

November 2017

# Role of Heat Shock Transcription Factor 1 in Ovarian Cancer Epithelial-Mesenchymal Transition and Drug Sensitivity

Chase David Powell

*University of South Florida*, [cdpowell@mail.usf.edu](mailto:cdpowell@mail.usf.edu)

Follow this and additional works at: <http://scholarcommons.usf.edu/etd>

 Part of the [Cell Biology Commons](#), [Molecular Biology Commons](#), and the [Oncology Commons](#)

---

## Scholar Commons Citation

Powell, Chase David, "Role of Heat Shock Transcription Factor 1 in Ovarian Cancer Epithelial-Mesenchymal Transition and Drug Sensitivity" (2017). *Graduate Theses and Dissertations*.  
<http://scholarcommons.usf.edu/etd/7079>

This Dissertation is brought to you for free and open access by the Graduate School at Scholar Commons. It has been accepted for inclusion in Graduate Theses and Dissertations by an authorized administrator of Scholar Commons. For more information, please contact [scholarcommons@usf.edu](mailto:scholarcommons@usf.edu).

Role of Heat Shock Transcription Factor 1 in Ovarian Cancer Epithelial-Mesenchymal Transition  
and Drug Sensitivity

by

Chase David Powell

A dissertation submitted in partial fulfillment  
of the requirements for the degree of  
Doctor of Philosophy  
Department of Cell Biology, Microbiology, and Molecular Biology  
College of Arts and Sciences  
University of South Florida

Major Professor: Sandy D. Westerheide, Ph.D.  
Brant R. Burkhardt, Ph.D.  
Younghoon Kee, Ph.D.  
Meera Nanjundan, Ph.D.

Date of Approval:  
November 3, 2017

Keywords: Heat Shock Factor 1, Ovarian Cancer, Epithelial to Mesenchymal Transition,  
Transforming Growth Factor  $\beta$ , HSP90 Inhibitors, Spheroid Culture, Intrinsic Disorder

Copyright © 2017, Chase D. Powell

## **DEDICATION**

I would like to dedicate this work to my wife, Anne T Powell, for all of her support, patience, and love. To my children Elise, Madeleine, Aidan, and Ethan for the encouragement and inspiration they have provided me. To my parents Christina and Chris Simcox for their continued belief in me. And lastly, to my mentor Sandy D. Westerheide for allowing me the opportunity to learn.

## **ACKNOWLEDGMENTS**

I would like to acknowledge my committee members, Brant Burkhardt, Ph.D., Younghoon Kee, Ph.D., and Meera Nanjundan Ph.D. for their guidance and understanding. I would most especially like to acknowledge my major professor, Sandy D. Westerheide, Ph.D., for her infinite patience.

## TABLE OF CONTENTS

List of Tables.....	iv
List of Figures.....	v
Abstract.....	vii
Chapter One: Introduction.....	1
Discovery of the Heat Shock Response.....	1
Regulation of the Heat Shock Response by HSF1 .....	2
Overview of Heat Shock Response Regulation by HSF1 .....	2
Activation of the HSR.....	3
Repression of the HSR .....	5
HSF1 Regulated Response.....	7
Heat Shock Proteins.....	7
HSP27 .....	7
HSP40 .....	8
HSP70 .....	8
HSP90 .....	8
HSP110.....	8
Other Cytoprotective Functions.....	9
Role of HSF1 in Cancer.....	11
Ovarian Cancer.....	12
Ovarian Cancer Types.....	12
Treatments.....	13
Epithelial to Mesenchymal Transition.....	13
Spheroid Model.....	15
Transforming Growth Factor $\beta$ .....	15
Studies.....	16
Chapter Two: Intrinsic Disorder in the HSF Transcription Factor Family and Molecular Chaperones.....	19
Abstract.....	19
Intrinsically Disordered Proteins: General Overview .....	20
Intrinsic Disorder and Transcription Regulation .....	22
An Overview of Intrinsic Disorder in Chaperones .....	25
The Heat Shock Response .....	28
HSF1- The Master Heat Shock Response Regulator.....	29
Domains of HSF1.....	29
DNA Binding Domain .....	30
Trimerization Domain.....	31
Transactivation Domain .....	31
Regulatory Domain .....	32

Conservation of HSF Across Different Species .....	32
Alternative Splicing of HSF1 .....	33
Post-Translational Modifications Regulate HSF1 Transcriptional Activity.....	33
Phosphorylation .....	33
Sumoylation.....	35
Acetylation.....	35
A Correlation between Intrinsic Disorder and Post Translational Modifications .....	36
HSF1 as an Interaction Hub .....	38
Other Heat Shock Transcription Family Members .....	40
HSF2.....	40
HSF4.....	41
HSF3, 5, X and Y .....	42
Chapter Three: The Heat Shock Transcription Factor HSF1 Induces Ovarian Cancer Epithelial-Mesenchymal Transition in a 3D Spheroid Growth Model .....	53
Abstract.....	53
Introduction.....	54
Materials and Methods .....	56
HSF1 Copy Number, Expression Determination and Survival Analysis.....	56
Cell Culture and Treatments .....	56
Lentiviral Creation and Infection for Stable, Inducible shRNA-Mediated HSF1 Knockdown .....	57
Protein isolation, SDS-PAGE, and Western analysis .....	57
Cell Viability Assay.....	58
Clonogenic Assay .....	58
Wound Healing Assay.....	59
Cell Migration .....	59
Spheroid Formation .....	59
Quantitative RT-PCR .....	60
Results.....	60
HSF1 is Overexpressed in Ovarian Cancer.....	60
Establishment of SKOV3 and HEY Inducible HSF1 Knockdown Ovarian Cancer Cell .....	61
HSF1 Knockdown Inhibits Colony Formation, Wound Healing, Cell Migration and Fibronectin Expression .....	63
The Induction of Fibronectin by TGF $\beta$ is Enhanced in 3D Cultures as Compared to 2D Cultures .....	64
3D Culturing Reveals a Marked Effect of HSF1 on the Induction of EMT Transcription Factors .....	64
Discussion.....	65
Chapter Four: Modulation of Heat Shock Transcription Factor HSF1 Affects Response to Multiple Drugs .....	74
Introduction.....	74
Overview of Drugs Tested.....	75
Cisplatin .....	75
Paclitaxel.....	75
Doxorubicin .....	75
Curcumin.....	76
17-AAG (Tanespimycin) .....	76

Ganetespib.....	77
Material and Methods .....	77
Cell Culture.....	77
Protein Isolation, SDS-PAGE, and Western analysis .....	78
Viability Assay.....	78
Results.....	79
Doxycycline Treatment Does Not Effect Drug Sensitivity .....	79
HSF1 Knockdown Sensitizes Cells to Multiple Chemotherapeutic Agents .....	79
Drug Treatment Does Not Induce Robust Heat Shock Response .....	80
Discussion.....	80
Chapter Five: Implication and Future Directions.....	90
Implications for Disorder in HSF Protein Family and Chaperones studies .....	90
Role of Disorder in HSF1 Function.....	90
Potential of HSF1 and Chaperones as Drug Targets .....	91
Implication for HSF1 in Ovarian Cancer Studies.....	92
Origin and of HSF1 Gene Duplications .....	92
Spheroids as a Model to Study EMT .....	93
Role of HSF1 in Cancer Treatment .....	93
Future Studies.....	95
Further HSF1 Structure Studies .....	95
Mechanism of HSF1 Effect of EMT .....	96
Modulation of $\beta$ -Catenin and Wnt Signaling.....	96
Direct Activation of EMT Transcription Factors.....	96
Direct Activation of Interleukin Genes.....	97
References.....	98
Appendices.....	119
Appendix A: Supplementary Figures .....	120
Appendix B: Supplementary Tables.....	124
Appendix C: Detailed Protocols .....	125
Appendix D: Copyright Permissions .....	140

## LIST OF TABLES

Table 4.1:	IC50 Values with and without HSF1 Knockdown.....	89
Table S.1:	List of Primers Used in Quantitative RT-PCR.....	124
Table S.2:	Location of HSEs in Epithelial to Mesenchymal Transition Genes.....	124
Table S.3:	Antibody Dilutions and Incubation Times .....	125



## LIST OF FIGURES

Figure 1.1:	Overview of Heat Shock Regulation by HSF1 .....	17
Figure 1.2:	TGF $\beta$ Pathway .....	18
Figure 2.1:	The HSF1 Activity Cycle .....	43
Figure 2.2:	Structural Characterization of Human HSF1 .....	44
Figure 2.3:	Sequence Alignment of HSF1s from Different Organisms Using BLAST .....	45
Figure 2.4:	Structural Characterization of the DBDs from <i>K. lactis</i> and from <i>D. melanogaster</i> .....	46
Figure 2.5:	Conservation of Intrinsic Disorder in HSFs from Different Species.....	47
Figure 2.6:	Effect of Alternative Splicing on Disorder Profiles of the C-terminal Regions of Mouse and Human HSF1 Proteins .....	48
Figure 2.7:	Post-Translational Modification Sites for HSF1 .....	49
Figure 2.8:	Evaluating the Intrinsic Disorder Propensity of Human HSF2 .....	50
Figure 2.9:	Evaluating Disorder Propensity Distribution in Human HSF4 by PONDR-FIT for Canonical and Alternatively Spliced Isoforms .....	51
Figure 2.10:	Evaluating the Intrinsic Disorder Propensity of Human HSF3, HSF5, HSFY and HSFX .....	52
Figure 3.1:	HSF1 levels are Elevated in Ovarian Cancer Patient Samples.....	68
Figure 3.2:	Validation of Inducible HSF1 Knockdown Ovarian Cancer Cell Lines.....	69
Figure 3.3:	HSF1 Knockdown Reduces Colony Formation .....	70
Figure 3.4:	HSF1 Knockdown Inhibits Wound Healing, Migration and Induction of Fibronectin .....	71
Figure 3.5:	Fibronectin Expression is Induced by 3D Growth .....	72
Figure 3.6:	TGF $\beta$ Induction of EMT Master-Switch Transcription Factors are Reduced upon HSF1 Knockdown, and the Effect is Enhanced upon 3D Culturing .....	73
Figure 4.1:	Cisplatin Chemical Structure .....	83

Figure 4.2:	Paclitaxel Chemical Structure .....	83
Figure 4.3:	Doxorubicin Chemical Structure.....	83
Figure 4.4:	Curcumin Chemical Structure .....	84
Figure 4.5:	17-AAG Chemical Structure.....	84
Figure 4.6:	Ganetespib Chemical Structure .....	85
Figure 4.7:	Doxycycline does not Affect Drug Response in Control Cells.....	86
Figure 4.8:	Effect of HSF1 Knockdown on SKOV3.shHSF1B Dose Response .....	87
Figure 4.9:	Effect of HSF1 Knockdown on HEY.shHSF1B Dose Response .....	88
Figure 4.11:	Drug Treatment does not Induce HSR .....	89
Figure S.1:	Doxycycline Treatment Alone does not Alter HSF1 Levels or Induce HSP90 Expression in Ovarian Cancer Cell Lines .....	120
Figure S.2:	Amplified Regions in Serous Ovarian Cancer .....	120
Figure S.3:	Knockdown of HSF1 Reduces IL-6 and MMP9 mRNA Induction During TGF $\beta$ Treatment in SKOV-3.shHSF1B Cells .....	121
Figure S.4:	SKOV-3 Short Tandem Repeat Analysis.....	122
Figure S.5:	HEY Short Tandem Repeat Analysis .....	123

## ABSTRACT

The heat shock response (HSR) is a robust cellular reaction to mitigate protein damage from heat and other challenges to the proteome. This protective molecular program in humans is controlled by heat shock transcription factor 1 (HSF1). Activation of HSF1 leads to the induction of an array of cytoprotective genes, many of which code for chaperones. These chaperones, known as heat shock proteins (HSPs), are responsible for maintaining the functional integrity of the proteome. HSPs achieve this by promoting proper folding and assembly of nascent proteins, refolding denatured proteins, and processing for degradation proteins and aggregates which cannot be returned to a functional conformation. The powerful ability of the heat shock response to promote cell survival makes its master regulator, HSF1, an important point of research. To garner a better understanding of HSF1, we reviewed the role of the highly dynamic HSF1 protein structure and investigated how HSF1 affects cancer cell behavior and drug response.

Cancers can be characterized in part by abhorrent replication, self-sufficient growth signaling, invasion, and evasion of apoptosis. HSF1 has been found to promote proliferation, invasion, and drug resistance in several types of cancer; including lung and ovarian cancer. Ovarian cancer has elevated levels of HSF1, but the role of HSF1 in ovarian cancer behavior had not been previously examined. Researching the role of HSF1 in ovarian cancer is merited, because treatment outcomes are poor due to the high frequency of late stage detection and drug resistance. We hypothesized that HSF1 is important in the malignant growth and drug resistance of ovarian cancer.

We have created ovarian cancer cell lines with inducible knockdown of HSF1 to investigate how HSF1 contributes to the behavior of ovarian cancer. This allowed us to examine the behavior of cells in the absence HSF1. Both 2D and 3D spheroid tissue culture models were used to study how HSF1 contributes to the growth and invasion of ovarian cancer cells after treatment with the transforming growth factor  $\beta$  (TGF $\beta$ ) cytokine. Additionally, we studied how HSF1 reduction modulates the response to multiple therapeutic drugs. Our research shows that HSF1 induces epithelial-mesenchymal transition (EMT) in a 3D growth model. Our work also demonstrates that reduction of HSF1 sensitizes ovarian cancer cells to multiple drugs.

## CHAPTER ONE: INTRODUCTION

### Discovery of the Heat Shock Response

The discovery of the heat shock response (HSR) came by way of a fortuitous accident in the early 1960s. The Italian geneticist, Ferruccio Ritossa, was researching nucleic acid synthesis associated with chromosomal puffs in *Drosophila* polytene salivary gland cells. These chromosomal puffing patterns offered a simple visual indication of gene transcription. During these studies a fellow researcher increased the temperature of the incubator by mistake [1].

When Ritossa observed the *Drosophila* that had been exposed to higher temperatures, he discovered a completely distinct puffing pattern. This change in chromosomal puffing represented one of the strongest examples of environmentally-induced changes in gene expression known at the time. Ritossa found that the response only took 2 – 3 minutes to occur, and that it was present in different tissues, developmental stages, and species of *Drosophila* [2, 3]. These observations led him to believe that the response he was observing was of importance. However, his work was not well received by the scientific community for many years.

In the 1970s, the study of the heat shock response focused on the nature of the response and the role of the induced proteins. It was established by protein and mRNA radiolabeling that a very specific set of mRNAs and corresponding proteins were being produced during the HSR. Simultaneously, basal protein production was halted [4]. These proteins induced by the heat shock response were called heat shock proteins (HSPs). The HSPs were named based upon the proteins size in kilo Daltons. Of the HSPs, HSP70 was found to be produced in the most abundance in *Drosophila* after heat shock [4]. As researchers sought to characterize HSPs, it was discovered that they were well conserved across *E. coli*, *Drosophila*, and many other organisms

[5-7]. While the homology across kingdoms suggested that HSPs were involved in foundational cell processes, it was not until the late 1980s that HSPs were understood to be molecular chaperones [8, 9].

To understand the regulation of the heat shock response, researchers studied the promoter of the rapidly inducible *hsp70* gene to investigate how the system is regulated. The critical region for heat shock induction of *Drosophila hsp70* was determined by creating promoter deletions and detecting gene activation by employing a S1 nuclease protection assay [10]. A short repeated sequence was found to be necessary for the HSR induction of *hsp70* and many other HSPs within a GC rich promoter region [10-12]. This promoter element was dubbed the heat shock element (HSE). The HSE is generally comprised of three contiguous inverted repeats: nTTCnnGAAnnTTCn [13, 14]. Shortly after the discovery of the HSE, promoter footprint analysis was used to discover a unique RNA polymerase II transcription factor which bound HSEs [15, 16]. This transcription factor was subsequently named heat shock transcription factor 1 (HSF1). HSF1 was shown to be required for HSR gene induction in *Drosophila* and human cells [17]. This research established the foundational understanding of the heat shock response. HSF1 binds HSEs in the promoters of target genes and strongly induces their transcription during HSR activation.

## **Regulation of the Heat Shock Response by HSF1**

### **Overview of Heat Shock Response Regulation by HSF1**

The heat shock response is presided over by the heat shock transcription factor (HSF) family of proteins in eukaryotes. While *C. elegans*, *S. cerevisiae* and *D. melanogaster* each have a single HSF, mammals possess 6 HSF family members [18]. Of these, heat shock factor 1 (HSF1) serves as the master regulator of HSR in mammals (Figure 1.1). This critical role in activating the heat shock response is demonstrated by the inability of *hsf*<sup>-/-</sup> mice and derived cell lines to undergo a heat shock response [19, 20].

HSF1 is constitutively expressed at low levels and is present in both the nucleus and cytoplasm as an inactive monomer. Upon activating stress, HSF1 forms trimers and accumulates in the nucleus where it aggregates as a part of nuclear stress bodies [21, 22]. HSF1 is concurrently hyper-phosphorylated and binds heat shock elements in the promoters of target genes [23-25]. There are often many HSEs within the promoters of strongly induced genes. After binding HSEs, the HSF1 trimer activates robust gene induction. Following stress, attenuation occurs due in part to acetylation of the HSF1 DNA binding domain and negative feedback from HSPs [26, 27].

### **Activation of the Heat Shock Response**

HSF1 protein is constitutively expressed and has a long half-life of approximately 13 -20 hours [28]. HSF1 is an inactive monomer during normal conditions. HSF1 is kept in an inactive monomer state by both intermolecular and intramolecular mechanisms. At the intramolecular level, HSF1 is stabilized in the monomer state by interactions between the hydrophobic repeat domains HR-A/B and HR-C (Fig 2.2). This interaction creates a coiled-coil structure which tethers the N and C termini together. The result is a semi stable monomer [29]. At the intermolecular level, HSF1 is repressed by interaction with the HSP90 complex, HSP70 and TRiC/CCT [27, 30, 31]. These chaperones bind HSF1 and maintain the inactive monomer state. When activated, HSF1 forms a homotrimer. Trimerization is generally induced by two mechanisms. It can be promoted by the loss of HSF1 associated chaperones to denatured proteins during ongoing stress. Alternately, it can be induced by elevated temperatures which cause the unfolding of the inhibited HSF1 monomer. While trimerization is required for HSF1 activation, it is not alone sufficient [32].

The next step in HSF1 activation is extensive phosphorylation. This occurs to such a degree that a marked shift in electrophoresis mobility occurs.[22] Some degree of phosphorylation is believed to be required for HSF1 transcription, because trimerization and DNA binding do not always result in transcriptional activity. This is demonstrated by the ability of salicylic acid to

induce trimerization and DNA binding, but not active transcription or phosphorylation [33]. The extensive phosphorylation occurs primarily on serine residues in the regulatory domain (Fig 2.2). Additionally, some studies have shown a small degree of threonine phosphorylation occurring [34-36]. Phosphorylation of ser326 by mTOR or p38 MAPK strongly supports activation [37, 38]. The phosphorylation of ser320 by Protein Kinase A leads to the nuclear accumulation HSF1 prompting activation [39, 40]. Many other serines are also known to be phosphorylated in HSF1 during the heat shock response: Ser121, Ser230, Ser292, Ser303, Ser307, Ser314, Ser319, Ser344, Ser363, Ser419, and Ser444. Interestingly, point mutation analysis of these sites showed none of them are individually critical for HSF1 transcriptional activity [36, 41]. It is reasonable to assume that these sites serve as a mechanism to finely modulate HSF1 activity, or interactions with its partners.

Concurrent with extensive phosphorylation, active HSF1 trimers accumulate in the nucleus. Transport into the nucleus is driven by a strong bipartite nuclear localization signal [21]. This signal is recognized by importin-alpha/beta [21]. Import into the nucleus occurs under basal conditions, but does not entirely accumulate in the nucleus due to export by 14-3-3  $\epsilon$  [42]. In unstressed cells, HSF1 location exists in an equilibrium between the cytoplasm and the nucleus. The primary location in unstressed cells varies. However, a literature review shows 31 of 38 studies found the nucleus is the primary location under basal conditions [21]. During stress, complete nuclear accumulation is achieved by the cessation of nuclear export. The rate of nuclear export by 14-3-3  $\epsilon$  is controlled by the phosphorylation of Ser303 and S307. Phosphorylation of both these site is required for export. These sites are phosphorylated by ERK, GSK3 $\beta$ , and possibly other kinases [43]. Regulation of nuclear export allows for fine tuning of HSF1 activity.

Active HSF1 accumulates in the nucleus and quickly congregates in nuclear stress bodies. These bodies form rapidly and range from 0.3 – 3  $\mu\text{m}$  in size [44]. Assembly of nuclear stress bodies is directed by blocks of satellite III DNA [44]. HSF1 binds these regions and recruits CREB binding protein which leads to chromatin remodeling and active transcription [44].



The discreet chromosomal locations of satellite III DNA sequences results in fixed locations for stress body formation. The resultant Satellite III RNA interacts with HSF1 and becomes part of the nuclear stress bodies. There HSF1 binds several splicing cofactors and suppresses translation of some non-heat shock proteins [45]. The full purpose of nuclear stress bodies is not fully understood. However, it is thought that the specific localization of nuclear stress bodies may serve to further direct and enhance transcription [46]. Surprisingly, nuclear stress bodies do not form in rodent cells, which suggests recent evolution.

Active HSF1 binds within the promoter regions of genes which are regulated during heat shock. HSF1 promoter binding activates transcriptions in all but few cases [47, 48] Promoter binding is mediated by the N-terminal DNA binding domain which interacts with the major groove and phosphate backbone [49, 50]. This binding is directed by a short sequence of DNA consisting of the sequence nGAAn, usually in three inverted repeats [51]. This is known as the Heat Shock Element (HSE) and was first identified in the *hsp70* promoter [11]. The multiple repeats of the nGAAn sequence serve to bind the three DNA binding domains in the active HSF1 trimer [46]. The number, spacing and sequence of the HSEs can vary some from the consensus sequence and still be recognized by HSF1. This is due in part to the co-operative nature of the DNA binding domain which interacts synergistically with other HSF1 DNA binding domains via a 'winged' structure [50]. The co-operative nature of HSEs and the HSF1 DNA binding domain allow HSF1 affinity to be greatly regulated by the strength, location and repetition of HSEs [52].

### **Repression of HSF1**

HSF1 activation is repressed through multiple mechanisms. The primary mechanism is believed to be negative feedback by heat shock proteins. Many of the HSPs expressed during heat shock inhibit HSF1 activation. These inhibitory HSPs include the HSP90 and its associated complex, HSP70, and TRiC [31, 53-55]. These inhibitory heat shock proteins achieve this by

binding and stabilizing HSF1. It is believed that these chaperones bind HSF1 in a repressed monomeric state. During damage to the proteome, denatured proteins are assumed to titrate away HSPs, alleviating inhibition. Multiple studies have found that HSF1 interacts with HSP90 and associated complex members including p23, Hip, and Hop [53]. Interestingly, co-immunoprecipitation research showing this interaction required cross-linking in both cases, suggesting that the interaction is of limited strength. Surprisingly, recent research has shown that HSP90 does not support or promote the monomeric state of HSF1 in *in vitro* studies. Instead, HSP90 facilitates transition to the active trimer form [29]. This suggests that HSP90 is important in the regulation of activation, but alone does not inhibit HSF1 activation. *In vitro* studies of HSF1 binding with TRiC and HSP70 found a stronger affinity which didn't require cross linking to examine [31, 56].

The ability of HSF1 to bind DNA can be reduced by post translational modification. This serves as another means by which to attenuate the heat shock response. Within the DNA binding domain lysine 80 and 118 are acetylated by p300 and other histone acetyltransferases [26, 57, 58]. This leads to the reduction of DNA binding affinity, presumably due to the loss of positive charges which facilitate interaction with negatively charged DNA. Acetylation which reduces HSF1 activity can be alleviated by the SIRT1 deacetylase [26].

HSF1 activity can also be regulated by changes in the available HSF1 protein itself. Active HSF1 can be targeted for degradation by the ubiquitin-proteasome system, which leads to the repression of the heat shock response. Multiple lysines can be ubiquitinated by NEDD4 and possibly other ubiquitin E3 ligases [59]. This leads to FILIP-1L mediated transport to the 19s proteasome subunit [60]. Surprisingly, HSF1 proteasome degradation can be inhibited by the acetylation of lysine residues by p300 and other acetyltransferases [57]. While p300 acetylation within the HSF1 DNA binding domain reduces HSF1 activity, the acetylation of lysine residues elsewhere prevents their ubiquitination and there by prevents degradation.

Additional means of HSF1 repression can be modulated by phosphorylation and sumoylation. While phosphorylation is a hallmark of HSF1 activation, multiple phosphorylation events serve to hamper activity. Phosphorylation of 303 and 307 by GSK3B leads to increased 14-3-3  $\epsilon$  mediated nuclear export [43, 61]. Phosphorylation can also inhibit transcriptional activity. Phosphorylation of serine 121 by MAPK activated protein kinase 2 reduces transcriptional activity and promotes HSP90 binding [55]. A reduction in transcriptional activity also occurs by sumoylation at lysine 289. Sumoylation of HSF1 requires phosphorylation of serine 203 as prerequisite [62]. The conjugation of SUMO is mediated by HSP27 oligomers [63].

### **The HSF1 Regulated Response.**

#### **Heat Shock Proteins**

**HSP27.** The small heat shock protein HSP27 functions primarily by binding and stabilizing unfolded protein intermediates [64]. This indirectly promotes the successful refolding or clearing of misfolded poly peptides. HSP27 works in a range of forms from monomers to large homo complexes [65]. These complexes passively stabilizes clients, as HSF27 has no ATPase function [66]. The co-operative aggregation is driven by the  $\alpha$ -crystallin domain [67].

In addition to its chaperone function, HSP27 plays a role in cytoskeletal organization and inhibits apoptosis. HSP27 interacts with actin to form cap ends which can inhibit actin polymerization [68]. This inhibition of actin polymerization is promoted the phosphorylation of HSP27 at multiple sites [69]. In the non-phosphorylated form HSP27 does not interact with actin and instead form oligomers which facilitate its chaperone function. HSP27 inhibits apoptosis via interacting pro-caspase 3 and inhibiting its activation [70].

**HSP40.** Acts as a co-chaperone and has two critical functions. It directs clients to HSP70 and it also controls the ATPase activity of HSP70 [71]. HSP70 has very weak ATPase activity alone and is dependent on HSP40 for its ATP dependent functions [72]. The J domain of

HSP40 is critical for HSP70 related functions. Outside of its role with HSP70, some members of the HSP40 family have functions in processing aggregates and inhibiting apoptosis [73].

**HSP70.** Of the heat shock proteins, the HSP70 family is one of the most highly induced proteins during heat shock response [13]. HSP70 functions in a large array of chaperone processes including, folding nascent proteins, complex assembly, and processing misfolded proteins for degradation. Hsp70 is composed of two domains, a N-terminal nucleotide-binding domain that regulates client interactions and a C-terminal substrate-binding domain, which recognizes exposed hydrophobic stretches in the client proteins [74]. HSP70 has a large number of clients. Because of this, HSP70 can affect many cellular processes including cells signaling, apoptosis and immune response [75, 76]. The client interactions are largely mediated by HSP40 which both shepherds client proteins and promotes HSP70 ATPase function.

**HSP90.** HSP90 processes larger proteins and protein complexes. It functions as a homodimer assisted by a bevy of co-factors which allows HSP90 to deal with large, complex clients. The large number of co-factors and client proteins make the HSP90 complex serve as a signaling hub in addition to a chaperone. This is illustrated by its role in regulating hormone receptor complexes, protein kinases and transcription factors functions [77, 78]. For these reasons, HSP90 is critical in the folding, activation and assembly of proteins and also ligand receptor binding interactions [79].

**HSP110.** The large HSP110 generally acts as a cochaperone. It is loosely related to HSP70 but possesses an extended loop structure within the C-terminus which allows interactions with larger clients [80]. Because of the similarity, HSP110 is often considered to be part of the HSP70 super family [81]. It works both by intrinsically stabilizing denatured proteins and directing clients to HSP70. Due in part to its large size, HSP110 excels at preventing irreversible aggregation [82]. It also has the ability to bind non-protein ligands, such as pathogen-associated molecules, and is implicated in immune response modulation [83].

Functioning as a co-chaperone, HSP110 assists in the activity of HSP70 by escorting client proteins and acting as a nucleotide exchange factor, similar to HSP40 [84].

### **Other cytoprotective functions**

HSF1 is capable of directing cellular responses through mechanisms outside of heat shock protein induction and their direct effects. HSF1 is able to modulate a variety of cellular functions including development, cell division, energy production, cytoskeletal organization, and vesicular transport [20, 85-89]. This is achieved through HSF1 direct interactions, alternative roles for expressed HSPs, and the expression of non-HSP genes.

In addition to activating transcription, HSF1 can inhibit genes under certain circumstances. Most notably, HSF1 is able to inhibit inflammatory response genes during a lipopolysaccharide-induced acute immune response [90-92]. This is achieved by both facilitating promoter interactions of transcriptional inhibitors and by direct inflammatory transcription factor inhibition [93, 94]. A variety of genes involved in the inflammation and immune response contain heat shock elements within their promoters, but are not strongly expressed during heat shock [48, 95]. Examples include multiple CXC chemokines, interleukin 6 (IL6) and tumor necrosis factor (TNF) genes [48, 93, 95]. In these instances, HSF1 is believed to be actively binding the promoter and directing the interaction of other transcription modulators. During heat shock, HSF1 has been shown to bind the promoter and facilitate an inhibitory effect on IL6, TNF, and CXCL5 [48, 92, 96, 97]. HSF1 is also able to affect the inflammatory response by directly binding and inhibiting the transcription factor CCAAT/enhancer binding protein beta (C/EBP- $\beta$ ), also known as nuclear factor of interleukin 6 (NF-IL6). C/EBP- $\beta$  is a key mediator of metabolic and inflammatory responses, and promotes expression of interleukins such as IL1- $\beta$  and IL6 along with other cytokines [94, 98-100]. The trimerization and regulatory domain HSF1 binds the basic leucine zipper domain of C/EBP- $\beta$  [94]. This leads to the inhibition of both transcription factors [94]. During

heat shock, C/EBP- $\beta$  inhibition by HSF1 leads to reduced induction of IL1- $\beta$  and G-CSF [101, 102].

Some of the heat shock proteins expressed during heat shock have protective functions outside of protein folding. HSP70 has a variety of specific functions and interactions which stave off apoptosis. HSP70 blocks mitochondrial translocation and activation of BCL-2 family member BAX, partially via direct interaction [103]. This prevents the mitochondrial release of pro-apoptotic factors [104]. HSP70 also directly inhibits apoptosis protease-activating factor 1 (Apaf-1), apoptosis-inducing factor (AIF), and death receptors DR4 and DR5 [105-107]. HSP27 is able to inhibit apoptotic signal by binding multiple apoptosis mediators including caspase-3, cytochrome c, and death-domain-associated protein (DAXX) [108-110].

HSF1 has been shown to directly and indirectly regulate expression of multiple non-HSP genes in order to promote survival. This is achieved through various means such as inhibiting apoptosis, enhancing autophagy, and regulating cell cycle. HSF1 mediated expression of Bcl-2-associated athanogene domain 3 (BAG3) leads to the stabilization of Bcl-2 family proteins which inhibit apoptosis [111, 112]. Similarly, HSF1 can regulate second mitochondria-derived activator of caspase (SMAC) which in turn affects apoptosis [113]. Activation of HSF1 can also promote autophagy, which enhances cell survival during metabolic stress [114]. This is accomplished by HSF1-dependent activation of the autophagy-related protein 7 (ATG7) gene and indirect activation of p62 [115, 116]. HSF1 has also been shown to regulate the cell cycle. Research suggests that HSF1 is required for proper mitotic progression, as is demonstrated by the increased rate of mitotic disturbances in *hsf1*<sup>-/-</sup> cell lines [85, 117]. Active HSF1 promotes FOXM1 expression which regulates G2/M cell cycle progression [118]. Additionally, HSF1 directly interacts with CDC20 and can modulate metaphase to anaphase transition [119].

## Role of HSF1 in Cancer

As the master regulator of the heat shock response, HSF1 has been postulated to be an important factor in oncogenesis. HSF1 plays many roles which could be beneficial to the progression and maintenance of the cancer phenotype. In addition to the canonical role in controlling the heat shock response, HSF1 is also involved in development, ageing, angiogenesis, inflammatory response, cell cycle signaling, metabolism, and translation [120-124]. Research over the last two decades has supported this idea and shown that HSF1 is important in cancer biology. HSF1 and many of its regulated targets are often overexpressed in cancers and support malignant behavior and survival.

Heat shock factor 1 and many associated HSPs are elevated in cancer cells compared to normal cells, which supports the theory that HSF1 can facilitate cancer development and survival. High HSF1 expression has been found in a wide array of cancers. These include breast, hepatocellular, ovarian, colorectal, multiple myeloma, glioma, oral squamous cell, and prostate cancers [125-132]. In addition to elevated levels of HSF1, many of these cancers also have increased nuclear accumulation of HSF1, which is indicative of activation [133]. Further, these elevated HSF1 levels correlate with poor outcomes in patients with breast cancer and hepatocellular carcinoma [129, 134]. Similarly, elevated levels of HSPs are found in many cancers including ovarian, breast, hepatocellular, and prostate cancer [135].

Continuing research has elucidated some of the ways HSF1 supports oncogenic behavior. Initial studies using *hsf*<sup>-/-</sup> mice and their derived cell lines demonstrated that HSF1 is required for RAS and mutant p53-induced transformation [136]. Subsequent studies determined that HSF1 supports cancers in a variety of ways. In many cases, HSF1 can improve survival of proteotoxic damage created by the malignant state [121, 137]. This is achieved through the general cytoprotective functions of the HSR. These functions include the anti-apoptotic effects of many HSPs and improved drug tolerance from increased efflux by ABC transporters [138, 139]. Other studies have found that HSF1 activation in cancer promotes malignant characteristics due to

effects outside of the classic HSR. In breast cancer and hepatocellular cancer, increased HSF1 is required to maintain aberrant signaling pathways including HER2 and MAPK pathways [140, 141]. This HSF1-driven maintenance of vital signaling pathways in cancer is thought to be supported in part by elevated levels of HSP90, because HSP90 serves many client proteins that are key in signal transduction [142]. The methods by which HSF1 facilitates cancer progression continue to be elucidated. Research using high-throughput techniques have found that in cancer, HSF1 can modulate many cell processes including energy metabolism, cell cycle signaling, DNA repair, apoptosis, cell adhesion, extracellular matrix formation, and translation [133].

## **Ovarian Cancer**

Ovarian cancer is the leading cause of cancer related deaths among gynecological malignancies [143]. It is projected that there will be 22,440 new cases of ovarian cancer and 14,080 ovarian cancer related deaths in 2017 [143]. Outcomes are typically poor; ovarian cancer has a low 46.5% 5 year survival rate. This high morbidity rate is due to the combination of late stage diagnosis coupled with a high rate of drug resistant recurrence. Failure to detect the disease in early stages is due in part to generalized symptoms such as abdominal and back pain, irregular vaginal discharge and pelvic pressure or bloat. Additionally, there is a lack of reliable diagnostic markers or tests. As a result, the vast majority of women are diagnosed at advanced stages III and IV [144]. Currently, there is work to establish diagnostic markers; however, this work has not yet substantially changed early stage detection rates [145].

### **Types of Ovarian Cancer**

There are multiple histological subtypes of ovarian cancer. Of these, epithelial ovarian cancers are the most common and account for about 90% of ovarian cancer cases [146]. Other less common histological subtypes include germ cell and stromal, which make up the remainder of cases. Epithelial ovarian cancer can be further divided into serous, endometrioid, clear cell,



and mucinous carcinoma subtypes [147]. The clear cell carcinoma and endometrioid subtypes are believed to come from endometriosis [148]. Of the types of epithelial ovarian cancer, serous accounts for the majority of cases [146]. Serous epithelial ovarian cancer can be further divided into high and low grade. Both types of serous ovarian cancer have traditionally been thought to come from the ovarian surface epithelium. There has been a recent debate over the origin of high grade serous, and current research suggests that it may actually originate from the fallopian tube [149]. High grade serous generally has an aggressive phenotype and is more common [146]. Low grade serous is less aggressive and sometimes has oncogenic drivers such as mutated KRAS, BRCA, and PTEN [148]. Both types are characterized by high genomic instability and frequent loss of p53 function [150, 151].

### **Treatments**

First line ovarian cancer treatment generally consists of surgical debulking and a combination of platinum and taxane chemotherapies. Initial response to these therapies is generally good, especially if resection was complete. Unfortunately, greater than 80% of patients will experience a recurrence, and most of these will be resistant to platinum and taxane therapies [146]. Other agents, notably bevacizumab and doxorubicin, are used in resistant cases. While these can increase progression-free survival, they very rarely achieve remission [152].

### **Epithelial to Mesenchymal Transition**

Epithelial to mesenchymal transition (EMT) is the shift of epithelial cells toward more mesenchymal characteristics. Cells which have undergone EMT have distinct changes in gene expression patterns which lead to the loss of epithelial morphology, and the gain of mesenchymal traits [153]. These include increased migratory behavior and stem cell like properties [154]. This mesenchymal like cell behavior facilitates migration through the surrounding extracellular matrix and the establishment of new growth. This behavior makes EMT an important part of early

development and wound healing [155]. However, it can also support aberrant conditions including cancer and fibrosis [153].

Epithelial to mesenchymal transition is believed to be an important step in the establishment of metastases because it promotes dissemination and invasive behavior [156]. In ovarian cancer, EMT is thought to be a critical step in progression for several reasons. The surface ovarian epithelium cells which serve as the source of most ovarian cancers, have a high degree of plasticity and naturally exhibit some mesenchymal properties [157]. This propensity to undergo EMT likely facilitates the detachment and dissemination within the peritoneal cavity [158]. This is a primary route which ovarian cancer spreads. Additionally, ascites fluids contain elevated levels of inflammatory and growth stimulating factors which drive the EMT process [159, 160]. For these reasons understanding EMT is an important part of understanding ovarian cancer.

On the molecular level EMT can be identified largely in part by the changes in cell to cell junctions and gene expression. This shift in cell interaction is driven by a handful of transcription factors which can serve as EMT markers [153]. During EMT there is reduction of E-Cadherin which destabilizes adherens junctions. Similarly claudins and occludins are reduced which weakens tight junctions [161]. N-cadherin is elevated, which promotes interaction with mesenchymal cells, increased invasion and migration, and disassociation with epithelial cells [162]. The extracellular matrix protein fibronectin is also more abundantly produced. This leads to further remodeling of the extracellular matrix and correlates with migration [163]. These changes in protein expression are driven principally by the transcription factors SNAIL1, SLUG (SNAIL2), TWIST and ZEB. SNAIL1 and SLUG are both zinc finger transcriptional repressors and function by binding E-box sequences within promoters and recruiting other repressors [164]. TWIST is a bHLH (basic helix-loop-helix) transcription factor which can activate or repress genes by directing histone modifications [164]. ZEB recognizes the E-box sequence motif, similar to SNAIL1 and SLUG, and can act as both a transcriptional activator and repressor depending on associated co-factors [165].

**Spheroid Models to Study EMT.** Standard tissue culture involves growing cells in a monolayer. This reinforces the cell polarity because the treated petri dish serves as the basal surface. This limits the usefulness of standard 2D cultures in studying EMT because the cells are not able to fully reorganize their interactions and transition away from the epithelial organization. Multiple studies have shown that culturing cells as 3 dimensional spheroids facilitates the signaling and gene expression changes that indicate EMT. Spheroid culture has been shown to increase TGF $\beta$ 1 and multiple growth factor levels as compared to 2D culture [166]. Additionally, the EMT transcription factors SLUG, SNAIL, and TWIST are elevated in spheroids versus 2D cultures [167]. In ovarian cancer patient ascites-derived cells, formation of spheroids is accompanied by increases the EMT transcription factors SNAIL, TWIST, and ZEB2 [168]. For these reasons, spheroid cell culture is an apt model for studying EMT and offers advantages over standard 2D culture.

### **Transforming Growth Factor $\beta$**

While many cytokines can promote EMT, transforming growth factor  $\beta$  (TGF $\beta$ ) is the principal driver of EMT in ovarian cancer [169, 170]. It is commonly overexpressed in cancer tissue, plasma and peritoneal fluid of ovarian cancer patients [171]. The TGF $\beta$  pathway controls multiple cell processes such as differentiation, apoptosis, migration and immune response [172]. TGF $\beta$  can act as either a tumor suppressor or promoter depending on cellular conditions. In primary and precancerous ovarian epithelial cells TGF $\beta$  induces cell death, but in ovarian cancer cells it promotes EMT [173]. Of the 3 forms of TGF $\beta$ , TGF $\beta$ 1 is most commonly associated with EMT in cancer [172].

The TGF $\beta$  pathway is activated by TGF $\beta$  ligand – receptor binding which triggers downstream changes in gene expression via the SMAD proteins (Fig 1.2). Extracellular TGF $\beta$  binds the TGF $\beta$ RII (TGF $\beta$  receptor II) and is incorporated into a hetero-tetramer receptor complex consisting of 2 TGF $\beta$ RII and 2 TGF $\beta$ RI receptors [174]. This activates the receptors' serine/threonine kinase activity resulting in the phosphorylation of receptor SMADs (R-SMADs)

in the cytoplasm. The activated R-SMADs associate with co-SMADs and accumulate in the nucleus. The SMAD complexes interact with various transcription factors and control expression of a wide set of genes [175]. . In addition to the canonical SMAD-mediated effects, TGF $\beta$  can activate the PI3K and MAPK pathways which can support EMT and proliferation [176, 177].

## **Studies**

To better understand the role of HSF1 in ovarian cancer we have done a review of the HSF family and associated chaperones, and completed studies to elucidate how HSF1 contributes to ovarian cancer cell behavior and drug resistance. Chapter 2 reviews the HSF and chaperone families with a focus on their general intrinsically disordered structure, which has implications for how they may function. Chapter 3 describes our work investigating how HSF1 induces ovarian cancer epithelial-mesenchymal transition, particularly in a spheroid growth model. Chapter 4 describes how HSF1 levels affect drug response in ovarian cancer cell lines to multiple agents. Chapter 5 discusses the implication of this work and future directions, including how HSF1 could translate to a potential drug target or prognostic marker.

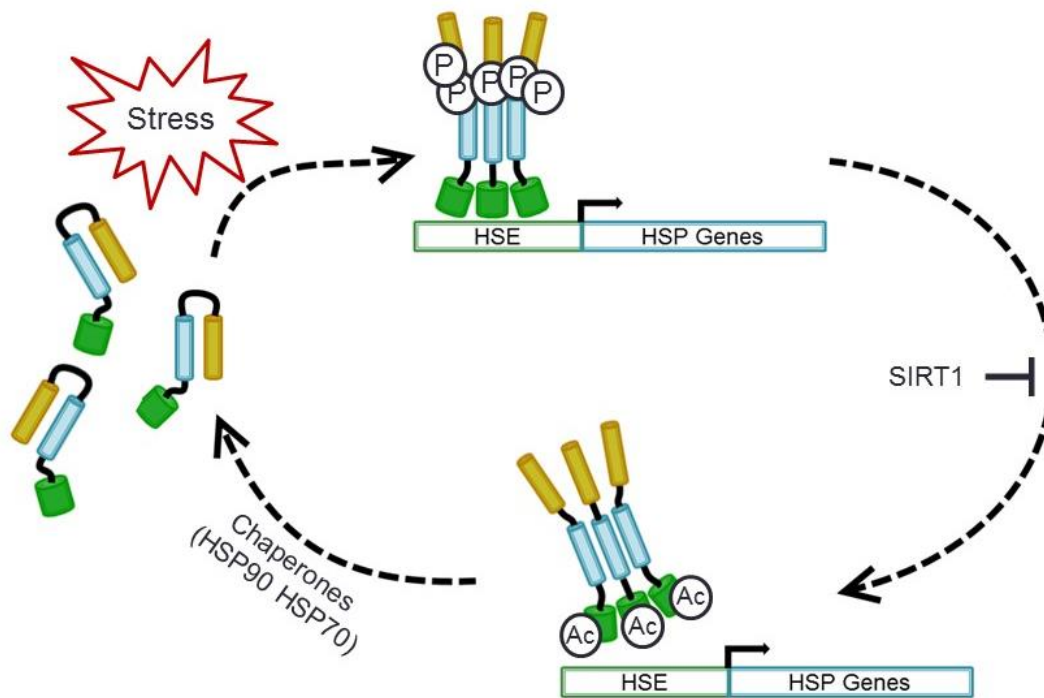


**Figure 1.1. Overview of Heat Shock Regulation by HSF1.** HSF1 forms trimers upon activating stress and is concurrently hyperphosphorylated. It accumulates in the nucleus, where it binds HSEs within the promoters of regulated genes. The response is shut off by negative feedback from HSPs and acetylation of the DNA binding domain. The DNA binding ability can be modulated by the deacetylase SIRT1.

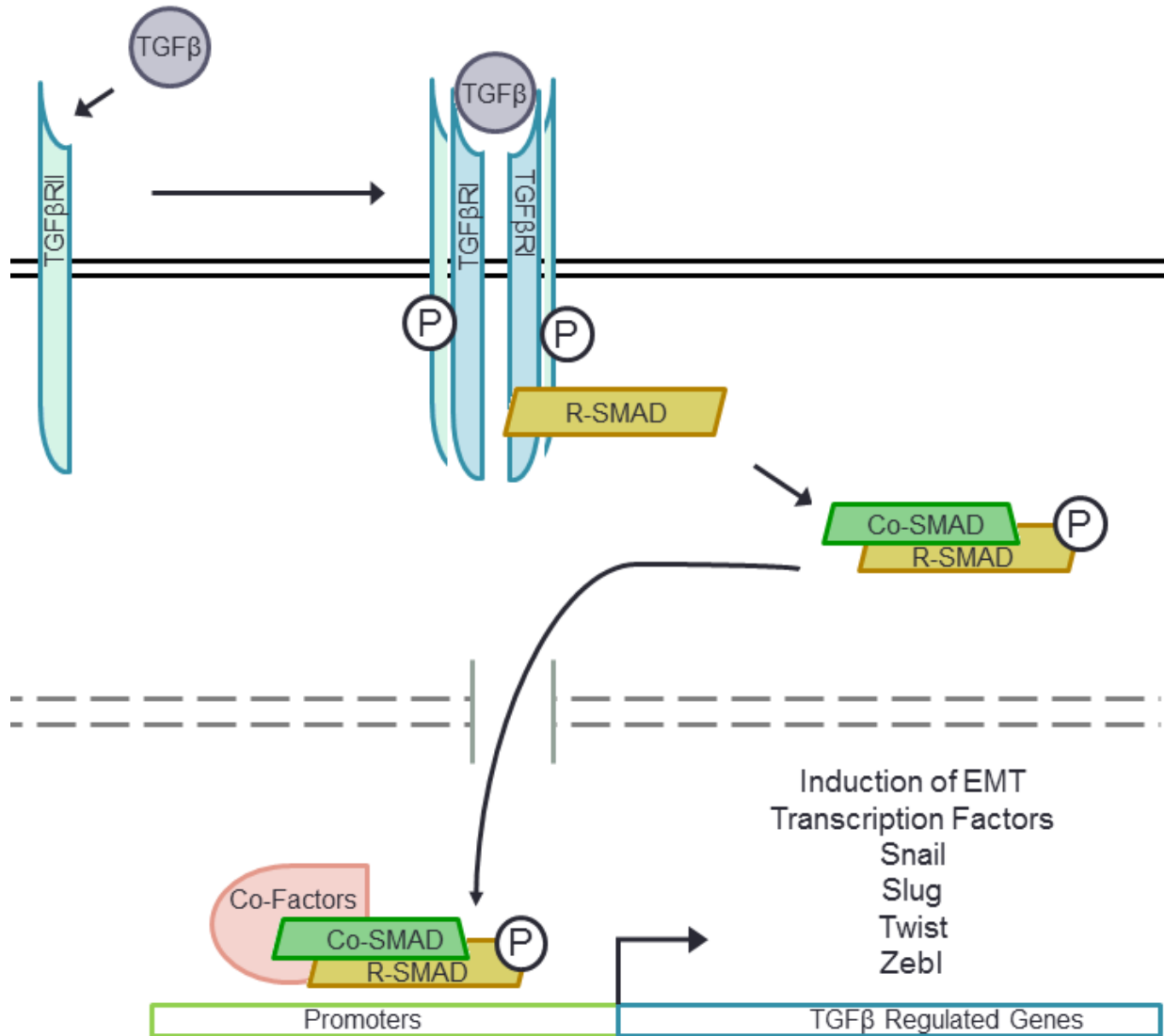


**Figure 1.2. TGFβ Pathway.** Active TGFβ binds the TGFβ receptor type II (TGFβRII) which results in the formation of the heteromeric complex with TGFβ receptor type I (TGFβRI) and autophosphorylation. This is followed by the phosphorylation of receptor-regulated SMAD (mothers against decapentaplegic homologue). R-SMAD forms complexes with co-mediator SMAD (Co-SMAD) and is translocated to the nucleus. The SMAD complex associates with DNA binding co-factors and transcriptional co-activators. These co-factors are largely responsible for directing the outcome of TGFβ signaling. In many ovarian cancers the TGFβ pathway leads to the induction of transcription factors which promote epithelial to mesenchymal transition (EMT).

## **CHAPTER TWO: INTRINSIC DISORDER IN THE HSF TRANSCRIPTION FACTOR FAMILY AND MOLECULAR CHAPERONS**

Authored by Sandy D. Westerheide, Rachel Raynes, Chase Powell, Bin Xue, and Vladimir N. Uversky

Published in *Current Protein and Peptide Science*. 2012 Feb;13(1):86-103. Review.

Authors contributed equally to the text. Background research and literature review performed by S. Westerheide, R. Raynes and C. Powell. Sequence and structure analysis was done by B. Xue and V. Uversky. See appendix D for copyright permissions.

### **Abstract**

Intrinsically disordered proteins are highly abundant in all kingdoms of life, and several protein functional classes, such as transcription factors, transcriptional regulators, hub and scaffold proteins, signaling proteins, and chaperones are especially enriched in intrinsic disorder. One of the unique cellular reactions to protein damaging stress is the so-called heat shock response that results in the upregulation of heat shock proteins including molecular chaperones. This molecular protective mechanism is conserved from prokaryotes to eukaryotes and allows an organism to respond to various proteotoxic stressors, such as heat shock, oxidative stress, exposure to heavy metals, and drugs. The heat shock response-related proteins can be expressed during normal conditions (e.g., during cell growth and development) or can be induced by various pathological conditions, such as infection, inflammation, and protein conformation diseases. The initiation of the heat shock response is manifested by the activation of the heat

shock transcription factor 1 (HSF1), part of a family of related HSF transcription factors. This review analyzes the abundance and functional roles of intrinsic disorder in various heat shock transcription factors and clearly shows that the heat shock response requires HSF flexibility to be more efficient.

### **Intrinsically Disordered Proteins: General Overview**

Research over the last decade or so made it absolutely clear that in addition to well-folded and highly structured transmembrane, globular and fibrous proteins, the protein universe includes intrinsically disordered proteins (IDPs) and proteins with intrinsically disordered regions (IDRs). These IDPs and IDRs are biologically active and yet fail to form specific 3D structure, existing instead as collapsed or extended dynamically mobile conformational ensembles [178-184]. These floppy proteins and regions are known as pliable, rheomorphic [185], flexible [186], mobile [187], partially folded [188], natively denatured [189], natively unfolded [180, 190], natively disordered [183], intrinsically unstructured [179, 182], intrinsically denatured, [189] intrinsically unfolded [190], intrinsically disordered [191], vulnerable [192], chameleon [193], malleable [194], 4D [195], protein clouds [196], and dancing proteins [197], among several other terms. The variability of terms used to describe such proteins and regions is a simple reflection of their highly dynamic nature and the lack of unique 3-D structure. None of these terms or their combinations is completely appropriate, as the majority of them have been borrowed from fields such as protein folding or crystallography, which are not directly related to the biologically active proteins that normally exist as structural ensembles.

Since these proteins are highly abundant in any given proteome [198], the role of disorder in determining protein functionality in organisms can no longer be ignored. Native biologically active proteins were conceptualized as parts of the "protein trinity" [181] or the "protein quartet" [199] models, where functional protein might exist in one of several conformations – ordered, collapsed-disordered (molten globule-like), partially collapsed-disordered (pre-molten globule-



like) or extended-disordered (coil-like), and protein function might be derived from any one of these states and/or from the transitions between them. Disordered proteins are typically involved in regulation, signaling and control pathways [200-202], which complement the functional repertoire of ordered proteins, which have evolved mainly to carry out efficient catalysis [203]. It is also important to remember that sites of posttranslational modifications (acetylation, hydroxylation, ubiquitination, methylation, phosphorylation, etc.) and sites of regulatory proteolytic attack are frequently associated with regions of intrinsic disorder [191].

Because of the fact that IDPs play crucial roles in numerous biological processes, it was not too surprising to find that many of them are involved in human diseases [204]. Originally, this hypothesis was based on numerous case studies where a particular IDP was shown to be associated with a particular disease. For example, the presence of disorder has been directly observed in several cancer-associated proteins, including p53 [205], p57<sup>kip2</sup> [206], Bcl-X<sub>L</sub> and Bcl-2 [207], c-Fos [208], thyroid cancer associated protein, TC-1 [209], and many others. Some other maladies associated with IDPs includes Alzheimer's disease (deposition of amyloid- $\beta$ , tau-protein,  $\alpha$ -synuclein fragment NAC [210-213]), Niemann-Pick disease type C, subacute sclerosing panencephalitis, argyrophilic grain disease, myotonic dystrophy, and motor neuron disease with neurofibrillary tangles (accumulation of tau-protein in the form of neurofibrillary tangles [212]); Down's syndrome (nonfilamentous amyloid- $\beta$  deposits [214]); Parkinson's disease, dementia with Lewy body, diffuse Lewy body disease, Lewy body variant of Alzheimer's disease, multiple system atrophy and Hallervorden-Spatz disease (deposition of  $\alpha$ -synuclein in a form of Lewy body, or Lewy neuritis [215]); prion diseases (deposition of PrP<sup>Sc</sup> [216]); and a family of polyQ diseases, a group of neurodegenerative disorders caused by expansion of CAG trinucleotide repeats coding for polyQ in the gene products [217].

Three computational and bioinformatics approaches have been elaborated to estimate the abundance of IDPs in various pathological conditions. The first approach was based on the assembly of specific datasets of proteins associated with a given disease and the computational

analysis of these datasets using a number of disorder predictors [200, 204, 218-221]. In essence, this was an analysis of individual proteins extended to a set of independent proteins. Using this approach, a prevalence of intrinsic disorder was detected in proteins associated with cancer [200], cardiovascular disease [219], neurodegenerative diseases [220, 222], various amyloidoses [223] and diabetes [204]. A second approach utilized the diseasome, a network of genetic diseases where the related proteins are interlinked within one disease and between different diseases [224]. A third approach was based on the evaluation of the association between a particular protein function (including the disease-specific functional keywords) with the level of intrinsic disorder in a set of proteins known to carry out this function [225-227]. Based on the fact that IDPs and proteins with long IDRs were commonly found in various diseases, the “disorder in disorders” or  $D^2$  concept was introduced to summarize work in this area [204] and the concepts of the disease-related unfoldome and unfoldomics were developed [228].

### **Intrinsic Disorder and Transcription Regulation**

Several protein functional classes (e.g., transcription factors [196, 229-231], transcriptional regulators [194, 232, 233], hub proteins [201, 233-238], scaffold proteins [239-242], signaling proteins [200], chaperones [243-250], etc.) were shown to be enriched in intrinsic disorder. Recent studies suggested that eukaryotic proteomes are highly enriched in IDPs relative to bacterial and archaeal proteomes [251-253], which may reflect the greater need for signaling and transcriptional regulation in nucleated cells [191, 200, 254]. Transcription factors (TFs) act through the recognition of specific DNA sequences and recruitment and assembly of the transcription machinery. Therefore, both protein-DNA and protein-protein recognition are central processes in TF function. It has been reported that protein-protein and protein-DNA interaction are often accompanied by a local folding in a protein molecule [255]. One of the important biological implications of this coupled binding and folding scenario is that protein backbone mobility may play an important role in the early stages of a binding event [256], where the specific

signal from the complex of protein with its binding partner emerges only after appropriate conformational changes take place [257].

Comprehensive computational analysis of several transcription factor datasets revealed that from 94.13% to 82.63% of TFs possess long regions of intrinsic disorder, and  $\geq 70\%$  proteins in the TF datasets were predicted to be wholly disordered [229]. Furthermore, the degree of disorder in eukaryotic TFs was shown to be significantly higher than in prokaryotic proteins. Eukaryotes have a well-developed gene transcription system, which probably requires a great deal of flexibility and plasticity. The intrinsically disordered TFs or partially unstructured regions can offer significant advantages in response to different molecular targets, allowing one protein to interact with multiple cellular partners and allowing fine control over binding affinity [229]. This analysis also revealed the existence of two distinct classes of DNA-binding domains (DBDs) in TFs. In one class, the DBDs are well-structured and specifically recognize DNA using the molecular surfaces they present to the environment. In another class, various DBDs such as basic domains and AT-hooks, are likely to be highly unstructured in isolation, and presumably undergo a disorder-to-order transition upon binding to specific DNA sequence. [229]. The high prevalence of intrinsic disorder in TFs suggested that it may play a critical role in the primary functions of TFs, which are molecular recognition, DNA binding, and transcriptional regulation.

This hypothesis is in a good agreement with several recent findings showing that eukaryotic TFs contain a variety of structural motifs that interact with specific DNA sequences [258] and are involved in activating the transcription. For example, based on the analysis of binding of multiple zinc fingers to cognate DNA a 'snap-lock' model has been recently introduced [259, 260]. According to this model, C<sub>2</sub>H<sub>2</sub>-type zinc finger domains consist of well-folded modules connected by highly conserved linker sequences that are mobile and unstructured in the absence of the cognate DNA. NMR analysis revealed that upon binding to the correct DNA sequence, the linker becomes highly structured and locks adjacent fingers in the correct orientations in the major groove [259, 260]. Furthermore, it has been shown that many alterations of this linker disrupt the

conformation of the bound linker, increase its flexibility, and impair DNA binding, thereby altering both the biological function and sub-nuclear localization of the protein [259, 260]. This model illuminates the sophisticated relationship between the function of a TF, its domain structure, and intrinsic disorder.

It is known that two totally disordered types of DBDs, AT-hook and basic domain, act as a versatile minor groove tether to anchor TFs to particular DNA sites. In addition to having sequence-specific DNA-binding activity, many TFs contain a region involved in activating the transcription of the gene whose promoters or enhancers they have bound. Usually, this trans-activating region enables the TF to interact with a protein involved in binding RNA polymerase. Many trans-activating domains were predicted either unstructured or partly structured [229]. This was in agreement with the accumulated experimental data that many trans-activating domains are significantly disordered in an unbound form and their interactions with their targets involve coupled folding and binding events [200, 252, 254, 261]. Recently, the kinase-inducible activation domain of CREB (cAMP response element binding protein) [262], the trans-activation domain of p53 [263], and the acidic activation domain of herpes simplex virus VP16 [264] were comprehensively examined. These studies revealed that the activation domains remained mostly unstructured in their normal unbound states, and form a helix or helices upon binding to the target proteins.

In another elegant computational study, the abundance and functional roles of intrinsic disorder in human TFs were investigated [230]. The authors emphasized that eukaryotic TFs, especially so-called *trans*-acting factors such as activators, repressors or enhancer-binding factors that specifically bind DNA *cis* elements, were noticeably larger than prokaryotic TFs. In fact, the average sequence of human TFs was more than twice as long as length of the TFs in prokaryotes. Furthermore, the fractions of sequence aligned to domains of known structure were 31% and 72% in human and bacterial TFs, respectively [230]. Therefore, as a rule, human TFs were long and poorly annotated. Analysis revealed that as high as 49% of the entire sequence of

human TFs was occupied by IDRs, and that more than half of the human TFs consisted of a small DBD and a set of long IDRs. In general, IDRs were shown to occupy a high fraction of TFs from eukaryotes, but not prokaryotes [230].

### **An Overview of Intrinsic Disorder in Chaperones**

Generally, a polypeptide chain of a protein contains all the information required to achieve functional conformation [265, 266]. Although this principle is generally correct for many proteins, the information contained in some potentially foldable proteins is not complete enough to guarantee the formation of a functionally active 3-D structure. Many such potentially foldable proteins cannot fold spontaneously and require the help of molecular chaperones; i.e., cellular proteins which act to ensure that the folding of certain polypeptide chains and their assembly into oligomeric structures occurs correctly [8]. Chaperones are an important part of the cellular quality control system, maintaining an intricate balance between protein synthesis and degradation and protecting cells from the devastating consequences of uncontrolled protein aggregation. In addition to chaperones, this system includes the ubiquitin-proteasome system and the autophagy-lysosome system. Molecular chaperones protect cells from apoptosis induced by toxic oligomers. There are several mechanisms by which chaperones fight devastating consequences of misfolding and aggregation. These mechanisms can be grouped into three major classes of action: prevention, reversal and elimination. At the prevention stage, chaperones bind to unfolded stretches in proteins and keep them in a folding-competent state while preventing aggregation. In the reversal mechanism, chaperones act as disaggregating and unfolding machines which help dissolve aggregates and give a misfolded protein a second chance for folding correctly. At the elimination step, chaperones target misfolded proteins for degradation by the ubiquitin-proteasome system and/or the autophagy-lysosome system.

The principal heat-shock proteins that have chaperone activity belong to five conserved classes: Hsp33, Hsp60, Hsp70, Hsp90, Hsp100, and the small heat-shock proteins. Molecular

chaperones have been divided into three functional subclasses based on their mechanism of action. "Folding" chaperones (e.g., DnaK and GroEL in prokaryotes, and Hsp60 and Hsp70 as well as the HspB group of Hsp including Hsp27 and HspB1 in eukaryotes) rely on ATP-dependent conformational changes to mediate the net refolding/unfolding of their substrates. "Holding" chaperones (e.g., Hsp33 and Hsp31) bind partially folded proteins and maintain these substrates on their surface to await the availability of "folding" chaperones. "Disaggregating" chaperones (e.g., ClpB in prokaryotes and Hsp104 in eukaryotes) promote the solubilization of proteins that have become aggregated as a result of stress.

Molecular chaperones are classified as either inducible or constitutively expressed according to their expression mechanisms. Both types of chaperones act by the selective binding of solvent-exposed hydrophobic segments of non-folded polypeptides, and, through multiple binding-release cycles, bring about the folding, transport, and assembly of the target polypeptides [267-269]. Some chaperones are ATPases; i.e., they use free-energy from ATP binding and/or hydrolysis to perform work on their substrates.

The concentration of inducible chaperones, also known as heat shock proteins (HSP), increases as a response to stress conditions. These molecular chaperones prevent and reverse the misfolding and aggregation of proteins that occur as a consequence of stress [270, 271]. On the other hand, constitutively expressed chaperones, also known as heat shock cognate proteins (Hscs), facilitate protein translation, help newly synthesized proteins fold, promote the assembly of proteins into functional complexes, and assist the translocation of proteins into cellular compartments such as mitochondria and chloroplasts [268, 272]. In the Hsp70 family of proteins, in addition to the inducible Hsp70 form, there is a constitutively expressed form, the heat shock cognate protein 70 (Hsc70), which has 85% identity with human Hsp70 and binds to nascent polypeptides to facilitate correct folding.

Molecular chaperones have evolved to protect proteins from misfolding and aggregation regardless of their classification as inducible or constitutively expressed. One important feature

of chaperones is that, although they assist the non-covalent folding/unfolding and the assembly/disassembly of other macromolecular structures, they do not occur in these structures when the latter are performing their normal biological functions. Generally, molecular chaperones have no effect on a protein's folding rate. Of course, apparent folding and assembly rates can be increased by the elimination of non-productive oligomer/aggregate formation. Furthermore, by binding to partially folded species and preventing their aggregation, chaperones increase the yield of functional folded/assembled proteins. However, these actions do not affect intramolecular folding rates. On the other hand, there is a last class of proteins - helpers which assist protein folding and are not present in the final folded/assembled functional form of a protein-substrate. Therefore, these helpers, known as foldases, belong to the family of chaperones. Contrary to the typical chaperones considered so far, foldases have evolved to catalyze the folding process by directly accelerating the protein folding rate-limiting steps. Well-known foldases include eukaryotic protein disulfide isomerase [273-275], peptidyl-prolyl cis/trans isomerase [275, 276], and lipase-specific foldases, Lifes, found in the periplasm of Gram-negative bacteria [275, 277].

Earlier, the prevalence of functional regions without a well-defined 3-D structure in RNA and protein chaperones was emphasized [250]. The analysis revealed a high proportion of predicted IDRs in chaperones, with 54% of residues of RNA chaperones falling into IDRs and with 40% of their residues being located within the disordered regions longer than 30 consecutive residues. Intrinsic disorder was also to be abundant in protein chaperones, for which corresponding values were 37% and 15%, respectively [250]. Based on the analysis of several individual cases it has been concluded that the IDRs in chaperones might function as molecular recognition elements solubilizing or locally loosening the structure of the kinetically trapped folding intermediate via transient binding to facilitate its conformational search. An "entropy transfer" model was proposed to account for the mechanistic role of structural disorder in chaperone function. According to this model, the binding of the disordered chaperone to the misfolded

substrate was proposed to be accompanied by ordering of the chaperone with a concomitant unfolding of the substrate [250].

Recently, it was confirmed that intrinsic disorder is highly abundant in protein chaperones and plays a number of important roles in the action of these intricate machines. IDRs determine the promiscuity of chaperones, act as pliable molecular recognition elements, wrap misfolded chains and participate in disaggregation and local unfolding of the aggregated and misfolded species. The functions of chaperones, co-chaperones and decorating proteins are precisely orchestrated. These proteins often act as large chaperone machines. They communicate with each other and form sophisticated chaperone networks. Protein intrinsic disorder plays a crucial role in the coordination and regulation of these chaperone machines and networks, thus helping form a flexible net of malleable guardians [243].

### **The Heat Shock Response**

The heat shock response is the cell's molecular reaction to protein damaging stress and results in the upregulation of heat shock proteins including molecular chaperones (reviewed in [13]). This response is conserved from prokaryotes to eukaryotes and allows an organism to respond to proteotoxic stressors, including heat shock, oxidative stress, heavy metals, and drugs, as well as cell growth and developmental conditions [278]. Pathology, such as inflammation or infection, may also induce the heat shock response, in addition to protein conformation diseases, such as Alzheimer's disease [278]. Upon initiation of the heat shock response, heat shock transcription factors (HSFs) are activated through trimerization and post-translational modifications [13]. A single, essential HSF1 gene exists in *Saccharomyces cerevisiae* and in *Drosophila melanogaster*, where this gene is responsible for both constitutive and heat-inducible heat shock gene expression [279-281]. Vertebrate species express a family of HSF proteins with diverse cellular roles.



## **HSF1- The Master Heat Shock Response Regulator**

HSF1 is the HSF family member responsible for stress-induced expression of heat shock proteins. Once the heat shock response is induced, HSF1 trimerizes, accumulates in the nucleus, and binds the heat shock elements (HSEs) located in the promoter regions of *hsp* genes (Figure 2.1). The HSEs consists of several adjacent and inverted repeats of the pentamer sequence nGAAn [282]. Activation of transcription occurs upon HSF1 hyperphosphorylation [34].

Attenuation of the heat shock response is important because the overexpression of HSPs is deleterious to the cell. Attenuation is regulated by a dual mechanism involving negative feedback inhibition from HSPs [27] and acetylation at a critical lysine residue within the DNA binding domain of HSF1 causing loss of affinity for DNA [26]. SIRT1 is a NAD-dependent histone deacetylase that deacetylates HSF1, thus promoting stress-induced HSF1 DNA binding ability and increased HSP expression [26]. The end result of the heat shock response is the upregulation of HSPs, thus promoting the cell's ability to cope with denaturing stress.

### **Domains of HSF1**

Similar to many eukaryotic TFs, HSF1 possesses a complex modular structure with several functional domains shown schematically in Figure 2.1a. These functional domains of HSF1 have been mapped by mutational analyses [281, 283-285]. Figure 2.1b represents the distribution of intrinsic disorder propensity within the human HSF1 sequence as estimated by two established disorder predictors, PONDR<sup>®</sup> VLXT (red line) and PONDR-FIT (black line). According to this analysis, more than a half of the protein is predicted to be disordered. In fact, only two of the HSF1 functional domains, DNA-binding domain (DBD, residues 15-120) and hydrophobic repeat HR-A/B domain (residues 130-203) are predicted to be ordered. Figure 1 also shows that the HR region C (which is located at the beginning of the transactivation domain (TAD), residues 384-409) is predicted to be partially ordered. These two domains are connected by a flexible

linker, and the remainder of the protein, including two important functional domains, the regulatory domain (RD, residues 221-310) and TAD (residues 371-529) and their linker, is mostly disordered.

### **DNA Binding Domain (DBD)**

The DBD is the most conserved domain of HSF1 from *Caenorhabditis elegans* to humans (Figure 2.4). Both the crystal structure of the DBD for *Kluyveromyces lactis* HSF and the solution structure of the DBDs for *K. lactis* and *D. melanogaster* HSF1 show that the DBD is a helix-turn-helix motif [49, 286, 287].

The helix-turn-helix structure contains 3 alpha helices, 4 beta strands, and an exposed loop. Upon trimerization, the DBD of each HSF1 monomer recognizes an inverted nGAAn repeat of the HSE [288]. The domains make contact with the major groove and with the DNA phosphate backbone by helix 3 of domain [50, 289]. Helix 3 is a region rich in positive charge and is the most conserved region of the DBD. Unlike other helix-turn-helix proteins, the loop in the HSF1 DBD does not bind DNA. Instead, the loop forms an interaction with the surface between adjacent HSF monomers [50].

The characteristic helix-turn-helix structure of the HSF1 DBD is shown in Figure 2.2a, b, and e representing both solution and crystal structures of DBDs from non-mammalian HSFs. Comparison of the crystal and NMR structures of *K. lactis* HSF (Figure 2.2b and c) revealed that DBD preserved the overall topology in solution. In fact, both structures contained a 4-stranded antiparallel beta-sheet and a 3-helix bundle [49, 286]. Seeing in the crystal structure an irregular segment defined as an  $\alpha$ -helical bulge in helix H2 was consistent with the NMR results. Furthermore, in the solution structure, the ill-defined loop connecting  $\beta$ -strands B3 and B4 was consistent with the results of the X-ray model, which showed larger B-factors in this region than in the rest of the structure, and the absence of electron density for residues 76-79 [49, 286]. These data are also consistent with the result of disorder prediction for the *K. lactis* HSF. In fact, Figure 2.2a clearly shows that the C-terminal part of the DBD is predicted to have significant amount of

intrinsically disordered residues. Comparison of Figure 2.2b, c, and e also shows that the overall structure of the DBD is conserved between *K. lactis* and *D. melanogaster*, but the DBD of the *D. melanogaster* HSF is bit less flexible in solution in comparison with the domain from *K. lactis*. Once again, this is consistent with the results of disorder predictions for these two domains, since according to Figure 2.2a and d, *D. melanogaster*'s DBD is expected to have less disorder propensity than its homologue from the yeast.

### **Trimerization Domains**

The HSF1 trimerization domain is composed of three arrays of hydrophobic heptad repeats (HR-A/B) [285]. HSF1 trimerization is unusual in that when the monomers come together, they form a leucine zipper, an artifact typically seen in dimerization. Trimerization is constitutive and is actively suppressed by the hydrophobic heptad repeat HR-C [290, 291]. When a mutation is introduced into the HR-C domain, trimerization and binding to the DNA is able to persist. *S. cerevisiae* and *K. lactis* HSFs have constitutive DNA-binding activity. In these HSFs, the HR-C is poorly conserved and does not actively suppress trimerization. Mutating the HR-C does not affect the oligomerization status of HSF in these organisms [292].

### **Transactivation Domains (TAD)**

Transcriptional elongation of *hsp* genes is regulated by the transactivation domains (TAD) of HSF1. In the absence of HSF1, RNA polymerase pauses at 46-49 bases downstream from the transcription start site even in the presence of excess free nucleotides [293]. The HSF1 transactivation domain can be divided into two distinct regions rich in hydrophobic and acidic residues: activation domain I and activation domain II, spanning amino acids 371-430 and 431-505, respectively [283, 294, 295]. These domains have been shown to equivalently stimulate both initiation and elongation of transcription [296]. This redundancy may be in effect due to the importance of heat shock proteins in maintaining protein homeostasis.

### **Regulatory Domain (RD)**

The regulatory activity of HSF1 is located between amino acids 221 and 310 and is functionally conserved between mammalian *hsf1* genes, but not between other members of the HSF family [283]. Upon non-stress conditions in which protein homeostasis is preserved, the transactivator activity of TAD I and TAD II is repressed by the regulatory domain and an exposure to stress leads to a reversal of this repression [283, 284]. The regulatory domain of HSF1 contains several serine residues that are responsive to protein kinases and lead to repression of the TADs upon phosphorylation. Phosphorylation by the MAP kinase ERK is responsible for this transactivator repression and mutation of these phosphorylation sites abolishes the suppression of the transactivation domains even in the absence of stress [297].

### **Conservation of HSF Across Different Species**

Figure 2.4 represents alignment of amino acid sequences of HSF from different species and clearly shows that the DBD and HR-A/B domains are highly conserved during evolution, whereas other functional domains of HSFs are much less conserved. Interestingly, two non-vertebrate HSFs possess long and poorly conserved N-terminal extensions. Figure 2.5 shows the conservation of the distribution of intrinsic disorder propensity in the HSF family. In agreement with sequence alignment data, Figure 2.5 shows that there is a great conservation of order propensity in the N-terminal parts of HSFs; i.e., in their DBDs and HR-A/B domains, with evolutionarily more advanced organisms typically showing very similar disorder patterns in this region Figure 2.5a and b. On the contrary, the C-terminal parts of these proteins generally do not show noticeable conservation except for the fact that all of them are predicted to be highly disordered. On the other hand, Figure 2.5c shows that the C-terminal fragments of these HSFs possessed relatively similar amino acid compositions, and also emphasizes that these regions, in general, have some features of typical disordered proteins, being depleted in major order-promoting residues and showing enrichment in major disorder-promoting residues.

## **Alternative Splicing of HSF1**

In mammalian cells, there are two distinct HSF1 mRNA isoforms that are produced via alternative splicing of the HSF1 pre-mRNA [298]. For example, in mouse, the two HSF1 mRNA isoforms differ by a single 66 bp exon of the HSF1 gene, which is present in the HSF1- $\alpha$  mRNA isoform but is skipped in the HSF1- $\beta$  mRNA isoform. The extra 22 amino acid sequence in the HSF1- $\alpha$  isoform is inserted immediately adjacent to a C-terminal leucine zipper motif [298]. The levels of the two HSF1 isoforms were shown to be regulated in a tissue dependent manner, with testis expressing higher levels of the HSF1- $\beta$  isoform, and with heart and brain expressing higher levels of the HSF1- $\alpha$  isoform [298]. In human, the shorter alternatively spliced isoform of HSF1 is different from the canonical isoform by lacking the last 40 residues and by in the shorter form and by changing the canonical residues GKQLVHYTAQPLFLDPPGSVDTGSNDLP<sub>462-489</sub> to the alternative sequence AGALHSAAVPAGPRLRGHREQRPAV<sub>462-489</sub>. Earlier, it has been pointed out that alternative splicing occurs mostly in regions of RNA that code for the disordered protein regions [299]. In agreement with these earlier findings, Figure 2.3 clearly shows that in both mouse and human HSF1 proteins, the regions affected by alternative splicing are predicted to be mostly disordered.

## **Post-Translational Modifications Regulate HSF1 Transcriptional Activity**

HSF1 is extensively modified by post-translational modifications including phosphorylation, sumoylation and acetylation (Figure 2.7). This extensive modification may form a code to allow fine-tuning of the activity of HSF1 to the precise needs of the cell.

### **Phosphorylation**

HSF is phosphorylated at several residues in order to promote or inhibit transactivation. HSF was first reported to display a reduction in electrophoretic mobility as a result of phosphorylation in *S. cerevisiae* [280]. Mammalian HSF1 also exhibits a similar electrophoretic shift due to

hyperphosphorylation upon activation of the heat shock response. Phosphorylation regulates transcriptional activity and not DNA binding, as some inducers of heat shock, such as the anti-inflammatory agent sodium salicylate, are capable of inducing HSF1 to bind to the DNA, but do not cause hyperphosphorylation [32]. Another example of the distinction between these two activities is observed in yeast. In *S. cerevisiae*, HSF exists as a trimer with constitutive DNA-binding activity. However, transcriptional activation only occurs in the presence of increased phosphorylation [280, 300, 301].

Through phosphoamino acid analyses and mass spectrometry, several phosphorylation sites within HSF1 have been mapped. While phosphorylation has been primarily mapped to serine residues, a low level of threonine phosphorylation has also been detected [34, 35, 297, 302, 303]. Of the first phosphorylation sites to be characterized are serine residues S303, S307, and S363 located within the C-terminal region of the regulatory domain. These sites are proline-directed and typically experience phosphorylation in the absence of stress. Upon stress, the repressive activity of these residues is superseded by the activation of HSF1 [34, 297, 304]. An HSF1 phosphorylation site that leads to transcriptional activation is serine residue 230, located within the N-terminal region of the regulatory domain [35]. Many sites within HSF1 can be phosphorylated, and a mass spectrometry analysis of HSF1 activated by heat shock found phosphorylation on Ser121, Ser230, Ser292, Ser303, Ser307, Ser314, Ser319, Ser326, Ser344, Ser363, Ser419, and Ser444 [41]. Phosphorylation of Ser326, but none of the other serine residues, was found to contribute significantly to activation of HSF1 upon stress in this study [41]. While the implications of HSF1 phosphorylation have yet to be fully characterized, it is clear that dynamic phosphorylation modulates HSF1 activity in both a positive and negative manner.

HSF1 phosphorylation is regulated by a number of kinases with several of the residues suspected to undergo modification by more than one kinase. MAP kinases have been shown to negatively regulate HSF1 activity and the HSF1 Serine residues S303, 307 and 363 have been found to be MAP kinase targets. The MAP kinase ERK1 has been shown to phosphorylate S307,

after which S303 is receptive to phosphorylation by glycogen synthase-3 kinase (GSK-3) [34, 297, 304]. The MAP kinase p38 has also been reported to phosphorylate S303 and/or S307, resulting in basal repression of HSF1 [305]. JNK, another MAP kinase family member, and the PKC isoforms alpha and zeta have been suggested to phosphorylate S363, there by contributing to the maintenance of HSF1 in an inert state [306, 307]. Inhibition has also been shown to occur through the phosphorylation of S121 by the proinflammatory protein kinase MK2, which may lead to an increase in affinity for Hsp90 [308]. Various kinases suspected of activating HSF1 have also been discovered. For instance, the Ca<sup>2+</sup>/calmodulin-dependent kinase II (CaMK II) phosphorylates S230 and promotes transcriptional activity [35]. Given the broad range of stimuli that induce the heat shock response and the vast number of HSF1 phosphorylation sites, it may be that different kinases regulate HSF1 depending on the nature of the stress. As an example, in yeast Snf1 protein kinase has been shown to regulate HSF1 in low glucose conditions, but does not phosphorylate HSF upon heat shock [309].

### **Sumoylation**

Upon stress, HSF1 is modified by SUMO-1 at the well-conserved lysine residue 298 within the N-terminal region of the regulatory domain [62]. In order for K298 to become sumoylated, S303 must first undergo phosphorylation, which has a repressive effect on HSF1 activation [62]. There may be a regulatory interplay of modifications at this residue as residue K298 is also an acetylation site [110].

### **Acetylation**

While the kinetics of phosphorylation and sumoylation are brought on rapidly upon stress, acetylation is delayed and coincides with a reduction of HSF1 DNA-binding activity at the decline of the heat shock response [26]. Acetylation of HSF1 by the histone acetyltransferase p300 occurs to attenuate HSF1 off of the DNA. The deacetylation of HSF1 is regulated by the NAD-

dependent deacetylase SIRT1. When SIRT1 is inhibited by siRNA, not only are the levels of heat shock-induced *hsp70* mRNA significantly decreased, but the ability of HSF1 to bind to the *hsp70* promoter region is also greatly reduced [26].

### **A Correlation Between intrinsic Disorder and Post Translational Modifications**

In the past, a correlation between intrinsic disorder and PTM sites was found. In fact, in a study of the functions associated with more than 100 long disordered regions, many were found to contain sites of protein posttranslational modifications (PTMs) [310, 311]. These PTMs included phosphorylation, acetylation, fatty acylation, methylation, glycosylation, ubiquitination, and ADP-ribosylation suggesting the possibility that protein modifications commonly occur in regions of disorder. A particular advantage of disorder for regulatory and signaling regions is that changes, such as protein modification, lead to large-scale disorder-to-order structural transitions: such large-scale structural changes are not subtle and so could be an advantage for signaling and regulation as compared to the much smaller changes that would be expected from the decoration of an ordered protein structure.

Protein phosphorylation and dephosphorylation are crucial for signaling. Indeed, about one-third of eukaryotic proteins are phosphorylated [312]. Many sites of protein phosphorylation were found to be in regions structurally characterized as intrinsically disordered [310, 311]. This conclusion was based on several lines of evidence, such as: very small number of PDB structures for both the un-phosphorylated and phosphorylated forms of the same protein [313, 314]; the fact that the residues of the phosphorylation site often have extended, irregular conformation consistent with disordered structure [314]; the fact that the segments containing phosphorylation site not only lack secondary structure but are held in place by side chain burial and also by backbone hydrogen bonds to the surrounding kinase side chains [315-320]; the fact that regions flanking the sites of phosphorylation are enriched in the disorder-promoting amino acids; [314] the fact that the sequence complexity distribution of the residues flanking phosphorylation sites



matches almost exactly the complexity distribution obtained for IDPs [314]. and the fact there is a high correspondence between the prediction of disorder and the occurrence of phosphorylation [314].

Ubiquitination, the reversible modification of proteins by the covalent attachment of ubiquitin, is implicated in the regulation of a variety of cellular processes and is involved in many diseases. Recently, 141 new ubiquitination sites were identified using a combination of liquid chromatography, mass spectrometry, and mutant yeast strains [321]. The detailed analysis of the sequence biases and structural preferences around known ubiquitination sites indicated that the properties of these sites were similar to those of IDPRs. In agreement with this computational study, structural information about the ubiquitination sites is sparse. In fact, despite the large size of PDB, only 7% of currently known ubiquitination sites in yeast could be confidently mapped to protein structures. The analysis of 3D structures of 32 homologous protein chains (with 15 of them being 100% identical with query proteins) containing 28 ubiquitination sites revealed that 10 ubiquitination sites were in crystal or interchain/intrachain contacts, and therefore the assignment of these sites to a specific structural element should be made with caution. Of the 18 sites that could be confidently assigned to ordered regions, 11 were located within coils (two of which were close to the observed disordered regions), four within helices, and three within strands. The majority of the sites within coils and helices were surface exposed and had high B-factor values indicating high flexibility [321]. The authors also pointed out that along with the lack of structural information for the majority of experimentally detected ubiquitination sites, there were several examples of ubiquitination sites located in the experimentally confirmed disordered regions [321]. Based on these observations it has been concluded that the involvement of flexible and disordered protein regions into various aspects of ubiquitination process provides a strong support for the functional importance of such regions. In addition to protease digestion, ubiquitination, and phosphorylation, several other types of PTMs, such as acetylation, fatty acid acylation, and methylation, have also been observed to occur in regions of intrinsic disorder [227, 311].

In agreement with all these earlier findings, Figure 2.1c shows that human HSF1 is not an exception and most of its experimentally verified PTM sites are located in the regions predicted to be disordered. From these findings, it is tempting to suggest that sites of protein modification in eukaryotic cells in general, and in HSF in particular, universally or at least very commonly exhibit a preference for intrinsically disordered regions. The likely explanation for this behavior is the fact that the modifying enzyme has to bind to and modify similar sites in a wide variety of proteins. If all the regions flanking these sites are disordered before binding to the modifying enzyme, it is easy to understand how a single enzyme could bind to and modify a wide variety of protein targets.

### **HSF1 as an Interaction Hub**

As expected for such an important and conserved transcription factor, HSF1 interacts with many molecules to allow it to carry out its diverse functions over the course of its activity cycle, including transcription factors, mRNA processing factors, molecular chaperones, and modifying enzymes. These interactions are transient and dynamic due to need for precise regulation under many stressful conditions.

During the resting state, chaperones including Hsp70 and Hsp90 contribute towards keeping HSF1 in an inactive state by preventing trimerization [27, 30, 53, 54]. Stress-induced activation of HSF1 may occur in part due to chaperones being titrated away from HSF1 by accumulating unfolded proteins, thus relieving the negative inhibition and allowing HSF1 to trimerize. In addition, heat actively promotes the trimerization of HSF1 through a heat-sensitive RNA called HSFR1 which has been proposed to act as a thermosensor [322]. Heat changes the conformation of HSFR1, and together with the translation elongation factor eEF1A, HSFR1 promotes the trimerization of HSF1 [322].

In order for HSF1 to be transcriptionally active, HSF1 must be hyperphosphorylated through transient interactions with the kinases described in the previous section.

Hyperphosphorylation may allow recruitment of basal transcription factors and coactivators required for transcription. HSF1 target promoters frequently contain a paused DNA polymerase that is poised to activate transcription rapidly upon stress. *D. melanogaster* HSF1 recruits elongation factors including pTEFb that allow release of the paused polymerase [323]. In addition, chromatin remodeling factors are recruited to target promoters by HSF1. The SWI/SNF chromatin-remodeling complex interacts with the activation domain of human HSF1, mediating the chromatin architecture changes required for proper Pol II elongation [324, 325]. *D. melanogaster* HSF1 also recruits the Mediator complex and the FACT complex to facilitate chromatin remodeling and promote transcription [326, 327]. Human HSF1 has been shown to interact with coactivators such as activating signal co-integrator 2 (ASC-2) to activate transcription on specific target promoters [328]. Interestingly, HSF1 is also linked to the recruitment of mRNA processing factors as evidenced by the binding of symplekin to human HSF1 [329]. Inhibition of this interaction inhibits *hsp70* mRNA polyadenylation, suggesting that HSF1 is involved in cotranscriptional mRNA processing.

During the attenuation phase, HSF1 is under negative control by its own targets including Hsp70 and Hsp90. Hsp70 and its cochaperone Hdj1/Hsp40 bind to the activation domain of HSF1 trimers and interfere with its function [27, 54, 330]. HSF1 trimers also interact with the Hsp90-immunophilin (FKBP52)-p23 complex, resulting in a loss of transcriptional activity [331]. Additionally, acetylation of HSF1 at a conserved lysine residue within the DNA binding domain promotes this phase [26]. HSF1 can be acetylated by p300 and deacetylated by SIRT1 [26], so interactions with these factors have important implications in the regulation of the heat shock response. The unstructured regions of HSF1 likely facilitate the multitude of interactions and modifications that HSF1 participates in.

## Other Heat Shock Transcription Family Members

The mammalian HSF family is composed of HSF1, 2, 3, 4, 5, Y and X [332]. While there is some redundancy, the HSF family members maintain different functionalities. Mammalian HSF1 is the ortholog of the single, essential HSF that is present in *S. cerevisiae* and *D. melanogaster*. HSF1 is the best characterized member of the HSF family and the factor responsible for the heat shock response. HSF2 and HSF4, on the other hand, have various roles in development and differentiation [333]. Mammalian HSF3, 5, Y and X have not yet been well-characterized.

### HSF2

HSF2 has been shown to recruit to satellite III repeats in nuclear stress bodies (NSBs) along with HSF1 [334]. At this colocalization site, HSF2 has been indicated to play a role in the heat shock response by modulating HSF1 in a heterocomplex formation [335]. HSF2 was originally discovered in tandem with HSF1 and similarly was shown to stimulate HSE-dependent transcription *in vitro* [336, 337]. While HSF2 is capable of inducing the transcription of heat shock proteins, it is not activated by heat and therefore has not been associated with the induction of the heat shock response [337, 338]. However, HSF2 has been shown to be involved in development and cellular differentiation [338-342].

Despite low amino acid sequence homology between HSF1 and HSF2, the DNA binding domain, as well as the N-terminal and C-terminal trimerization domains, are conserved. Figure 2.6a represents the distribution of disorder propensity within the human HSF2 sequence evaluated by PONDR® VLXT (red line) and PONDR-FIT (black line). Similar to human HSF1, more than a half of HSF2 is predicted to be disordered. Similar to HSF1, HSF2 possesses several ordered functional domains, DBD (residues 7-112), HR-A/B domain (residues 119-192), and HR-C (residues 360-385). The remainder of HSF2 is mostly disordered. Figure 2.6b compares PONDR® VLXT predictions for HSF2 (red line) and HFS1 (blue line) and shows that despite

relatively low sequence homology, these two proteins possess remarkably similar disorder profiles. However, the manner of DNA-binding differs between the two proteins. HSF2 appears to regulate a different set of target genes compared to HSF1 and also experiences variable expression patterns in different tissues and cell types [338, 342]. The DNA binding-specificity of HSF1 is determined by the loop within the DNA binding domain. Chimeric HSF2 containing the HSF1 DBD loop is capable of binding to HSF1 target genes upon heat shock stress [343]. In addition, the transactivation activity of HSF2 is considerably weaker than HSF1, possibly as a result of a dispersed AD [344]. As mentioned previously, in addition to the role of HSF2 in development, evidence has indicated that HSF2 may act as a modulator of HSF1 transcription. While HSF2 has not been shown to directly regulate the heat shock response, HSF2 has been shown to interact with HSF1, is recruited to nuclear stress bodies along with HSF1, and has been shown to stimulate HSF1-mediated transcription upon heat shock stress [345].

#### **HSF4**

HSF4 exhibits limited sequence homology to the other HSF family members, but regions of similarity correspond to the DNA binding domain and the N-terminal hydrophobic repeats (HR-A/B). Like other HSF family members, HSF4 is able to bind to HSEs. However, when HSF4 is co-transfected into Cos7 cells along with a transcriptional HSE-reporter construct, HSF4 is unable to induce transcription and is therefore not a typical activator for the transcription of *hsp* genes [346]. In addition, HSF4 lacks the *cis*-regulatory domain that represses HSF1 under non-stress conditions [283].

HSF4 has also been shown to exhibit crosstalk with HSF1. Together, HSF1 and HSF4 are involved in the maintenance of sensory organs and are critical during lens development [179]. HSF4 expression is specific to the brain and lungs and has been indicated to play a role in lens development and quality control [347, 348]. Mutations of HSF4 have been shown to lead to cataractogenesis and the breakdown of the lens microarchitecture [349, 350]. Two HSF4

missense mutations have been identified by screening age-related cataract patients [351]. These mutations appear to have an effect on HSF4 DNA-binding to HSEs resulting in an under-expression of heat shock proteins in the lens, which consequently lead to an increase in protein aggregates that cause cataracts.

### **HSF3, 5, X and Y**

HSF3 was first identified in chicken, where it is the HSF that is essential for activation of the heat shock response in this species [352]. Mammalian HSF3 has only recently been identified in mouse, and is capable of activating non-classical heat-shock genes during heat shock by binding to the PDZ domain-containing 3 (Pdzk3) promoter [175]. Although sequences related to HSF3 have also been found in the orthologous region of the human genome, this sequence is thought to be a pseudogene as no transcripts corresponding to this gene have been found [332].

HSF5 has recently been discovered as part of a large gene characterization project [180] and has been identified as a potential transcription factor within the HSF family, but has not undergone characterization. HSFY and HSFX are the only members of the HSF family found on the sex chromosomes. HSFY is present on the Y chromosome as well as murine chromosome 2. It is predominantly expressed in the testes and may potentially have a role in spermatogenesis [181-183]. Even less has been characterized regarding HSFX, but both HSFs have been found to exist as two identical copies [183].

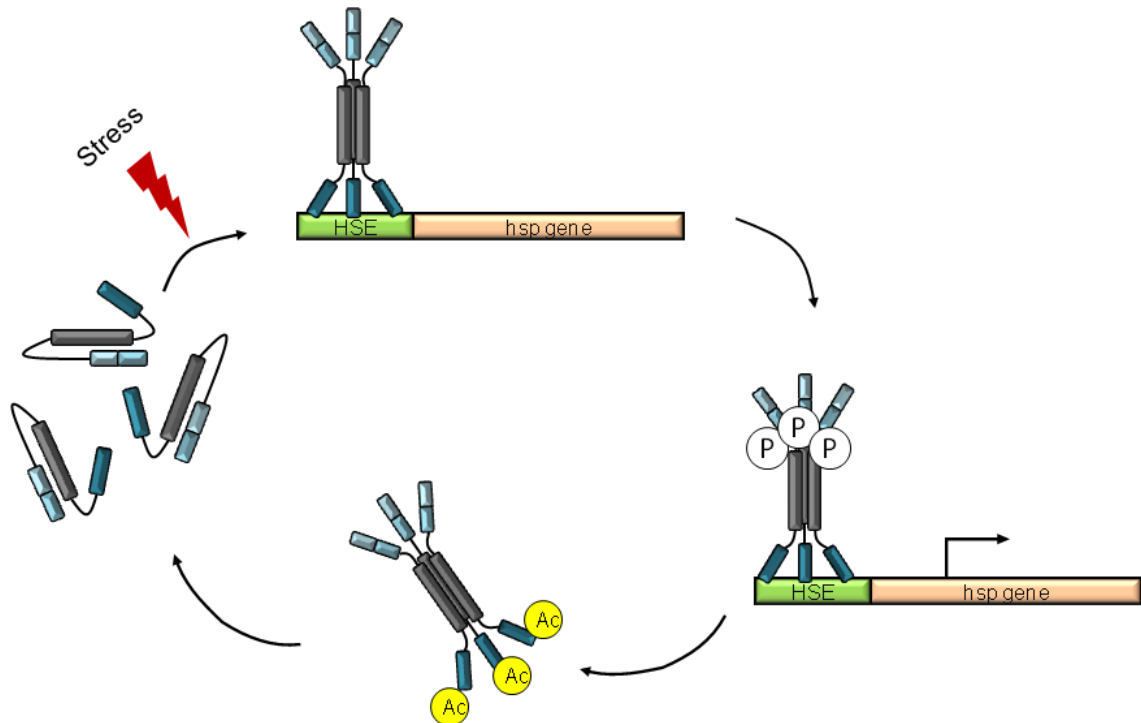


**Figure 2.1. The HSF1 Activity Cycle.** HSF1 in unstressed cells is a monomer in both the cytoplasm and nucleus. Following heat shock, HSF1 accumulates in the nucleus in a trimeric form and is capable of binding to heat shock elements (HSE). Transcriptional activity requires hyperphosphorylation of HSF1 by various kinases. Attenuation of the cycle involves negative feedback by chaperones as well as acetylation of a conserved lysine within the DNA binding domain. P and Ac reflects the hyperphosphorylation and acetylation sites.

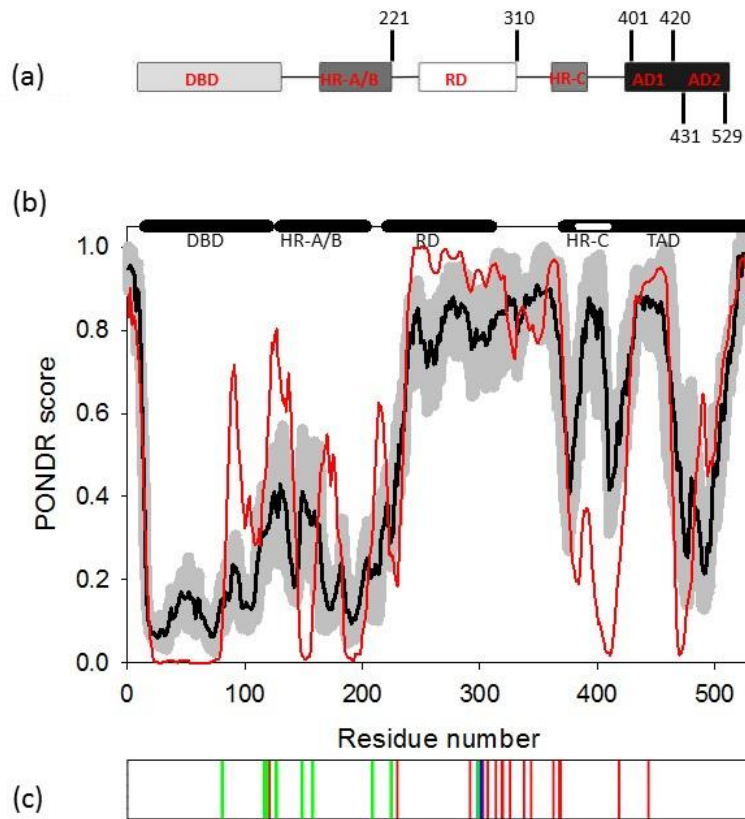


**Figure 2.2. Structural Characterization of Human HSF1.** (a) Domain structure of human HSF1. (b) Intrinsic disorder propensity evaluated by PONDRL® VLXT (red line) and PONDRL-FIT (black line). Gray shadow represents standard errors of disorder prediction by PONDRL-FIT. Thick bars on the top of this plot represent localization of the major domains. PONDR scores above 0.5 correspond to predicted disordered residues. (c) Localization of PTM sites within the human HSF1 sequence. Phosphorylation, acetylation and SUMOylation sites are shown by red, green and blue bars, respectively. DBD, HR-A/B, RD, HR-C, AD1, and AD2 correspond to the DNA-binding domain, hydrophobic heptad repeat regions A/B, regulatory domain, hydrophobic heptad repeat region C, activation domain 1 and activation domain 2, respectively.



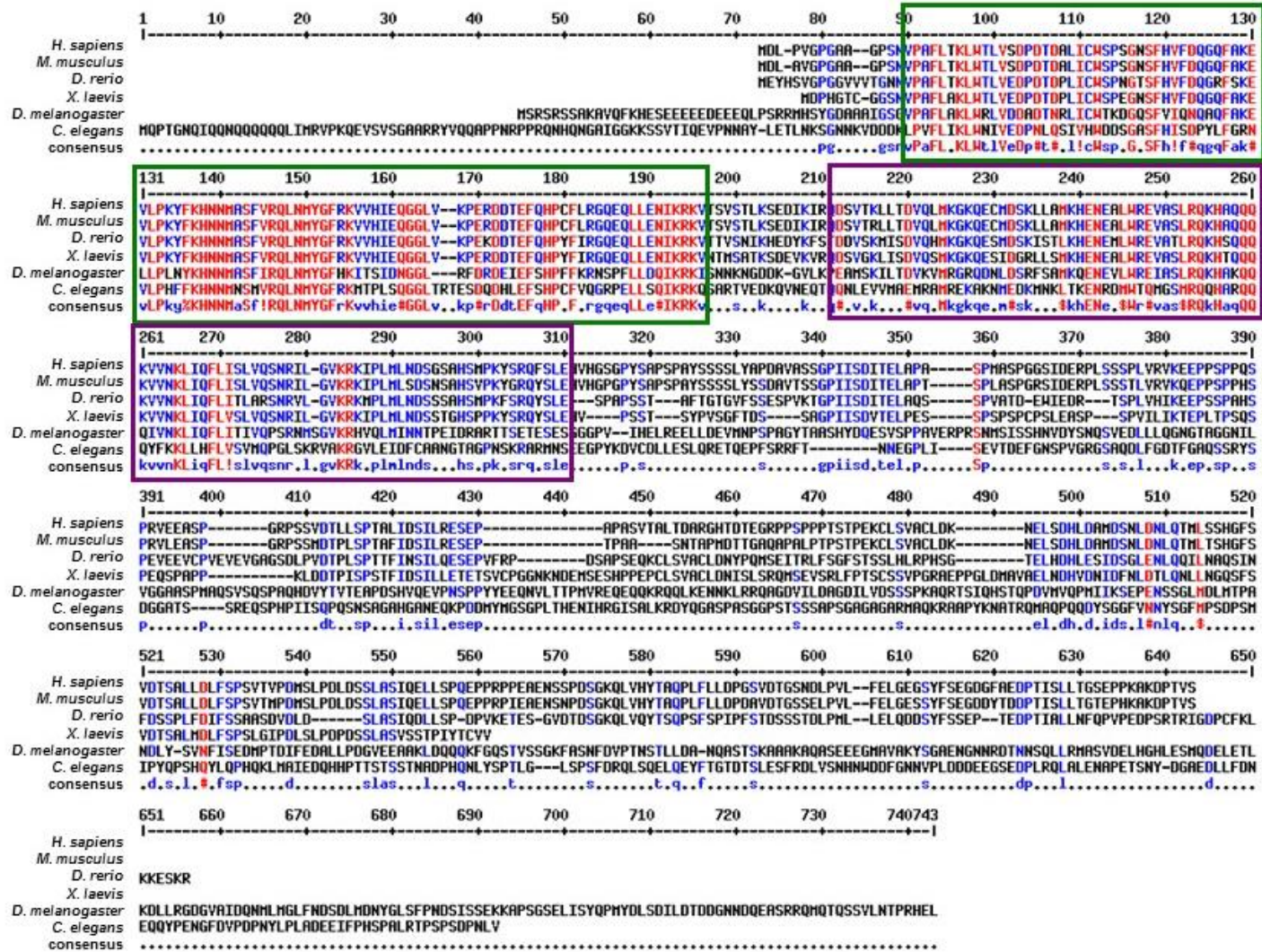
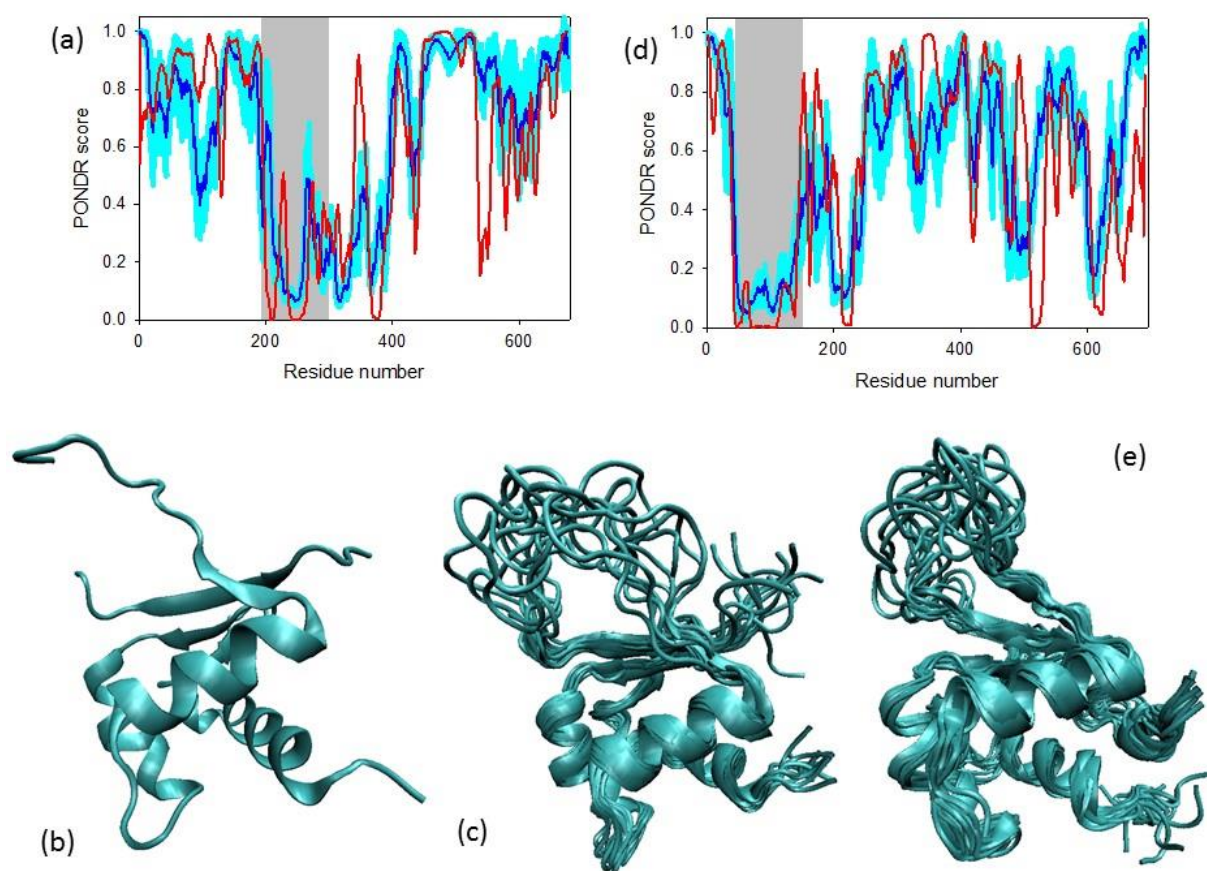
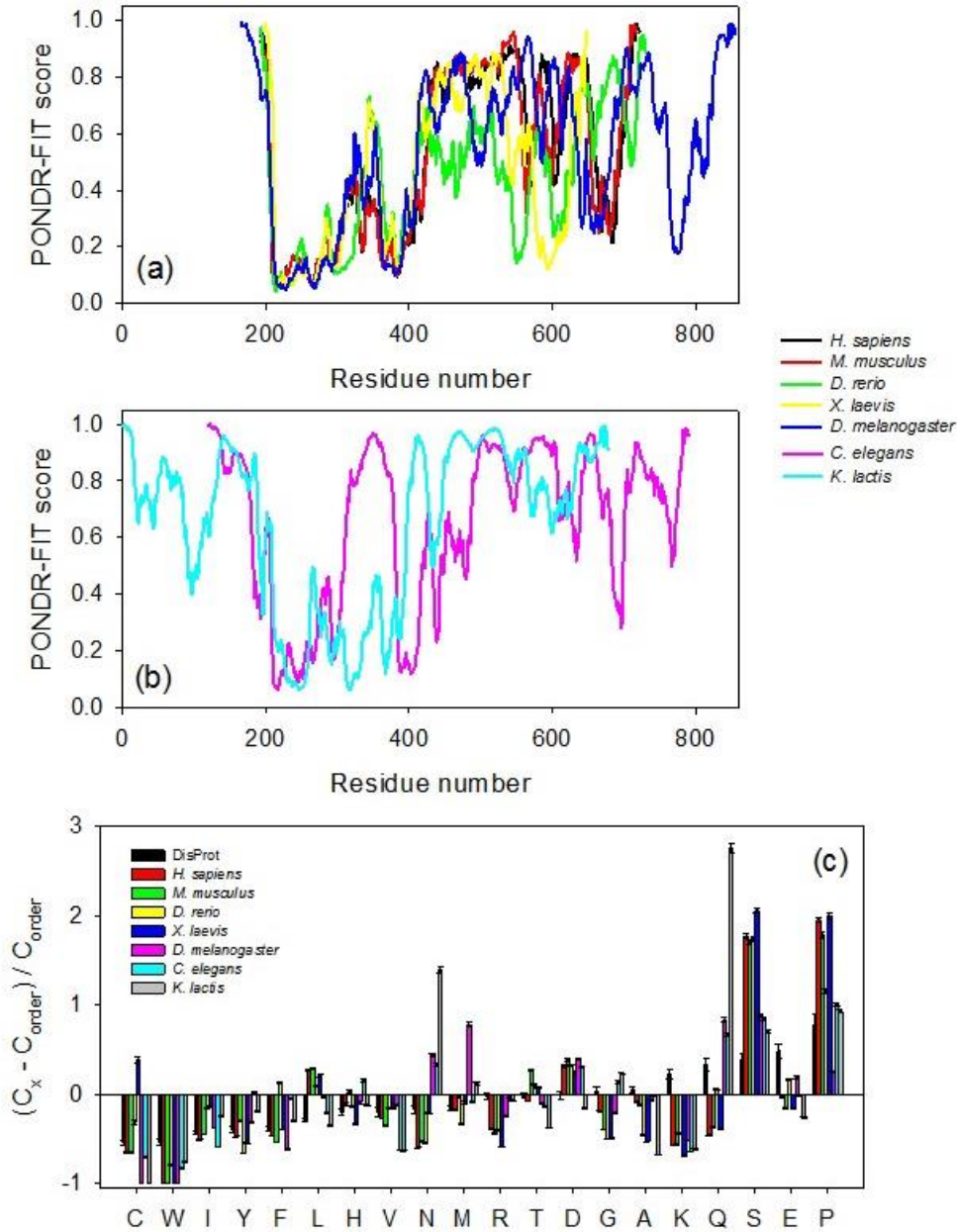


Figure 2.3. Sequence Alignment of HSF1s from Different Organisms Using BLAST. Green and violet rectangles correspond to the DBD and HRA/B, respectively.



**Figure 2.4. Structural Characterization of the DBDs from *Kluyveromyces lactis* (plots (a), (b) and (c)) and from *Drosophila melanogaster* (plots (d) and (e)).** (a) and (d) Intrinsic disorder propensity evaluated by PONDOR@ VLXT (red lines) [190, 191] and PONDOR-FIT (blue lines) [192]. Cyan shadow represents standard errors of disorder prediction by PONDOR-FIT. DBDs are shown as shaded gray areas. (b) and (c) Crystal and solution structures of DBD of the *K. lactis* HSF, respectively. (e) Solution structure of the *D. melanogaster* HSF1 DBD.



**Figure 2.5. Conservation of Intrinsic Disorder in HSFs from Different Species.** (a) PONDR-FIT plots for the evolutionary more-advanced organisms. (b) PONDR-FIT profiles of the evolutionary less-advanced organisms. (c) Compositional profiling of the C-terminal fragments of HSFs. The bar for a given amino acid represents the fractional difference in composition between a given protein and a set of ordered proteins. The fractional difference is calculated as  $(C_x - C_{order}) / C_{order}$ , where  $C_x$  is the content of a given amino acid in a given protein, and  $C_{order}$  is the corresponding content in a set of ordered reference proteins and plotted for each amino acid [14, 193]. The amino acid residues are arranged according to the abundance of residues in a set of well-characterized IDPs from the DisProt database [194, 195]. Negative values indicate residues that a given protein has less than the reference set, positive values correspond to residues that are more abundant in a given protein in comparison with the reference set.

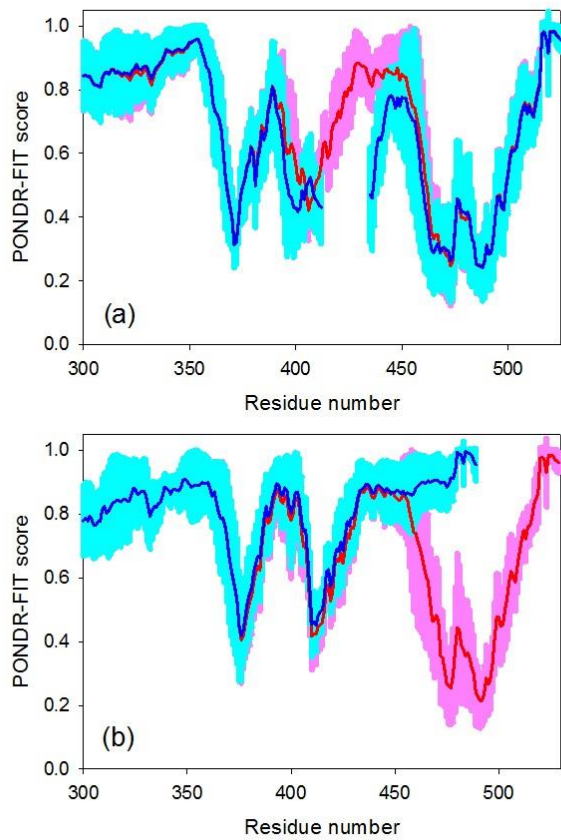


**Figure 2.6. Effect of Alternative Splicing on Disorder Profiles of the C-terminal Regions of Mouse (a) and Human (b) HSF1 Proteins.** Propensity for intrinsic disorder was evaluated by POND-R-FIT for canonical (red) and short (blue) isoforms of these proteins. Standard errors of disorder predictions for long and short forms are shown as red and cyan shadows, respectively.

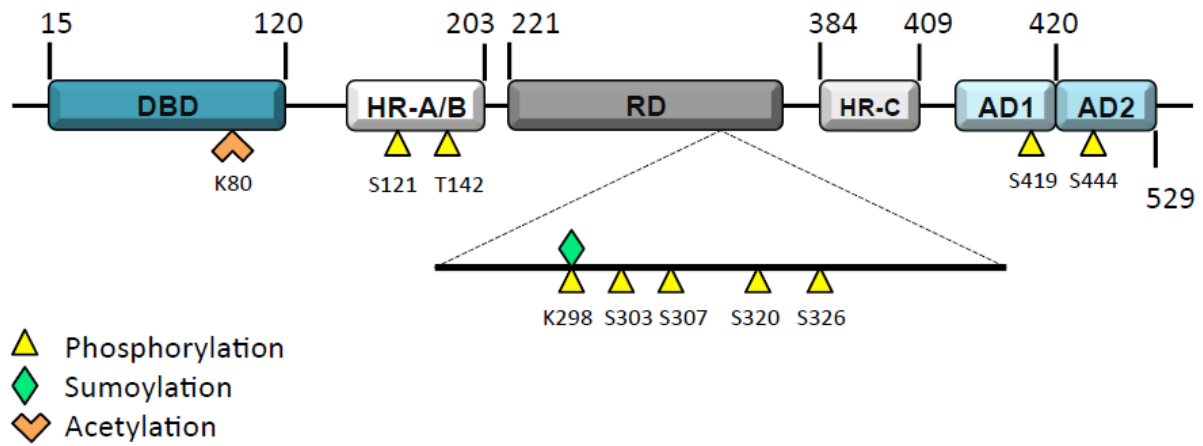


**Figure 2.7. Post-Translational Modification Sites for HSF1.** In addition to these sites, additional phosphorylation sites include serine residues 97, 230, 292, 314, 319, 344, and 363 [137]. While K80 is a critical lysine residue that when acetylated will cause a loss of affinity for DNA, other uncharacterized sites for acetylation include lysine residues 116, 118, 126, 148, 157, 208, 224, and 298 [110].

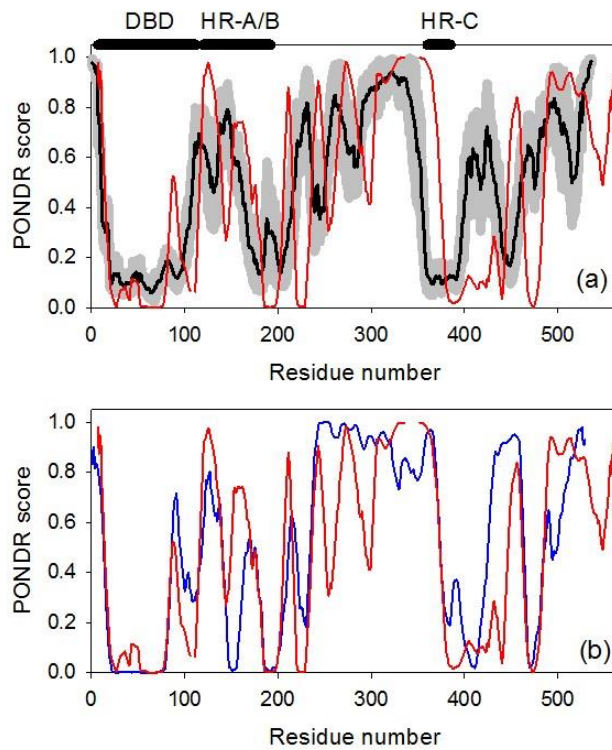


**Figure 2.8. Evaluating the Intrinsic Disorder Propensity of Human HSF2.** (a) Per residue intrinsic disorder propensities evaluated by PONDNR@ VLXT (red line) and PONDNR-FIT (black line). Gray shadow represents standard errors of disorder prediction by PONDNR-FIT. Thick bars on the top of this plot represent localization of the major domains. (b) Conservation of intrinsic disorder in human HSF2 (red line) and HSF1 (blue line) as evaluated by PONDNR@ VLXT.

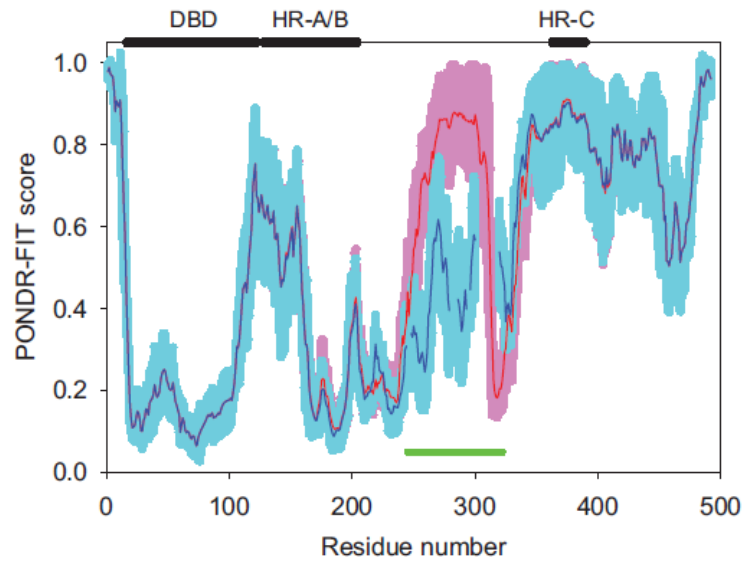


**Figure 2.9. Evaluating Disorder Propensity Distribution in Human HSF4 by POND-R-FIT for Canonical (red) and Alternatively Spliced Isoforms (blue).** Standard errors of disorder predictions for long and short forms are shown as red and cyan shadows, respectively.

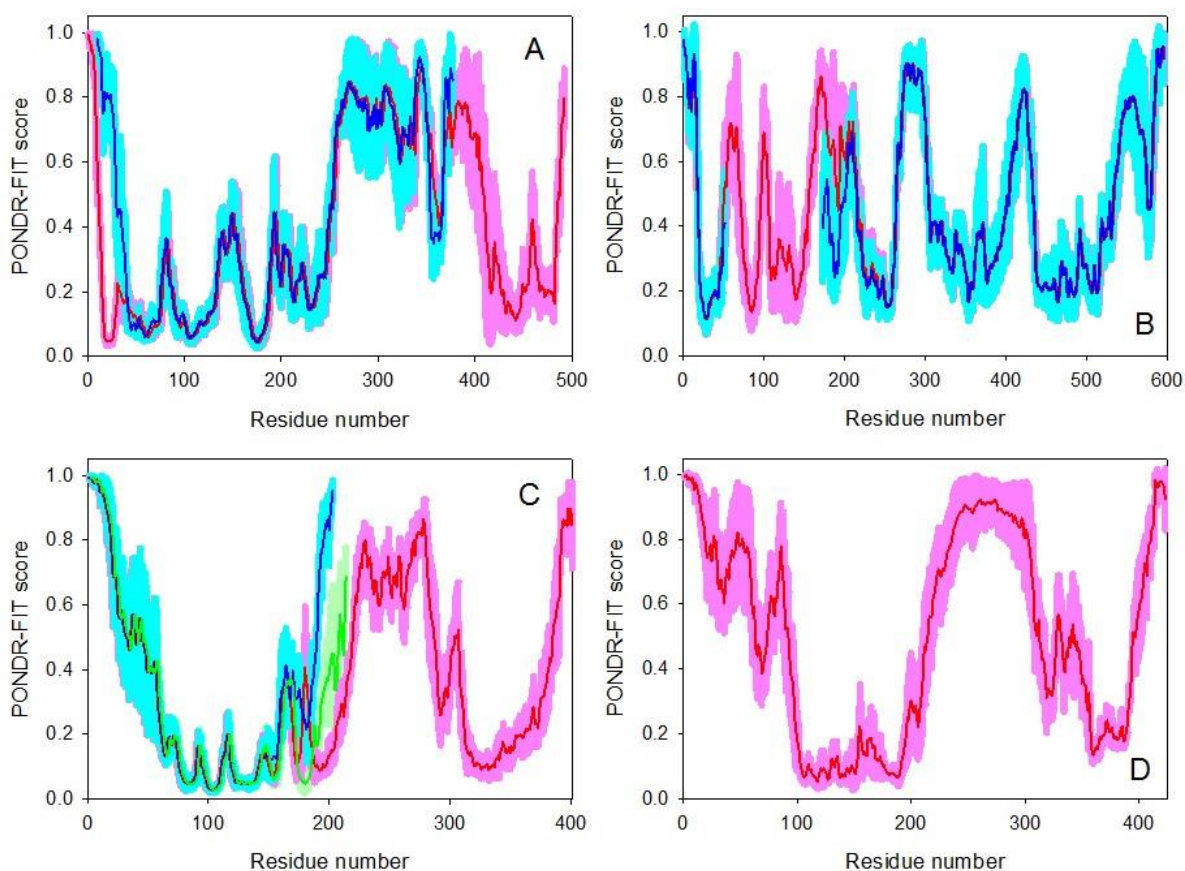


**Figure 2.10. Evaluating the Intrinsic Disorder Propensity of Human HSF3 (a), HSF5 (b), HSFY (c) and HSFX (d).** Propensity for intrinsic disorder was evaluated by PONDR-FIT for canonical (red) and short (blue) isoforms of these proteins. Alternatively spliced isoforms of HSFX were not described as of yet, whereas HSFY has two short alternatively spliced isoforms (shown by blue and green lines in plot (c)). Standard errors of disorder predictions for long and short forms are shown as red and cyan (and light green) shadows, respectively.



**CHAPTER THREE: THE HEAT SHOCK TRANSCRIPTION FACTOR HSF1 INDUCES  
OVARIAN CANCER EPITHELIAL-MESENCHYMAL TRANSITION IN A 3D SPHEROID  
GROWTH MODEL**

Authored by Chase D. Powell, Trillitye Paullin, Candice Aoisa, Christopher Menzie, Ashley Ubaldini, and Sandy D. Westerheide

Published in *PLoS One*. 2016 Dec 20;11(12):e0168389. doi: 10.1371/journal.pone.0168389.

Experimental design created by C. Powell. All experiments and analysis, with the exception of qRT-PCR, were performed by C. Powell with the assistance of A. Ubaldini. T. Paullin, C. Aoisa and C Menzie performed and analyzed qRT-PCR experiment. The manuscript was written by S. Westerheide, C. Powell, and T. Paullin. See appendix D for copyright permissions.

**Abstract**

Ovarian cancer is the most lethal gynecological cancer, with over 200,000 women diagnosed each year and over half of those cases leading to death. The proteotoxic stress-responsive transcription factor HSF1 is frequently overexpressed in a variety of cancers and is vital to cellular proliferation and invasion in some cancers. Upon analysis of various patient data sets, we find that HSF1 is frequently overexpressed in ovarian tumor samples. In order to determine the role of HSF1 in ovarian cancer, inducible HSF1 knockdown cell lines were created. Knockdown of HSF1 in SKOV3 and HEY ovarian cancer cell lines attenuates the epithelial-to-mesenchymal transition (EMT) in cells treated with TGF $\beta$ , as determined by western blot and

quantitative RT-PCR analysis of multiple EMT markers. To further explore the role of HSF1 in ovarian cancer EMT, we cultured multicellular spheroids in a non-adherent environment to simulate early avascular tumors. In the spheroid model, cells more readily undergo EMT; however, EMT inhibition by HSF1 becomes more pronounced in the spheroid model. These findings suggest that HSF1 is important in the ovarian cancer TGF $\beta$  response and in EMT.

## **Introduction**

Ovarian cancer is the number one cause of death related to gynecological malignancies [353]. This is partially due to a lack of physical symptoms during early cancer stages as well as shortcomings in screening techniques. In fact, a majority of newly diagnosed ovarian cancer cases present with stage III and IV disease [354]. Recent advances in surgery and chemotherapy treatment have led to improvement in short-term survival of ovarian cancer patients, however long-term survival remains bleak [355]. Conventional chemotherapy agents used to treat ovarian cancer include platinum and taxol-based drugs. While these agents are largely effective upon initial treatment, the patient commonly develops resistance to the drugs, yielding them inefficient should the patient relapse [356]. In addition, agents such as cisplatin can be toxic to the patient's organs, such as the kidneys and gastrointestinal tract, indicating a need for more efficient, as well as safer, treatment options [357].

The heat shock response (HSR), driven by the heat shock transcription factor HSF1, is a cytoprotective response to proteotoxic stressors, including heat shock, that results in the induction of various genes including molecular chaperones essential for recovery from cellular damage [278]. Chaperones function to guide protein folding and protect cells against proteotoxic stress [84]. The HSR is regulated at the transcriptional level by the heat shock transcription factor 1 (HSF1) [278].

Multiple lines of evidence suggest that HSF1 is important in promoting tumorigenesis. For instance, studies in HSF1 null mice show they are refractory to chemically-induced tumors, and HSF1  $-/-$  mouse embryonic fibroblasts resist oncogene-induced transformation [136]. In cancer, HSF1 controls many genes that may support the transformed phenotype, including genes involved in cell-cycle regulation, signaling, metabolism, adhesion and translation [133]. HSF1 is elevated in breast, colon, lung and hepatocellular cancers, and activated or elevated HSF1 often couples with poor cancer prognosis [129, 133].

The dissemination of primary tumors occurs through a multi-step process called the epithelial-to-mesenchymal transition (EMT). EMT consists of detachment of primary tumor cells, infiltration of local stroma, spread through cavities or vascular and lymphatic vessels, and adhesion followed by colonization at distant sites [358]. Sweeping changes are made in the cytoskeleton and extracellular matrix during EMT, and cells develop a spindle-like morphology. TGF $\beta$  inhibits proliferation in normal tissues, but this effect is lost in advanced cancer where it strongly promotes EMT [359]. The expression of a number of transcription factors are induced by TGF $\beta$  and support the EMT process, including SNAI2/SLUG, SNAI1/SNAIL, TWIST1 and ZEB1 [358]. Once the mesenchymal-like cell has migrated into a new organ, it can then undergo the reverse mesenchymal-to-epithelial transition (MET) and begin to form a secondary tumor [360].

Here, we have established two ovarian cancer inducible HSF1 knockdown cell lines to study the effect of HSF1 on ovarian cancer. We show that HSF1 knockdown inhibits colony formation, wound healing, migration and the induction of FN1/fibronectin, a protein important in the EMT process. We also show that the induction of EMT markers by TGF $\beta$  is enhanced when cells are grown as 3D spheroid cultures vs. 2D monolayer cultures. Upon 3D culturing, there is a marked effect of HSF1 on the induction of transcription factors known to promote EMT. HSF1 knockdown also alters spheroid morphology. Thus, we conclude that HSF1 plays a striking role in regulating the EMT process under 3D growth conditions.

## **Materials and Methods**

### **HSF1 Copy Number, Expression Determination and Survival Analysis**

Data comparing HSF1 copy number across multiple cancers with GISTIC analysis was obtained from The Cancer Genome Atlas (TCGA) via the cBio portal [361, 362]. HSF1 expression levels across multiple cancers were assessed from TCGA RNA seq V2 data via the cBio portal. Data for the comparison of ovarian cancer and normal ovarian tissue were obtained from GEO and the TCGA. The datasets analyzed were: GSE18520, consisting of 10 normal ovary and 53 ovarian cancer samples assayed on Affymetrix HG-U133 Plus 2.0 GeneChips, and TCGA data, consisting of 8 normal ovary and 568 ovarian cancer samples assayed on Affymetrix HG-U133A GeneChips. Gene intensity was compared by one-sided unpaired T-test.

### **Cell Culture and Treatments**

HEY, SKOV3 and T80 cells were authenticated using short tandem repeat (STR) DNA profiling (Genetica, Inc.) and comparing profiles to ATCC profiles and other previously published profiles [363]. Cells were cultured in RPMI 1640 medium supplemented with 10% fetal bovine serum (GIBCO) and 1% Pen-Strep-Glutamine (CellGro) in a humidified incubator at 37°C with 5% CO<sub>2</sub>. Heat shock treatment was performed by wrapping plates in parafilm and submerging them in a 42°C circulating water bath for designated times. Cells were treated as indicated with 1 µg/ml doxycycline (Sigma-Aldrich) and 5 ng/mL TGFβ1 (Thermo Fisher).

## **Lentiviral Creation and Infection for Stable, Inducible shRNA-mediated HSF1 Knockdown**

To allow for inducible knockdown of HSF1, we utilized the doxycycline-inducible TRIPZ shRNAmir system (Thermo Scientific). Two shRNA sequences targeting HSF1 were obtained from the RNAi codex database [364]: CGCAGCTCCTTGAGAACATCAA (shHSF1A) and CCCACAGAGATACACAGATATA (shHSF1B). These two sequences were cloned into the pTRIPZ vector. For lentiviral packaging, a 2<sup>nd</sup> generation lentiviral system was used with the pCGP packaging and pVSVG envelope plasmids (Addgene). HEK293T cells, cultured in RPMI medium, were used as the packaging cell line. Transfection was achieved using Polyfect Transfection Reagent (Qiagen) according to the manufacturer's protocol using a 1:1:1 ratio of lentiviral vectors. 24 hours post-transfection, medium with transfection reagent was removed and replaced with fresh RPMI. Medium containing viral stock from the HEK293T cells was harvested 48 hours post-transfection. A 0.45 micron PVDF filter was used to filter viral stock and infection of the HEY and SKOV3 cell lines was performed in a single round with the addition of 8 µg/mL of hexadimethrinebromide (Sigma-Aldrich). Selection of stable HEY and SKOV3 cells was achieved with 1 µg/ml and 0.5 µg/ml of puromycin (Thermo Fisher) for the HEY and SKOV3 cell lines, respectively. Infection was verified via immunoblotting analysis for knockdown of HSF1 after doxycycline-induced expression of the shRNAs.

## **Protein Isolation, SDS-PAGE, and Western Analysis**

Cells were washed once and scraped in chilled PBS. After pelleting the cells, protein was extracted using the M-PER lysis buffer (Thermo Scientific) with a protease inhibitor cocktail (Halt™ Protease Inhibitors, Thermo Scientific). A Bio-Rad Protein Assay was then utilized to quantify protein concentrations. 20 µg of lysate was resolved on 8% to 12% sodium dodecyl sulphate

polyacrylamide gel electrophoresis (SDS-PAGE) gels and transferred to Immun-Blot® 0.2µm PVDF Membrane with a Trans-Blot semi-dry transfer cell (Bio-Rad). Membranes were blocked in 2% w/v non-fat milk in TBS with 0.1% Tween (TBST milk). Blots were probed with primary and secondary antibodies before incubation in ECL Prime Western Blotting Detection System (Amersham™) and film exposure. Primary antibodies used were: HSF1 (Assay Designs), HSF1 P-S326 (Abcam) fibronectin (BD Biosciences), HSP90 (Cell Signaling), HSP70 (Cell Signaling) and Actin (Santa Cruz). HRP-conjugated secondary antibodies were from Millipore and Jackson ImmunoResearch.

### **Cell Viability Assay**

Cells at a concentration of  $2 \times 10^5$  cells/ml were seeded in a 96-well plate at 100 µl per well with eight replicates for each test condition. The cells were then incubated either with or without doxycycline treatment for 72 hours. After incubation, 10 µl of PrestoBlue® Cell Viability Reagent (Invitrogen) was added to each well and incubated for 1 hour at 37°C. The reduction of the reagent was measured by fluorescence (excitation 570 nm, emission 600 nm) using a microplate reader (BioTek®). Mean percent viability and standard error were then plotted.

### **Clonogenic Assay**

Cells were seeded at 500 cells per well in 6-well plates and were treated with or without 1 µg/ml doxycycline to induce HSF1 knockdown. Treated wells were given an additional treatment with 1 µg/ml doxycycline on day 4 to maintain doxycycline levels. After 8 days, colonies were stained with 1% crystal violet (w/v) in methanol and rinsed 3X in deionized water. Stained colonies were subsequently photographed and counted.

### **Wound Healing Assay**

Cells were plated at  $3 \times 10^5$  cells per well in a 6-well plate, and then either treated with 1  $\mu\text{g/ml}$  doxycycline 48 hours prior to the assay or left untreated. Once the cells reached confluency, a 2  $\mu\text{l}$  pipet tip was used to scrape the cells in 2 vertical and 2 horizontal lines yielding 4 intersections per well. Cells were washed twice with PBS to remove debris and serum-free medium was added. Pictures were taken immediately and again 12 hours after the creation of the wound, using an EVOS inverted microscope (Advanced Microscopy Group). The experiment was performed in triplicate and wound closure was determined using TScratch software [365]. Significant differences were calculated by ANOVA and Bonferroni post-hoc tests.

### **Cell Migration**

For the transwell migration assay, cells were treated with or without 1  $\mu\text{g/ml}$  doxycycline 48 hours prior to the assay to induce HSF1 knockdown, and cells were then serum-starved 24 hours before performing the assay. Cells were then resuspended in serum-free medium, and seeded at  $2.5 \times 10^4$  cells per upper chamber. 400  $\mu\text{L}$  of complete medium containing FBS was added as a chemoattractant to the lower chamber. After a 16-hour incubation, non-migrating cells on the upper surface of the filter were removed by scrubbing with a cotton swab. The remaining cells on the lower surface were fixed and stained with 1% (w/v) crystal violet in methanol. Migrated cells were counted from 10 random fields of view from each well and each condition was performed with triplicate samples. Statistical analysis done by paired t-test.

### **Spheroid Formation**

The hanging drop method was utilized to form spheroids [366]. Briefly, cells released with trypsin were resuspended at  $1 \times 10^6$  cells/mL in RPMI medium, supplemented as described

above. Cell suspension droplets of 25  $\mu$ l were placed on the plate lids, which were then inverted and put back on plates containing phosphate buffered saline (PBS) and incubated for 48 hours. Upon incubation, cells aggregated into spheroids. Prior to plating the cells, TGF $\beta$ 1 was added to the suspension as indicated at a final concentration of 5 ng/mL. Following aggregation for 48 hours, spheroids were collected in 1X PBS. Pictures were obtained using an EVOS (Advanced Microscopy Group) inverted microscope.

### **Quantitative RT-PCR**

Cells were harvested in cold 1X PBS and RNA extraction was completed utilizing the TRIzol reagent (Thermo Fisher) according to standard protocol. Reverse transcription reactions of the RNA were performed with the High Capacity cDNA Reverse Transcription Kit (Applied Biosystem), as per the manufacturer's protocol. The cDNA samples were then used as a template for qRT-PCR. Applied Biosystem's Step One Plus Real-time PCR machine was used with BioRad's iTaq<sup>TM</sup> Fast SYBR<sup>®</sup> Green Supermix with ROX according to the manufacturer's protocol. The primer sets used for each gene can be found in Supplementary Table 1. GAPDH was used as the endogenous reference control. Statistical significance was measured by Student's T-test.

## **Results**

### **HSF1 is Overexpressed in Ovarian Cancer**

We analyzed data from The Cancer Genome Atlas (TCGA) database to compare HSF1 levels across multiple cancer types. Interestingly, we find that HSF1 gene duplication is more common in ovarian cancer than in any other cancer type in this database by a large margin (Fig. 3.1A). Additionally, we find that HSF1 mRNA transcripts are elevated in ovarian cancer tumor



tissue vs. normal epithelial tissue from matched patient samples (Fig. 3.1B). Other cancers with high HSF1 mRNA levels include liver cancer, head and neck cancer, and breast cancer (Fig. 3.1B). Two distinct data sets of matched ovarian tumor tissue vs. normal tissue show that HSF1 mRNA expression is significantly higher in tumor tissue (Fig. 3.1C-D). Given this data, we postulate that HSF1 may drive ovarian cancer progression. We thus sought to study the effect of HSF1 knockdown in ovarian cancer cell lines.

### **Establishment of SKOV3 and HEY Inducible HSF1 Knockdown Ovarian Cancer Cell Lines**

We chose two epithelial ovarian cancer cell lines for our studies, SKOV3 and HEY. These cell lines were authenticated by using short tandem repeat (STR) DNA profiling (Genetica, Inc.) and comparing the profiles to ATCC profiles and other previously published profiles [363]. We first wanted to test whether the cell lines we selected exhibited a normal response to heat, including the characteristic activation of HSF1 and induction of chaperones. We find that both SKOV3 and HEY cells exhibit multiple hallmarks of activation of the heat shock response (Figure 3.2A).

Upon treatment with a 42°C heat shock over a 6 hour timecourse, we observe stress-induced hyperphosphorylation of HSF1 followed by a return to the hypophosphorylated state. This result is characteristic of HSF1 activation by heat shock and can be readily detected by electrophoretic retardation on SDS-PAGE and Western blot analysis [367]. Interestingly, while SKOV3 cells contain a similar level of basal and activated HSF1 as compared to normal ovarian epithelial T80 cells, HEY cells express higher levels of HSF1, corresponding to the higher levels of HSF1 expression we identified in ovarian cancer patient databases. Upon heat shock, we also observed that both SKOV3 and HEY cells show HSF1 phosphorylation at serine 326, a marker of activated HSF1 [41]. Additionally, the chaperone HSP70 was induced by heat shock in both

SKOV3 and HEY cells, and HSP90 was induced in HEY cells. Overall, we conclude that both SKOV3 and HEY cells express HSF1 and respond to heat shock, validating the choice of these two ovarian cancer cell lines for our studies.

We next wanted to generate HSF1 knockdown SKOV3 and HEY cell lines. Our initial attempts to create stable HSF1 knockdown in these cell lines were not successful, perhaps due to selective pressure for the cancer cells to re-express HSF1. We therefore employed a doxycycline-inducible shHSF1 system (pTRIPZ vector, Open Biosystems). To ensure that doxycycline treatment alone would not alter HSF1 levels or activity, we treated SKOV3 and HEY cells with both 0.5 and 2.0  $\mu\text{g/ml}$  of doxycycline for 48 hours and found no changes in HSF1 levels or hyperphosphorylation status (Figure S.1). We also found no change in HSP90 levels (Figure S.1). We therefore concluded that a doxycycline-inducible system would be a viable option for HSF1 knockdown in our studies.

We used two shHSF1 sequences obtained from the RNAi codex database [364], shHSF1A (CGCAGCTCCTTGAGAACATCAA) and shHSF1B (CCCACAGAGATACACAGATATA), as well as a control sequence that is non-targeting, to create SKOV3.shControl, SKOV3.shHSF1A, SKOV3.shHSF1B, HEY.shControl, HEYshHSF1A and HEY.shHSF1B stable cell lines (Figure 3.2B).

The shHSF1A sequence knocks down HSF1 expression by about 75%, while shHSF1B knocks down HSF1 expression more completely. Knockdown of HSF1 resulted in only a marginal reduction of cell viability in the SKOV3 or HEY cell lines over a 72 hour doxycycline treatment time course (Figure 3.2C). We thus have established an effective means of knocking down HSF1 to varying degrees in two different ovarian cancer cell lines.

## **HSF1 Knockdown Inhibits Colony Formation, Wound healing, Cell Migration and Fibronectin Expression**

We then assayed our HSF1 knockdown cell lines to determine whether HSF1 is important for ovarian cancer tumorigenicity. As a measure of the ability of HSF1 to allow cell survival and growth upon plating at a low cell density, clonogenic assays were performed (Fig. 3). SKOV3.shControl, SKOV3.shHSF1B, HEY.shControl and HEY.shHSF1B stable cells were treated with or without doxycycline to induce HSF1 knockdown and then plated at 250 cells per well in 6-well plates in triplicate. Colonies, stained after 8 days, show that HSF1 knockdown strongly inhibits colony formation in both HEY and SKOV3 cells.

To assess the ability of HSF1 to affect cellular motility, we used a wound healing assay as well as a cell migration assay. For the wound healing assay, cells were seeded in equal numbers into 6-well plates and grown to approximately 80% confluence prior to introducing scratches in straight lines through the monolayers. TScratch software was then used to automatically analyze wound healing rates (Figure 3.4A).

HSF1 knockdown in SKOV3 and HEY cells inhibits wound-healing ability by 25% and 28%, respectively. Next, cell migration assays were employed to assess the ability of cells to pass through a matrigel-coated transwell membrane (Fig. 4B). Cells were seeded in equal numbers into the insert of a transwell plate, with no cells in the lower chamber. The number of cells that passed through the membrane were then calculated and plotted after 48 hrs. HSF1 knockdown was found to inhibit cell migration by 29% in SKOV3 cells and 33% in HEY cells. These experiments in sum support a role for HSF1 in promoting cell motility in ovarian cancer.

We next wanted to test whether HSF1 knockdown can suppress the EMT process. Fibronectin, a mesenchymal marker, is upregulated during EMT and plays a crucial role in altering cell adhesion and migration processes, allowing for transition to the mesenchymal state [368].

We tested protein expression levels of fibronectin using Western blot analysis of SKOV3.shHSF1B and HEY.shHSF1B cells treated with and without doxycycline and with and without the EMT inducer TGF $\beta$  (Figure 3.4C). As expected, TGF $\beta$  treatment induces fibronectin expression (Figure 3.4C, compare lanes 1 with lanes 3). Interestingly, HSF1 knockdown in both SKOV3 and HEY cells reduces both the basal expression levels of fibronectin (Figure 3.4C, compare lanes 1 and 2) as well as the TGF $\beta$ -induced levels of fibronectin (Figure 3.4C, compare lanes 3 and 4). Therefore, HSF1 may promote the EMT process by enhancing TGF $\beta$ -induced fibronectin expression.

### **The induction of Fibronectin by TGF $\beta$ is Enhanced in 3D Cultures as Compared to 2D Cultures**

As ovarian cancer cells typically spread throughout the peritoneal cavity in the form of 3D spheroids, we cultured cells in 3D culture using the hanging drop method [369] in order to create a more biologically-relevant *in vitro* system for our studies. We first tested whether the induction of fibronectin by TGF $\beta$  is altered in 3D cultures as compared to 2D cultures.

In both monolayer and spheroid SKOV3 cells, TGF $\beta$  increased fibronectin expression (Figure 3.5). Surprisingly, this effect was enhanced in the SKOV3 spheroid model as compared to monolayer cells (Figure 3.5, compare lanes 2 and 4). The HEY cells also showed enhanced fibronectin expression upon 3D growth, although this effect was not enhanced by TGF $\beta$ . Therefore, we conclude that 3D culturing enhances fibronectin expression.

### **3D Culturing Reveals a Marked Effect of HSF1 on the Induction of EMT Transcription Factors**

Various transcription factors, including snail, slug, twist, and zeb, help to coordinate the EMT process [358]. We tested whether 3D growth affected the expression of these genes (Fig.

6). We find that 3D growth enhances TGF $\beta$  induction of these transcription factors as shown by qRT-PCR (Fig. 6, compare lanes 2 and 4). We wondered whether HSF1 may regulate the expression of these EMT transcription factors. We thus tested our HSF1 knockdown cell lines, grown under both 2D and 3D conditions, to test for effects on the expression of *SNAIL*, *TWIST1*, *SLUG* and *ZEB1* mRNAs (Figure 3.6). SKOV3.shControl, SKOV3.shHSF1B, HEY.shControl, and HEY.shHSF1B stable cell lines, grown both as 2D and 3D cultures, were treated with and without doxycycline treatment to induce HSF1 knockdown. We find that HSF1 knockdown in most cases slightly inhibits the expression of EMT transcription factors in SKOV3 and HEY cells grown in 2D (Fig. 6, compare lanes 2 with lanes 3). Interestingly, the effect of HSF1 knockdown on the expression of these genes is magnified for most of the genes upon growth in 3D conditions (Figure 3.6, compare lanes 4 with lanes 5). Therefore, using a 3D ovarian cancer culturing system, we have uncovered a positive effect of HSF1 on the ability of TGF $\beta$  to induce EMT genes. We thus conclude that HSF1 promotes EMT in ovarian cancer 3D spheroids at least in part through regulating the levels of EMT-inducing transcription factors.

## **Discussion**

As ovarian cancer is highly lethal and has few treatment options, identifying new therapeutic targets for this disease is highly important. Through mining patient data, we find that HSF1 DNA levels are most highly amplified in ovarian cancer as compared to other cancers, and also that ovarian cancer is one of the top cancer types with amplified HSF1 mRNA levels. A previous study of 37 malignant vs. benign ovarian tumors has shown that HSF1 expression is higher in the malignant tumors [132]. Our findings thus add to this data and suggest that HSF1 may be an important therapeutic target for ovarian cancer.

We have identified HSF1 as a critical player in promoting ovarian cancer tumorigenicity by multiple measures in both SKOV3 and HEY ovarian cancer cells. Via HSF1 knockdown and

colony formation assays, we show that HSF1 promotes the ability of cells to grow under conditions of low cell density, a hallmark of cancer cells. Cell motility is another characteristic of cancer cells. Previous work has shown that cell motility is inhibited in immortalized mouse embryonic fibroblast cells derived from *hsf1* *-/-* mice [370]. In addition, HSF1 knockdown reduces the invasiveness of multiple types of tumor cells [129, 371-374]. Consistent with these findings, we show that HSF1 knockdown inhibits wound healing and cell migration in SKOV3 and HEY ovarian cancer cell lines. Our results thus add further evidence that HSF1 enhances tumorigenicity in multiple types of cancer.

EMT is essential for cell migration and is a key rate-limiting step in metastasis. Previous studies have shown that HSF1 promotes EMT in breast cancer cells through a mechanism that requires HER2 [140, 375]. As ovarian cancer cells typically spread throughout the peritoneal cavity in the form of 3D spheroids [376], culturing ovarian cancer cells as spheroids is likely to better mimic the *in vivo* growth conditions as compared to conventional 2D culturing conditions. Here, we show that HSF1 knockdown reduces the ability of TGF $\beta$  to induce EMT. Interestingly, we find that this effect is stronger upon growth in 3D spheroids. We also show that HSF1 is required for the compact morphological structure of spheroid growth.

Our data suggests that HSF1, either directly or indirectly, controls the expression of transcription factors that are important for the EMT process. Interestingly, upon promoter analysis, we find consensus heat shock element (HSE) sequences containing three inverted arrays of the sequence nGAAn [377] in the promoters of the EMT transcription factor genes *SNAIL*, *ZEB* and *TWIST1* (Table S2). Putative HSEs are also present in the *FN1* (*fibronectin*), *VIM* (*vimentin*), and *CDH2* (*N-cadherin*) promoters, additional genes that are associated with EMT (Table S2). Future experiments will be required to determine whether any of these genes are direct HSF1 targets. This is plausible given that HSF1 was recently found to bind to the *SLUG* promoter through an imperfect HSE motif [375].

In summary, we have identified HSF1 as a critical player in ovarian cancer progression, and have identified EMT as a process that is promoted by HSF1. The effects for HSF1 are more striking when cells are grown as 3D spheroids, which more closely mimic the *in vivo* growth conditions of ovarian cancer. Therefore, HSF1 deserves further research and development as a promising anticancer strategy for ovarian cancer.

### **Acknowledgements**

The authors would like to thank Dr. Meera Nanjundan for donation of the SKOV3 and HEY cell lines, and Dr. Marc Mendillo for the suggestion to analyze TCGA data.

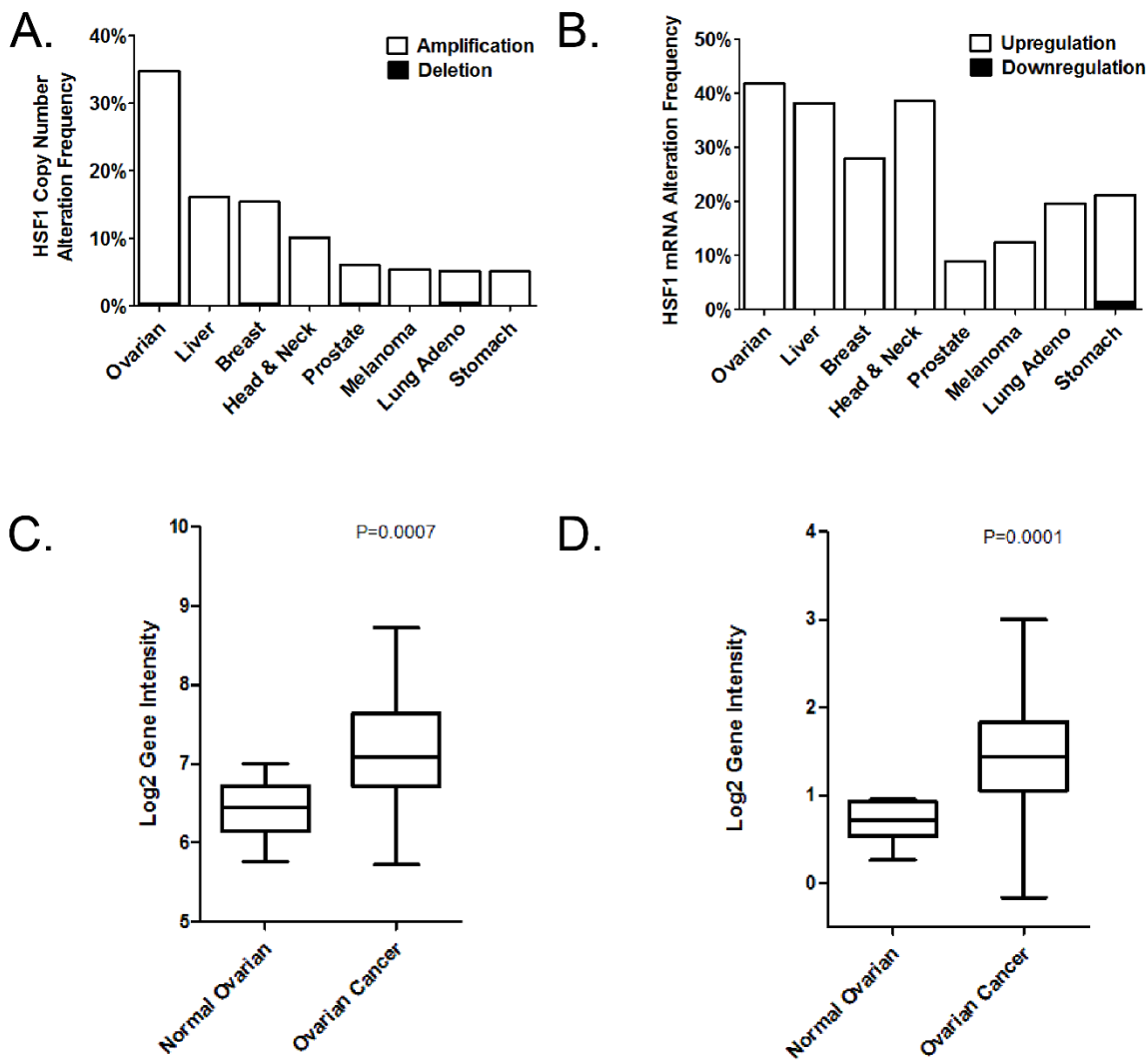


**Figure 3.1. HSF1 Levels are Elevated in Ovarian Cancer Patient Samples.** A, HSF1 copy number is increased most frequently in ovarian cancer. HSF1 copy number was analyzed in a variety of cancers using TCGA data and GISTIC analysis with a threshold CNA change of +/-2. B, HSF1 transcripts are elevated in a variety of cancers. Samples from tumor tissue and matched normal tissue were compared in the TCGA database using RNA Seq V2 RSEM data with a z-score threshold of +/-2. C, HSF1 is increased at the mRNA level in an ovarian cancer data set GSE18520 consisting of 10 normal ovarian samples and 53 late stage, primary site, high grade ovarian cancer samples. D, HSF1 is increased at the mRNA level in a TCGA ovarian cancer data set consisting of 8 normal ovarian samples and 568 ovarian cancer samples.



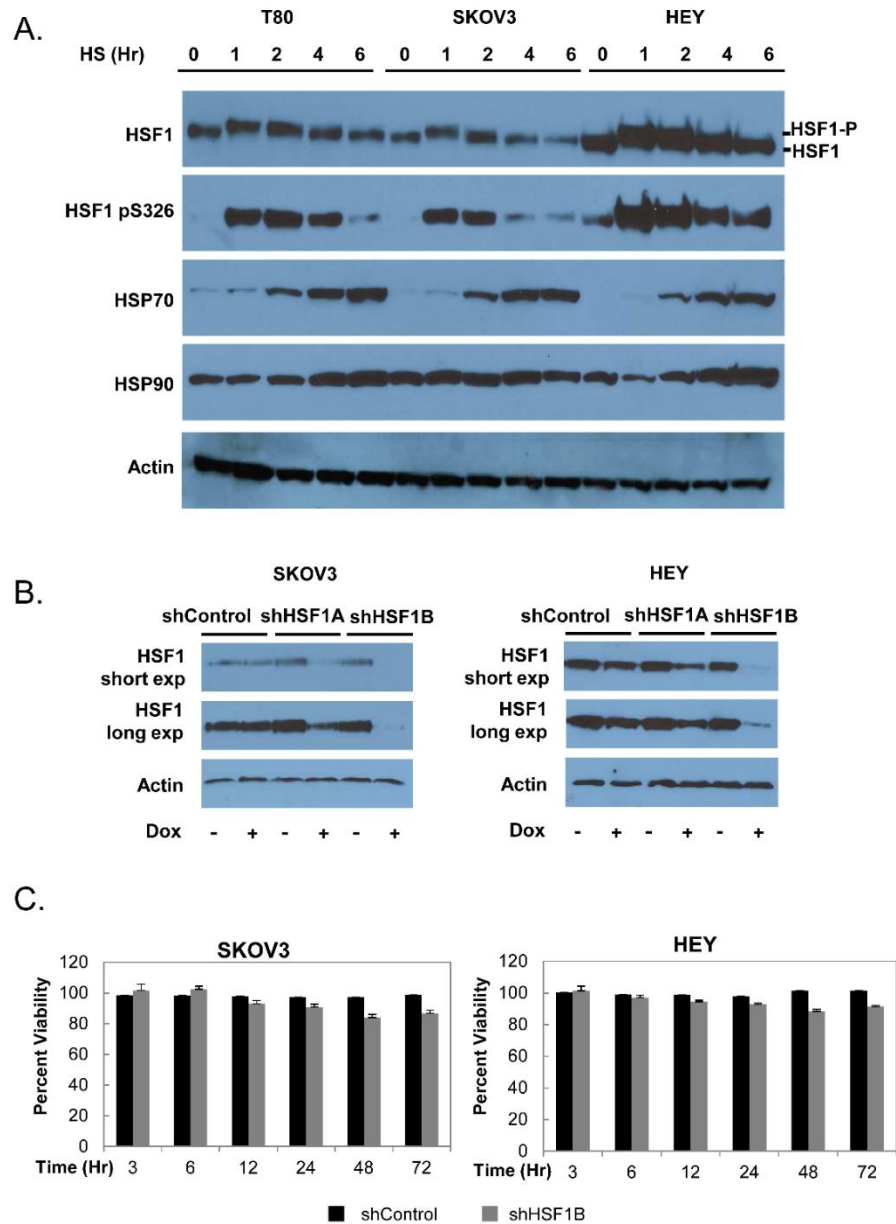


**Figure 3.2. Validation of Inducible HSF1 Knockdown Ovarian Cancer Cell lines.** A, The heat shock response in the epithelial ovarian carcinoma cell lines SKOV3 and HEY as compared to normal ovarian epithelial T80 cells. T80, SKOV3, and HEY cells were treated with a 42°C heat shock for the indicated times and harvested immediately after. Cell lysates were subjected to Western blot analysis using antibodies recognizing HSF1, HSF1 phosphorylated at S326, HSP90, HSP70, and actin as a loading control. B, The pTRIPZ system was used to create the doxycycline-inducible HSF1 knockdown cell lines SKOV3.shHSF1A, SKOV3.shHSF1B, HEY.shHSF1A and HEY.shHSF1B. After treatment with 1 µg/ml doxycycline for 48 hours, cell lysates were subjected to Western blot analysis using antibodies recognizing HSF1 and actin as a loading control. Both short and long exposures are shown for the HSF1 blot. C, HSF1 knockdown does not cause a large decrease in cell viability. The viability of the SKOV3.shHSF1B and HEY.shHSF1B cell lines as compared to shControl cells was assessed after treatment with 1 µg/ml doxycycline for the indicated times using the PrestoBlue cell viability assay. Mean percent viability (n=8) and standard error is shown.

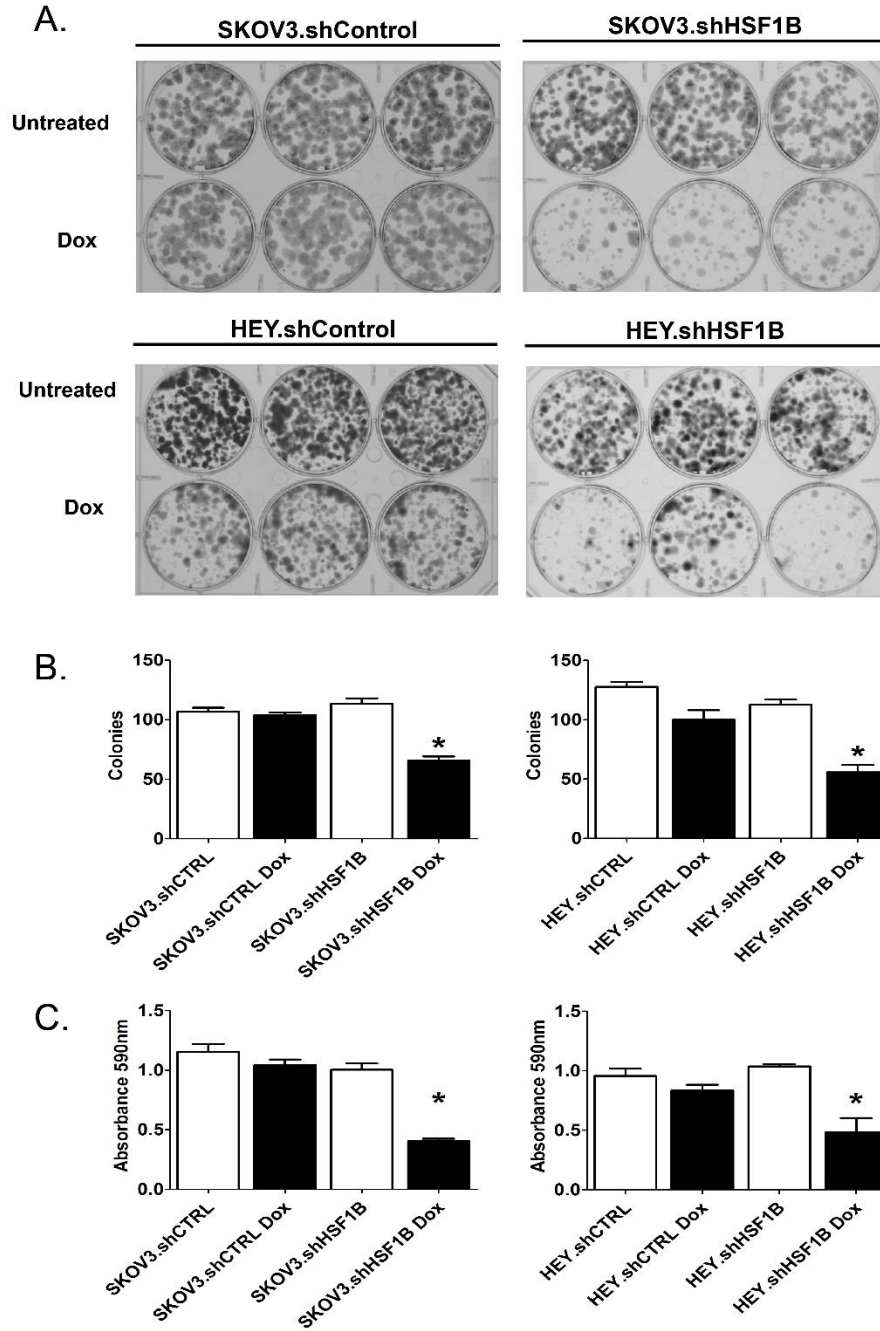


**Figure 3.3. HSF1 Knockdown Reduces Colony Formation.** SKOV3.shHSF1B, HEY.shHSF1B and control cell lines were plated 250 cells per well in 6-well plates in triplicate. Cell were treated with or without 1  $\mu$ g/ml doxycycline (Dox) to induce HSF1 knockdown and were given an additional dose after 4 days. Cells were stained with crystal violet after 8 days to visualize colonies.

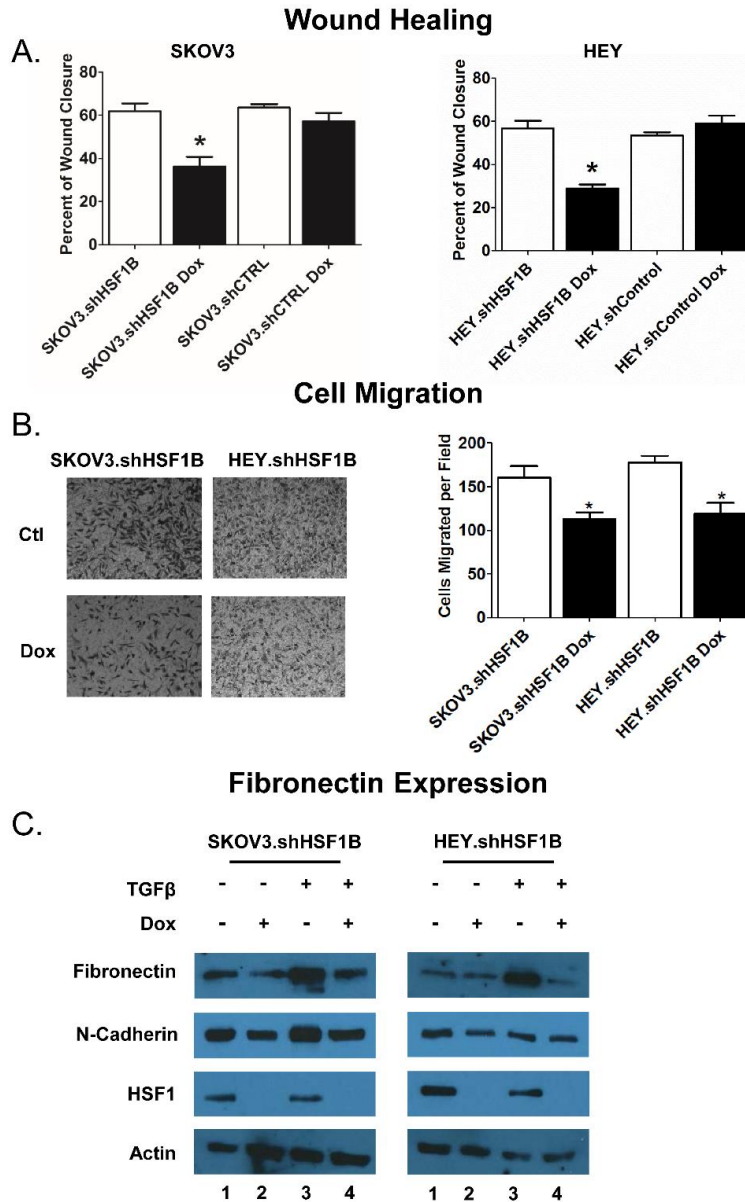


**Figure 3.4. HSF1 Knockdown Inhibits Wound Healing, Migration and Induction of Fibronectin.** A, HSF1 knockdown reduces wound closure. Cells treated with or without 1  $\mu\text{g/ml}$  doxycycline were grown in 6-well plates to confluency. Cells were scraped to create wounds, the cells were washed and serum-free media was added. The intersections of perpendicular scratches were photographed immediately and 12 hours after and analyzed using Tscratch software. Asterisk denotes significant difference from all other samples calculated by ANOVA ( $P < 0.05$ ). B, HSF1 knockdown reduces migration. After treatment with or without 1  $\mu\text{g/ml}$  doxycycline and 12 hours of serum starvation, cells were added to a Boyden chamber at  $2.5 \times 10^4$  cells per chamber. Serum was used as the chemoattractant in the lower chamber. After 16 hours, nonmigrating cells were scrubbed and cells which had migrated stained. The experiment was done in triplicate and analysis done by paired t-test. Asterisk marks significant difference ( $P < 0.05$ ). C, HSF1 KD reduces TGF $\beta$ -induced expression of fibronectin. SKOV3.shHSF1B and HEY.shHSF1B were treated with 1 $\mu\text{g/ml}$  doxycycline, 10 ng/ $\mu\text{l}$  TGF $\beta$ , or both, and cell lysates were harvested for immunoblotting. Cell lysates were subjected to Western blot analysis using antibodies recognizing fibronectin, HSF1, and actin as a loading control.

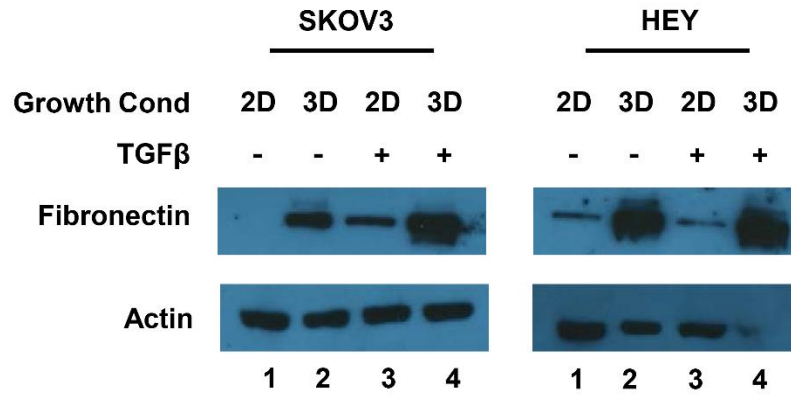


**Figure 3.5. Fibronectin Expression is Induced by 3D Growth.** SKOV3 and HEY cells were cultured under 2D or 3D conditions, with or without TGF $\beta$ , as indicated. Cell lysates were subjected to Western blot analysis using antibodies recognizing fibronectin, and actin as a loading control.

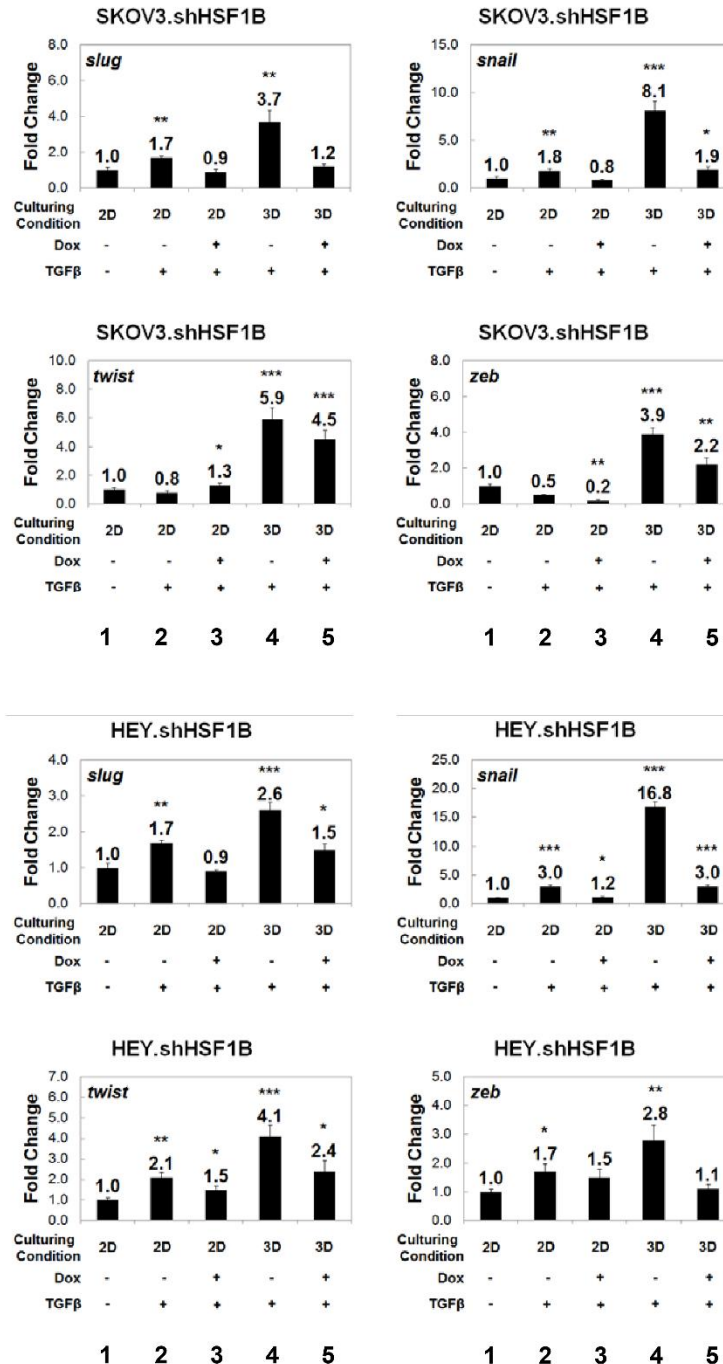


**Figure 3.6. TGFβ Induction of EMT Master-Switch Transcription Factors are Reduced Upon HSF1 Knockdown, and the Effect is Enhanced Upon 3D Culturing.** Quantitative real-time polymerase chain reaction (qRT-PCR) of selected genes shows that the EMT master-switch transcription factors *SNAI1/SNAIL*, *TWIST1*, *ZEB1*, and *SNAI2/SLUG* are upregulated when HSF1 inducible knockdown SKOV3.shHSF1B and HEY.shHSF1B cells are cultured as 3D spheroids. This effect is significantly reduced upon knockdown of HSF1 via doxycycline treatment. Gene expression was normalized to the housekeeping gene *GAPDH*, and fold change was calculated relative to monolayer non-treated conditions. Statistical significance was measured by Student's t test as compared to untreated monolayer cell culture (\* $p < 0.05$ ; \*\* $p < 0.01$ ; \*\*\* $p < 0.001$ ).

## CHAPTER FOUR: MODULATION OF HEAT SHOCK TRANSCRIPTION FACTOR HSF1 AFFECTS RESPONSE TO MULTIPLE DRUGS

### Introduction

The heat shock transcription factor HSF1 is an important component in the cellular survival response to a multitude of stressors. HSF1 acts as the master controller for the HSR, which mitigates damage from heat and a variety of other stresses. Examples include proteasome inhibition, translational inhibition, heavy metals, ischemia, osmotic pressure and protein aggregation [378-381]. The HSR promotes survival in part through increased expression of molecular chaperones including HSP25, HSP70, and HSP90 [13]. These HSPs are capable of conferring resistance to multiple treatments in *in vitro* studies, including doxorubicin and paclitaxel [382-384]. In addition, HSF1 is required for the some aberrant signaling pathways that are vital in highly malignant cancers, such as HER2, BRAF, RAS, and AKT signaling [133, 136, 372, 385, 386].

HSF1 has become an attractive target for the treatment of cancer because it is implicated in facilitating aberrant oncogenic pathways and drug resistance in multiple cancers such as breast and hepatocellular cancers. Previous studies have found that HSF1 promotes resistance to doxorubicin, paclitaxel, and HSP90 inhibitors in hepatocellular, breast, and melanoma cancers [115, 139, 387]. High levels of HSF1 are common in approximately a third of ovarian cancer cases, which suggests that HSF1 may play an important role in the drug resistance of ovarian cancer [388]. We performed a knockdown study on the HSF1 in two ovarian cancer cell lines, SKOV-3 and HEY. We determined how the knock down of HSF1 affected the cell survival

response to cisplatin, paclitaxel, doxorubicin, curcumin, 17-AAG, and ganetespib. These drugs are either commonly used chemotherapeutic agents or prospective chemotherapeutic drugs.

### **Overview of Drugs Tested**

**Cisplatin.** Cisplatin is the general name for cis-diamminedichloroplatinum(II) and is a very stable planar platinum coordination compound (Figure 4.1). It was discovered to have cytotoxic properties in the 1960s and in 1978 became the first FDA approved metallic based cancer therapy [357]. The primary mechanism of action is through DNA damage. This is accomplished mostly through the interaction with purine bases creating interstrand and intrastrand DNA-DNA crosslinks and also through the creation of DNA-protein crosslinks [389]. Of these DNA adducts, intrastand adducts are believe to be the source of most damage. While these nuclear lesions affect DNA synthesis, it is the triggering of the DNA damage response which ultimately leads to cell cycle arrest and apoptosis [389]. Cisplatin and other platinum therapies are the first line treatment for ovarian cancer. While initially effective in the majority of cases, resistance usually develops with cancer recurrence [390].

**Paclitaxel.** The compound paclitaxel was originally derived the pacific yew tree, *T. brevifolia* and was found to have cytotoxic effects in the late 1970s (Figure 4.2) [391]. It was the first of the taxol family to be discovered and was FDA approved for the treatment of refractory ovarian cancer [392]. Paclitaxel functions by stabilizing the microtubule assembly. This stabilization results in cellular arrest during mitosis at high doses [393]. At low doses, cell death occurs after undergoing irregular mitosis [394]. Paclitaxel is often combined with platinum based therapies as first line chemotherapy regime [395].

**Doxorubicin.** Doxorubicin is the most commonly used of the anthracycline class of drugs (Figure 4.3). It was originally derived from daunorubicin, an antibiotic from *Streptomyces peucetius*. Doxorubicin is very potent and is used in the treatment of a variety of cancers. It is

limited in application by its toxicity profile, in particular its cardiotoxicity [396]. The primary mechanism of action is through the inhibition of topoisomerase II [397]. This is accomplished by the formation of a doxorubicin-DNA-topoisomerase II ternary complex, stabilized in part by the intercalation of the DNA minor groove by the planar ring system [398]. Doxorubicin is not typically a first line chemotherapy agent. It is usually employed to treat recurrent cases of ovarian cancer that are resistant to platinum therapies [399].

**Curcumin.** Curcumin (diferuloylmethane) is a polyphenol derived from *Curcuma longa*, which is commonly known as turmeric. The chemical structure for curcumin is shown in figure 4.4. Its recent use in clinical trials is preceded by use in traditional Chinese and Indian medicines [400]. Curcumin has antioxidant and anti-inflammatory properties. It induces functions through multiple means including the inhibition of proliferation, invasion, and angiogenesis [401]. This is accomplished by the inhibition of signaling proteins such as NF- $\kappa$ B, AP-1 and STAT3 [402]. The potential for clinical use of curcumin is hindered by its low aqueous solubility and poor bioavailability. However, analogues and different delivery strategies are being created to circumvent this. Curcumin as a single agent and in combination has advanced to phase II trials for treating colorectal and pancreatic cancer [403]. Curcumin was included in this study due to a significant correlation between HSF1 transcript levels and curcumin LD50 values in the NCI-60 cell line panel. This was found using the CellMiner suite of tools [404].

**17-AAG (Tanespimycin).** 17-AAG is a benzoquinone ansamycin antibiotic (Figure 4.5). It was developed a less toxic analogue geldanamycin, which was limited by its high liver toxicity. It interrupts many oncogenic signaling pathways through inhibition of cytosolic HSP90 function [405]. Inhibition is achieved through affinity with the ATPase N-terminal domain of the HSP90 complex, which prevent ATP dependent client refolding by HSP90 [406]. This has the effect of interrupting the critical oncogenic signal pathways HER2, EGFR, MEK, Akt, Src, and many others [407].



**Ganetespib.** Ganetespib was developed as a second generation HSP90 inhibitor with a substantially different chemical structure. The critical difference is the absence of the benzoquinone moiety which is the cause of the high liver toxicity that hampered first generation HSP90 inhibitors in clinical trials (Figure 4.6) [408]. Despite the difference in chemical structure, ganetespib functions by inhibiting the N-terminal ATPase domain like earlier HSP90 inhibitors. In addition to having a better pharmacological profile, ganetespib is roughly 20 times more potent than 17-AAG [409]. Ganetespib has made it as far as phase II clinical trials when included in combinatorial therapy for treatment of hepatocellular, pancreatic, and prostate cancers [410-412]. The biggest challenge for the development of treatment with ganetespib is identifying patients most likely to respond to the therapy. Ganetespib works best on cases where the cancer is reliant on constitutively active kinases (including c-KIT, EGFR, and B-RAF).

## **Material and Methods**

### **Cell Culture**

The HEY and SKOV3 cell lines with inducible HSF1 knockdown were created as previously described in Chapter 2. The doxycycline-inducible TRIPZ shRNAmir system (Thermo Scientific) was used in conjunction with shRNA targeting HSF1. The shRNA sequences for targeting HSF1 were obtained from the RNAi codex database [364]. Two sequences were cloned into the pTRIPZ vector and tested for efficacy: CGCAGCTCCTTGAGAACATCAA (shHSF1A) and CCCACAGAGATACACAGATATA (shHSF1B). Infection was done using a 2<sup>nd</sup> generation lentiviral system with pCGP packaging and pVSVG envelope plasmids (Addgene). Packaging was done with HEK293 cells cultured in RPMI medium. Transfection was performed using Polyfect Transfection Reagent (Qiagen) based on the manufacturer's suggested protocol. After a single round of infection, stable HEY and SKOV3 cells were selected with 1 µg/ml and 0.5 µg/ml

puromycin (Thermo Fisher) respectively. Knockdown efficacy was tested by western blot after a 48 hour treatment with 1 µg/ml doxycycline (Figure 2.2B). In all subsequent experiments, HSF1 knockdown was achieved with a 1 µg/ml doxycycline treatment 48 hours prior.

### **Protein Isolation, SDS-PAGE, and Western Analysis**

Treated cells were washed and released by scraping in chilled PBS. Cells were then pelleted and protein was extracted using M-PER lysis buffer (Thermo Scientific) containing Halt™ Protease Inhibitors (Thermo Scientific). Protein concentration was determined using Pierce™ 660nm protein assay (Thermo Scientific) following the manufacturers recommended procedures. 15 µg of cell lysate run on 10% sodium dodecyl sulphate polyacrylamide gel electrophoresis (SDS-PAGE) gels and then transferred using a Trans-Blot semi-dry transfer cell (Bio-Rad) to 0.2 µm Immun-Blot® PVDF membrane. The membranes were blocked with 1% w/v non-fat milk in TBS with 0.1% Tween. Blots were probed with primary overnight, followed by secondary the next day. Blots were developed using ECL Prime Western Blotting Detection System (Amersham™) and film exposure. The primary antibodies used were: Actin (Santa-Cruz), HSF1 (Cell Signaling), HSF1 P-S326 (Abcam) and HSP70 (Cell Signaling). Secondary HRP-conjugated antibodies were from Millipore and Jackson ImmunoResearch.

### **Viability Assay**

Cells at a concentration  $1.5 \times 10^5$  cell/ml were plated in clear bottom, black walled 96-well plates at 100 µl per well. After a 6 hour incubation to allow cell to adhere, cells were treated with drugs or vehicle control in triplicate. DMSO was used as vehicle control for all drug treatments with the exception of cisplatin, which used saline water. The drugs used were: cisplatin (Tocris), 17-AAG (Selleck Chemical), paclitaxel (ACROS), doxorubicin (Fisher), curcumin (Sigma-Aldrich) and ganetespib (Selleck Chemical). After a 16 hour treatment, cells were washed 3 times with

PBS, followed by the addition of 50  $\mu$ l RPMI medium. After rinsing, 5  $\mu$ l of PrestoBlue® Cell Viability reagent (Invitrogen) was added to each well followed by a 45 minute incubation at 37°C. Fluorescence (excitation 570nm, emission 600nm) was measured using a microplate reader (BioTek). Viability was determined by comparing treated and control samples after subtracting a dead cell control reading. Dead cell control was generated by treatment with lethal dose of cycloheximide (Fisher). Curve calculations were done using variable slope linear regression analysis with GraphPad prism® 7 software (GraphPad Software, Inc.).

## **Results**

### **Doxycycline Treatment Does Not Effect Drug Sensitivity**

Doxycycline is known to have a variety of effects on cancer cells when used at higher doses, such as the inhibition of Protease-Activated Receptor 1 (PAR1) and Matrix Metaloproteinases (MMPs) [413, 414]. To determine if the use of doxycycline changed the drug response, HEY.shControl and SKOV3.shControl cells were treated with and without 1  $\mu$ g/ml doxycycline for 48 hours. This was followed by a drug response assay. Treatments were performed in triplicate for doses previously determined to be IC50 values. The results of the viability assay show that doxycycline does not substantially effect the sensitivity of HEY.shControl or SKOV3.shControl cell lines to any of the drugs tested (Figure 4.7).

### **HSF1 Knockdown Sensitizes Cells to Multiple Chemotherapeutic Agents.**

Previous studies have indicated that HSF1 levels can increase cancer cell tolerance to therapeutic agents [139]. Elevated HSF1 levels have been found to raise melanoma and breast cancer cell line resistance to doxorubicin, paclitaxel, trastuzumab, and carboplatin [115, 139, 415]. We used HEY.shHSF1B and SKOV3.shHSF1B ovarian carcinoma cells lines with inducible HSF1

knockdown to test if HSF1 contributed to ovarian cancer cell survival when challenged with drug treatment. After pretreatment with or without 1 µg/ml doxycycline for 48 hours, HEY.shHSF1B and SKOV3.shHSF1B cells were treated with different drugs for 16 hours. These included cisplatin, paclitaxel, doxorubicin, curcumin, 17-AAG, and ganetespib. Response curves were generated and the IC50 values compared (Figure 4.8 – 4.10). Knockdown of HSF1 in SKOV3.shHSF1B cells significantly reduced the IC50 values for treatment with paclitaxel, doxorubicin, 17-AAG, and ganetespib based on an extra sum of squares F test (P=0.01). Similarly, knockdown of HSF1 reduced tolerance in HEY.shHSF1B cells for paclitaxel, doxorubicin, 17-AAG, and ganetespib, but not cisplatin and curcumin (Figure 4.9 and 4.10). While the sensitivity of SKOV3.shHSF1B cells to cisplatin was increased in the absence of HSF1, the change in response slope results in the significance being undetermined.

#### **Drug Treatment Does Not Induce Robust Heat Shock Response.**

Some previous reports have suggested that some cancer therapeutics elicit the HSR, or at least prime it by promoting the trimerization and phosphorylation of HSF1 [115, 139, 416]. HSP90 inhibitors are especially known to be HSR activators. This is due to feedback which activates HSF1 to replenish the pool of functional HSP90 [417]. To determine if the compounds being tested activated the HSR, SKOV3 cells were treated with semi-lethal doses of cisplatin, paclitaxel, doxorubicin, curcumin, 17-AAG, and ganetespib. Treatments were performed for 16 hours and activation of the HSR was determined by western blot analysis (Figure 4.11). Exposure to a 42°C heat shock followed by a 2 hour recovery resulted HSF1 phosphorylation at S326 and expression of HSP70. Surprisingly, none of the drug treatments induced a heat shock response.

#### **Discussion**

The heat shock response results in a robust increase of molecular chaperones including HSP27, HSP70, and HSP90. Given that these chaperones individually can promote survival

under stress, we sought to determine if HSF1, the master regulator of the HSR, supported resistance to therapeutic agents in ovarian cancer cells. We found that the knockdown of HSF1 sensitizes both HEY and SKOV3 ovarian carcinoma cells to paclitaxel, doxorubicin, 17-AAG, and ganetespib. Our results also showed that HSF1 knockdown did not affect cisplatin or curcumin sensitivity. Additionally, we found that treatment with the selected drugs does not activate HSF1 or induce HSR at the interval and doses used.

HSF1 knockdown reduces tolerance to all drugs tested to some degree. While the reduction in tolerance to cisplatin and curcumin was not as pronounced as other treatments, knockdown of HSF1 did lower the IC50 dose. In particular, the reduction of HSF1 appears to sensitize cells to low doses as evident by the change in slope (Figure 4.8 and 4.9). Low, non-lethal doses result in a broader curve during HSF1 knock down which suggests the cells may struggle to deal with minor stressors. This shift is most evident in the response curves of SKOV3.shHSF1B to cisplatin and curcumin, and HEY.shHSF1B to cisplatin, doxorubicin, and 17-AAG.

The increase in drug sensitivity during HSF1 knock down is reasonable given the protective and wide ranging roles HSF1 plays in cellular processes. In addition to controlling chaperone levels, HSF1 has been shown to promote cell survival under stress in other ways. For example, HSF1 can attenuate apoptosis through indirect stabilization of the anti-apoptotic Bcl-2 protein family [111]. HSF1 has also been shown facilitate drug efflux of doxorubicin and paclitaxel when over expressed in melanoma cells [139]. Interestingly, that study reported a 2 – 3 fold increase in IC50 values when HSF1 is overexpressed. Conversely, our studies show a 2 – 4 fold decrease when HSF1 is reduced. The HSF1-driven increase in drug efflux was found to be caused by an increase in ABC transporters.

The ability of HSF1 to increase chaperone levels was assumed to mitigate HSP90 inhibitors shortly after their discovery. Experiments using *hsf1*<sup>-/-</sup> mouse embryonic fibroblast cells

showed a modest increase in HSP90 inhibitor sensitivity compared to control cells [418]. A later study also found the same conclusions using hepatocellular carcinoma cell lines [387]. Interestingly, the mechanism by which HSF1 mitigates the effects of HSP90 inhibitors is dependent in part on the expression of DEDD proteins. This demonstrates that the protection conferred by the activation of HSF1 is not based solely on elevating HSP90 levels. Our findings are consistent with previous research in demonstrating that HSF1 attenuates the effects of HSP90 inhibitors such as 17-AAG and ganetespib. There is also some evidence to suggest that the degree to which HSF1 knockdown sensitizes cells correlates with HSF1 levels. The HEY cells, which express higher levels of HSF1, had a slightly larger increase in HSP90 inhibitor sensitivity after treatment with doxycycline compared to the SKOV3 cells.

The drug treatments used in this study did not induce HSF1 activation as determined by western blot analysis. This deviates from previous findings that HSP90 inhibition activates the heat shock response [373, 387, 419]. There are multiple possible explanations for this. The most likely cause is the duration of treatment used. Our experiments used a 16 hour dose time while other studies used 2 – 5 day treatment durations. Another possibility is that the HSR elicited by HSP90 inhibitors is weak compared to a traditional heat shock treatment, causing the results to appear negative. Lastly, the dose of inhibitor may have been too high or low. This is a possibility that cannot be ruled out since only a single dose of each HSP90 inhibitor was tested.

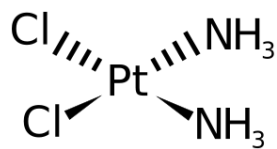


**Figure 4.1. Cisplatin Chemical Structure.** Cisplatin, also known as CDDP, is a DNA damage inducing alkylating agent. It is usually used in combination with a taxane as first round treatment.

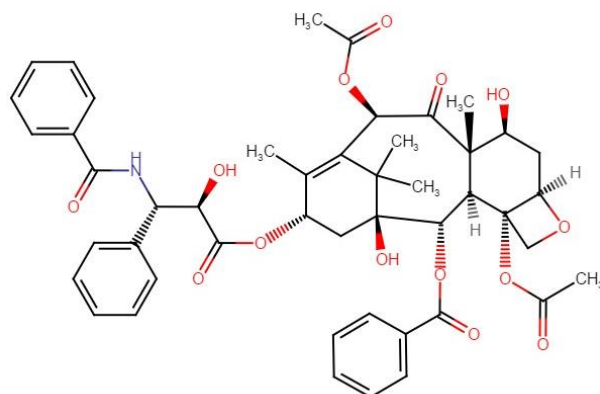


**Figure 4.2. Paclitaxel Chemical Structure.** Paclitaxel, a plant derived alkaloid, was the first member of taxane family. It functions as an anti-microtubule agent and is usually combined with platinum therapies as a first line of treatment.

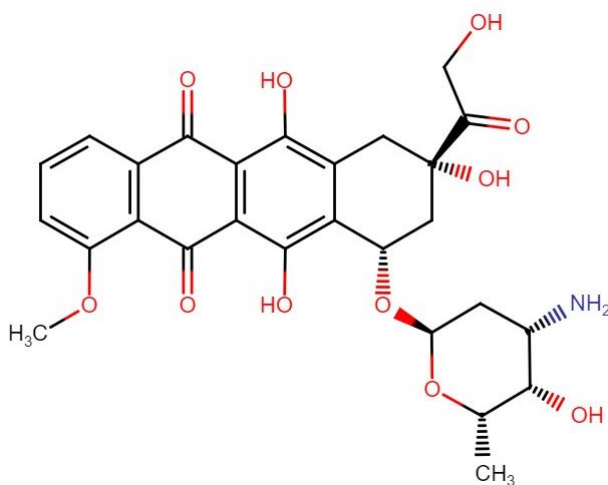


**Figure 4.3. Doxorubicin Chemical Structure.** Doxorubicin is an anthracycline antibiotic which is commonly used to treat platinum-resistant recurrence.

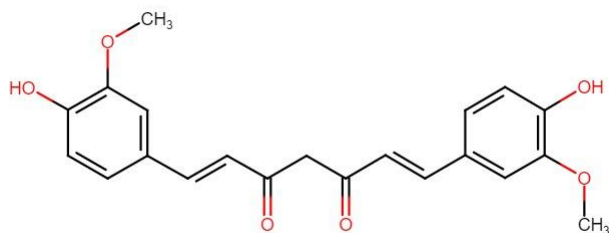


**Figure 4.4. Curcumin Chemical Structure.** Curcumin is a polyphenol which has anticarcinogenic effects. It has been used in combination with traditional therapies in clinical trials.

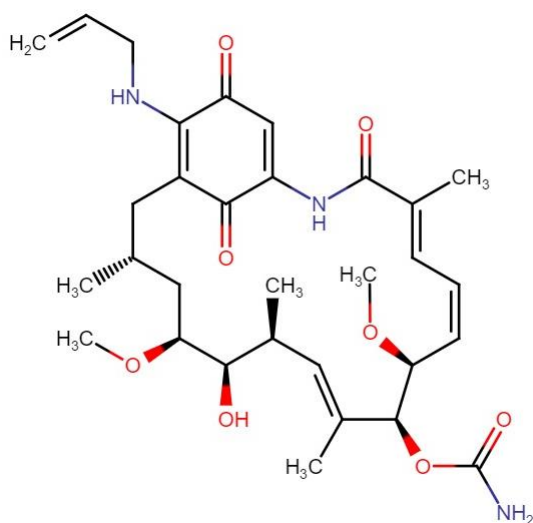


**Figure 4.5. 17-AAG Chemical Structure.** 17-AAG is a derivative of the antibiotic geldanamycin, which acts as a HSP90 inhibitor. It has been used in clinical trials for solid tumors and leukemia.



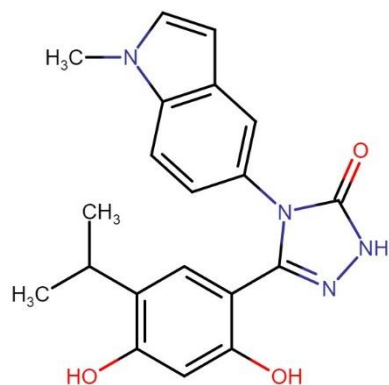


**Figure 4.6. Ganetespib Chemical Structure.** Ganetespib is a HSP90 inhibitor with lower toxicity and greater potency than earlier inhibitors. It is currently being used in phase II ovarian cancer trials.

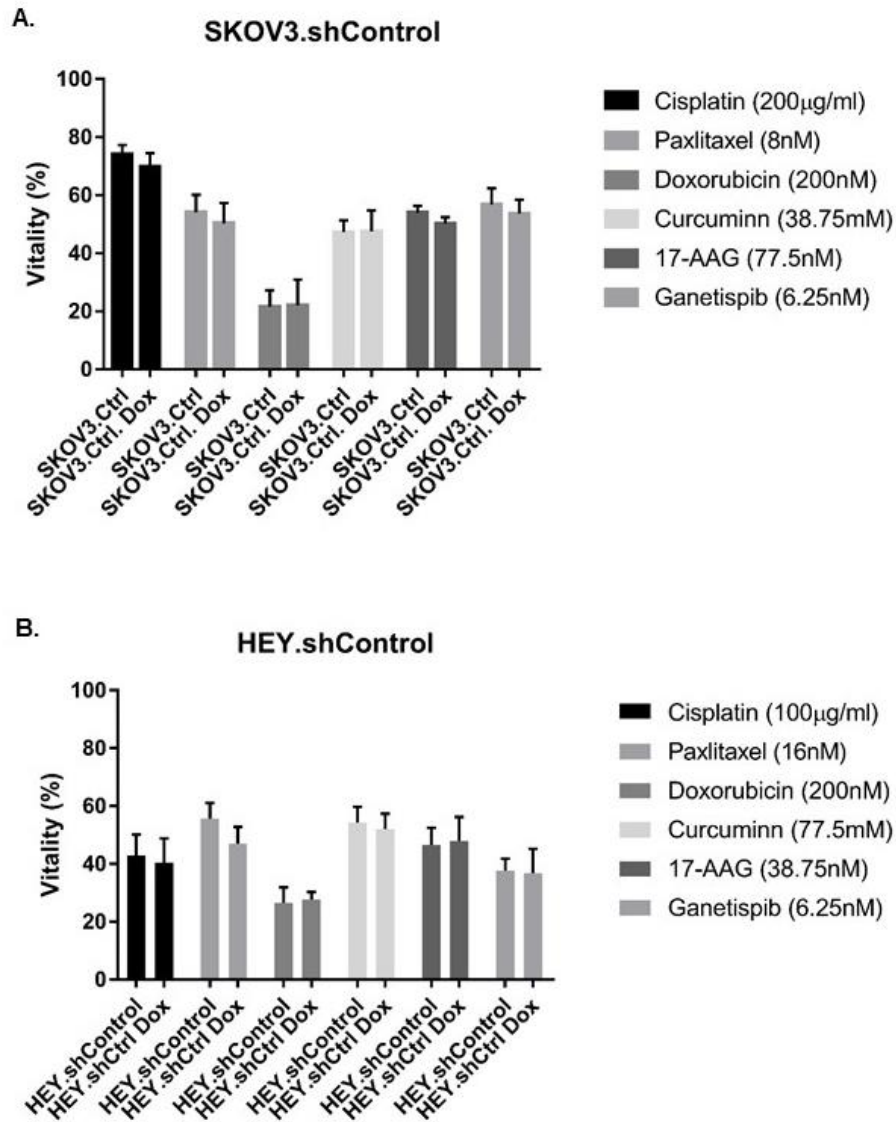


**Figure 4.7. Doxycycline Does Not Affect Drug Response in Control Cells.** SKOV3.shControl and HEY.shControl cells were treated with or without doxycycline in combination with a variety of drugs to determine if doxycycline affects IC50 values. Test was performed in triplicate using previously determined IC50 treatment values. Treatment with doxycycline did not significantly change the SKOV3.shControl and HEY.shControl IC50 values for any of the drugs tested. Statistical analysis was performed using a paired t-test.

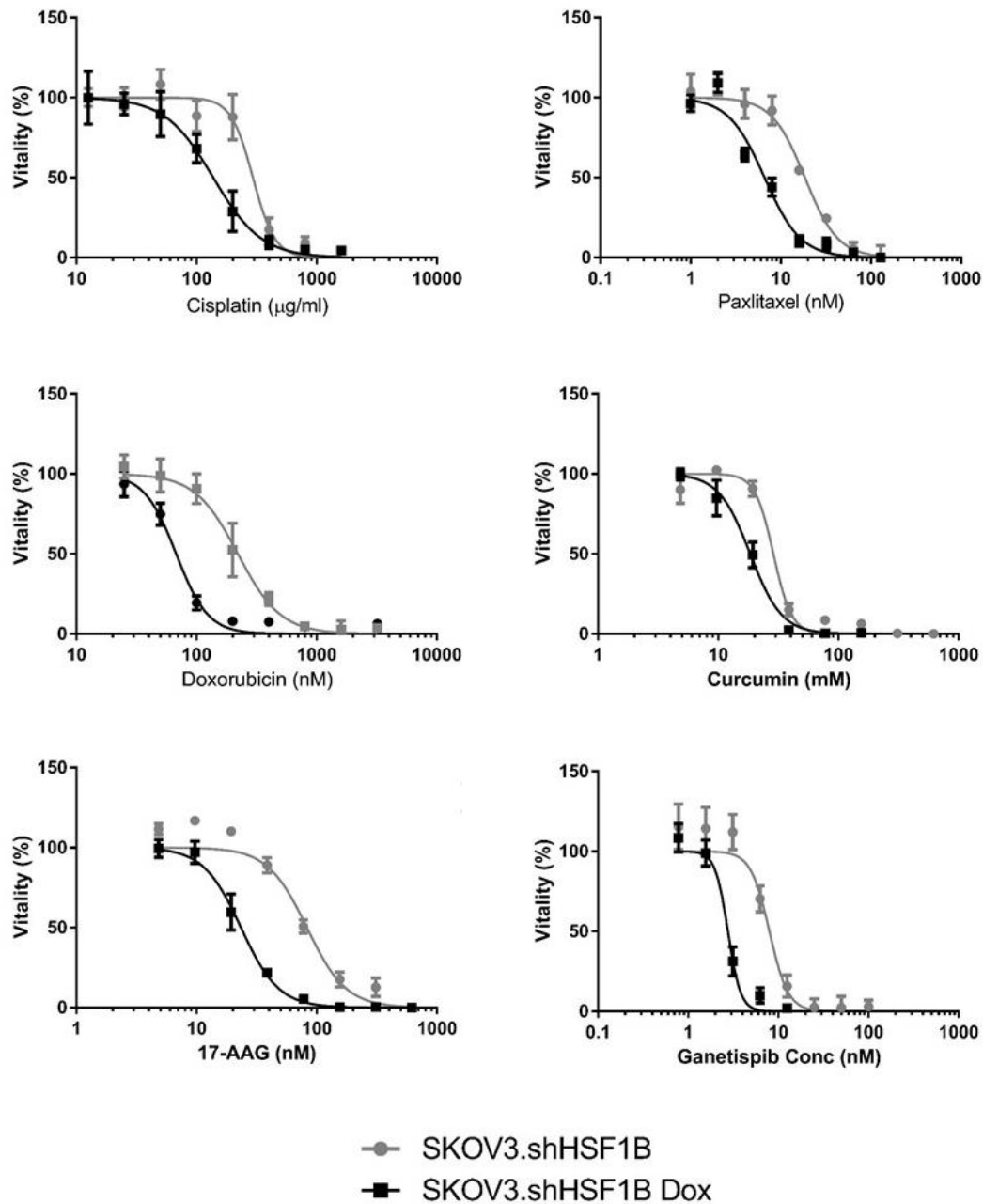


**Figure 4.8. Effect of HSF1 Knockdown on SKOV3.shHSF1B Dose Response.** SKOV3.shHSF1B cells were treated with or without doxycycline and then treated with serial dilutions of different drugs. After a 16 hour incubation, viability of the cells was assessed by PrestoBlue® assay.

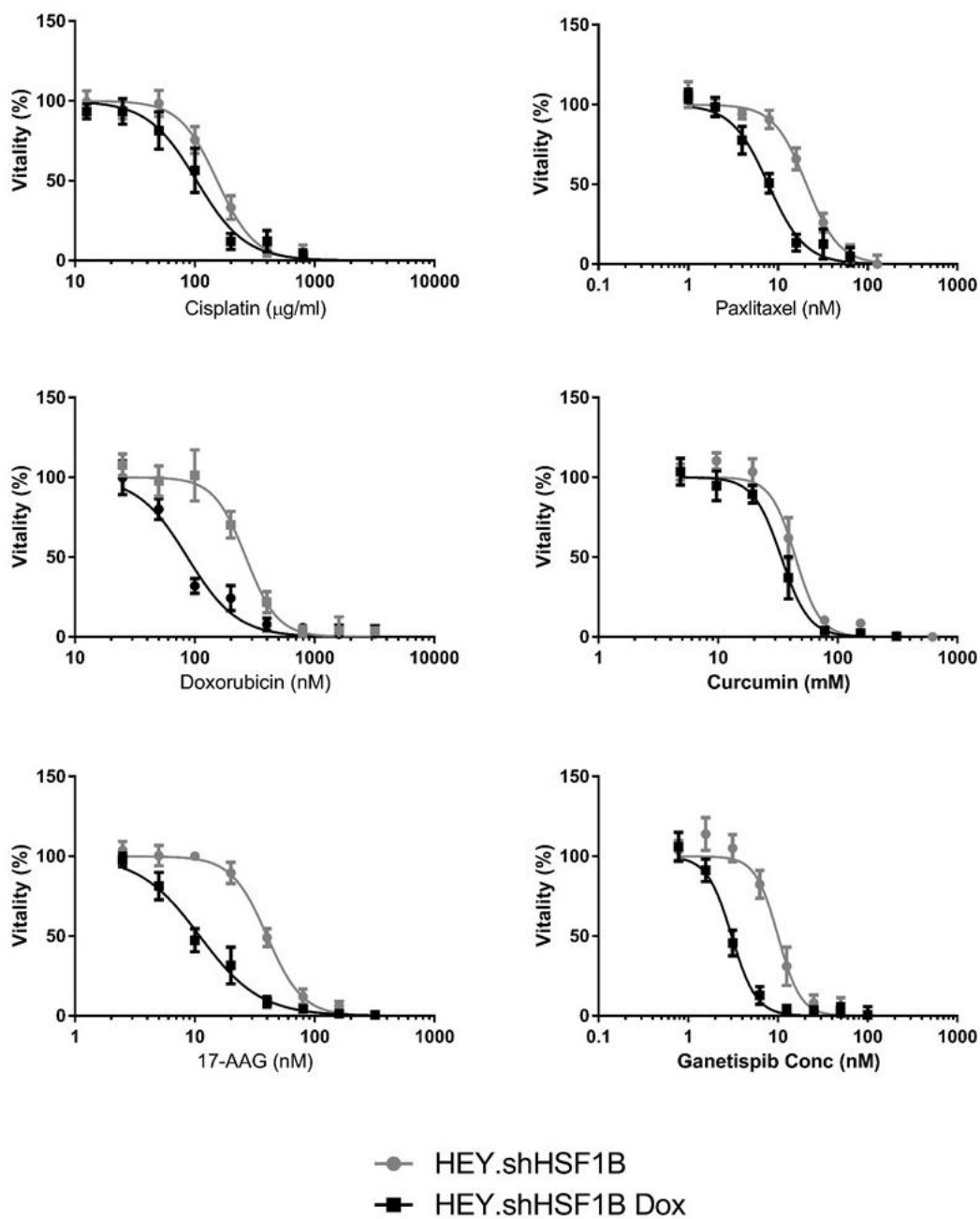


**Figure 4.9. Effect of HSF1 Knockdown on HEY.shHSF1B Dose Response.** HEY.shHSF1B cells were treated with or without doxycycline and then treated with serial dilutions of different drugs. After a 16 hour incubation, viability of the cells was assessed by PrestoBlue® assay.

**Table 4.1. IC50 Values with and without HSF1 Knockdown**

Dox	HEY.shHSF1B		SKOV3.shHSF1B	
	-	+	-	+
Cisplatin	153.6µg/ml	103.4µg/ml	294.4µg/ml	137.7µg/ml
*Paxlitaxel	20.8nM	7.8nM	18.5nM	6.6nM
*Doxorubicin	267.1nM	86.7nM	221.1nM	67.7nM
Curcumin	44.3mM	33.7mM	28.7mM	18.5mM
*17-AAG	40.07nM	10.98nM	82.72nM	23.4nM
*Ganetespib	10nM	3.05nM	7.96nM	2.76nM

\*Denotes significant difference between doxycycline treated and untreated as determined by extra sum-of-squares F test (P<0.01).

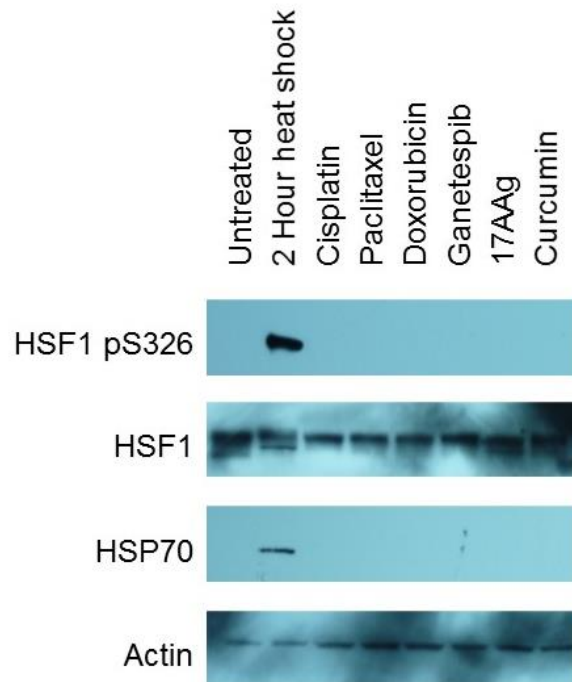


**Figure 4.11. Drug Treatment Does Not Induce HSR.** SKOV3 cells were treated with half the IC50 value for a variety of drugs. After a 16 hour treatment, cells were collected and analyzed by western blot analysis. Untreated cells, and cells that were heat shocked at 42°C for 2 hours followed by a 2 hour recovery were included as controls.

## CHAPTER FIVE: IMPLICATIONS AND FUTURE DIRECTIONS

### Implications for Disorder in HSF Protein Family and Chaperones Studies

#### Role of Disorder and Structure in HSF1 Function

The activation of human HSF1 is a multistep process which includes the conversion of the monomer to a trimer. The trimerization of HSF1 can be induced by elevated temperatures without any cofactors *in vitro* [290]. This serves as the primary step in the activation of HSF1. It was proposed that the HR-A/B and HR-C hydrophobic repeats form a coiled-coil interaction. This is known to stabilize the monomer but dissolves at activating temperatures. This model was supported by initial studies, and was proposed to act as a thermodynamic switch to activate HSF1 [420]. Further studies showed transfected human HSF1 in *Drosophila* cells formed trimers at temperatures below the 42°C activation threshold [421]. This led to the conclusion that trimer formation was not controlled by temperature-dependent unfolding of the inactive HSF1 monomer. Subsequently, a thermally activated model of trimer formation was considered not plausible. More recent research has returned to a model which includes temperature-dependent conformation changes and trimerization [29]. Notably, it was discovered that disassociation of the HR-A/B and HR-C domains occurs slowly at basal temperatures, but usually re-associates before the complete unfolding of the monomer occurs. This is due to the high apparent concentration of the intramolecular interaction. The proposed model based on these findings has the monomer concentration and stability of the unfolded or intermediate forms as limiting factors in the

conversion to trimer. This model allows for both temperature-induced trimerization, and concentration/interaction dependent trimerization.

During activation HSF1 is hyperphosphorylated. However, the role of most of these post-translational modifications in activation is poorly understood. Point mutation studies have shown that most of sites are not individually significant [36]. Assuming trimerization occurs as proposed by Hentze *et al.*, it is possible that the many phosphorylation sites with no known function collectively serve to promote the unfolding of the monomer form, presumably because the hyperphosphorylation is substantial enough to greatly increase the hydrophobicity of the regulatory domain. The increased hydrophobicity in the regulatory domain, which is located between the HR-A/B and HR-C domains, would be expected to promote the unfolded, disordered state. As demonstrated in our work, most of the regulatory domain tends towards disorder based on *in situ* analysis (Figure 2.2). It is reasonable to assume the increased hydrophobicity and charge repulsion would shift the conformation equilibrium toward the unfolded, disordered state. In the Hentze model of trimerization, this would promote the formation of trimers.

### **Potential Benefit of HSF1 Conformation Changes in Activation**

HSF1 conformation and oligomer status is a critical part of its function and regulation in higher organisms. The transition from a monomer to a trimer serves as a primary step in heat shock response activation; however, transition from a monomer to a trimer is not found in lower organisms. In *S. cerevisiae* and *K. lactis*, HSF1 is constitutively a trimer, whereas in metazoans HSF1 trimerization is the first activation step [300, 422]. This suggests that the regulation of HSF1 trimerization is a more recently evolved step of HSF1 activation. This is further supported by the absence of a conserved HR-C hydrophobic repeat domain which is critical in the control of the HSF1 oligomer state (Figure 2.5) [292]. The regulation provided by this additional step allows for further tuning of the response in a way that responds to temperature changes in the environment.

Interestingly, this coincides with the ability of organisms to move and seek environments with amendable temperatures. It is possible that organisms with a better ability to choose the environmental temperatures they are exposed to could benefit from a heat shock response with a more specific activation temperature. Possessing a heat shock response with a biological thermo-sensor would allow cells to react directly to heat stress instead of reacting to damage created by heat stress. This would be especially beneficial in organisms which regulate body temperature and have a narrow temperature threshold in which proteome damage begins to occur when exposed to heat stress [423].

## **Implications for HSF1 in Ovarian Cancer**

### **Origin of HSF1 Gene Duplications**

Our work illustrates that HSF1 gene duplications are common in serous ovarian cancer (Figure 3.1). The reason the HSF1 gene copy number is higher than most other genes is not known. The selection of sub populations with specific gene duplications is driven by the advantage those duplications confer [424]. Our study and others show that HSF1 acts to shift the cellular programs toward survival and invasion in cancer, but does not generally act as a prototypical proliferation-promoting oncogene [380, 425-427]. Myc, a well-established oncogene that promotes proliferation, is near the HSF1 locus and might be an implicating factor for the increase in HSF1 gene copy number [428-430]. Myc gene duplication often occurs by translocation [431]. Myc is located at 8q.24.21 and HSF1 is located at 8q24.3. Duplication of Myc by translocation of the distal chromosome 8q arm will subsequently result in HSF1 gene duplication [432]. This notion is supported by the elevated copy number of the distal chromosome 8q arm up to the Myc locus (Figure S2). While it might be happenstance that HSF1 is duplicated in this scenario, our work demonstrates that it substantially modifies serous ovarian cancer behavior.



### **Spheroids as a Model to Study EMT**

The hanging drop spheroid culture method has been established for over a decade but has seen only limited use [369]. It has primarily been proposed as a model for studying rudimentary angiogenesis and drug penetration [433, 434]. More recent bodies of work demonstrate spheroids are useful in studying EMT [168, 435]. Our work augments this and shows that spheroids are a good model for studying EMT in serous ovarian cancer cell lines. This is demonstrated by increased levels of EMT markers in 3D vs 2D cultures (Figure 3.5 and 3.6). The mRNA levels for the *SNAIL*, *TWIST1*, *ZEB1*, and *SLUG* transcription factors, which in part drive EMT, were elevated in spheroid cultures. The increased potential of spheroids to undergo EMT may allow future studies to more robustly examine EMT and uncover aspects not apparent in 2D culture. Future work should continue to establish spheroids as a sound model for emulating the tumor microenvironment and studying EMT. This will allow the simple and economical spheroid model to bridge the gap between 2D culture and animal models.

### **Role of HSF1 in Cancer Treatment**

The ultimate goal for studies examining the role of HSF1 in drug response are finding applications in medicine. There are two ways in which HSF1 could be relevant to cancer treatment. It is possible that HSF1 could be used as a biomarker to guide which therapies are selected. Additionally, HSF1-targeted treatments could be used to sensitize cancers to other chemotherapeutic agents. Currently there are multiple ways HSF1 might be targeted, though none have been tested clinically. HSF1 could be targeted by therapeutic siRNA. However, despite great progress, there are huge challenges that still need to be overcome before siRNA therapy is a plausible treatment [130]. Another approach is through use of small molecule HSF1 inhibitors. There are currently multiple inhibitors already available on the market for research use. These include quercetin, KNK437, triplotide, and MTOR inhibitors which work indirectly to inhibit HSF1

[31, 436, 437]. Unfortunately, these inhibitors all have low specificity and multiple off target effects. Both siRNA and molecular inhibitor methods have shown efficacy in cell culture and xenograft mouse models, but are still far from clinical testing. Multiple studies, including our own, have established that the reduction or inhibition of HSF1 sensitizes cancer to multiple treatments. Research should continue to find a HSF1 inhibitor with relevant clinical applications for cancer patients [115, 139, 438, 439].

Given the strong affect HSF1 has on ovarian cancer cells, it is possible that HSF1 could be a biomarker to predict the behavior of a given cancer case. This has already been established for some cancers; elevated HSF1 is correlated with poor prognosis in esophageal, breast, non-small cell lung, and hepatocellular cancers [140, 440, 441]. While predicting outcomes for individual cases is valuable, it doesn't improve treatment. A more valuable use of HSF1 as a biomarker would be to guide treatment choices for personalized medicine. Our work adds to previous findings that HSF1 plays a role in the sensitivity to multiple drugs [115, 139, 438, 439]. It is possible that HSF1 protein or mRNA levels could be used to better select treatment options.

HSP90 inhibitors are the most likely drug for which HSF1 levels may significantly predict treatment response. Based on our research and that of others, reduced levels of HSF1 increase sensitivity to HSP90 inhibitors 2 – 3 fold (Table 4.1) [419, 442, 443]. It has been reported that HSF1 is activated by HSP90 inhibitors; thereby creating a feedback mechanism to compensate for the loss of chaperone function [387]. Interestingly, our data did not corroborate robust HSF1 activation by HSP90 inhibition. This suggests there may be other or additional causes for the increase in sensitivity. Regardless of the mechanism, cancers with low levels of HSF1 should be more sensitive to HSP90 inhibitor given our findings. In theory, this would make cases with low HSF1 expression good candidates for treatment with HSP90 inhibitors. Surprisingly, phase II clinical trials for HSP90 inhibitors have not selected for cases with low levels of HSF1. This is

most likely because HSP90 inhibitors have been touted as a broad spectrum approach, due to their ability to disrupt a variety of oncogenic signaling pathways [444, 445].

## **Future Studies**

### **Further HSF1 Structure Studies**

The mechanism by which HSF1 converts from the active trimer back into the monomer is not known. Understanding this step would give a more complete idea about how HSF1 is regulated. It would also offer a point for potential therapeutic regulation. Multiple studies have found that formation of the human HSF1 homotrimer is irreversible [29, 290]. This suggests that the active trimer form is more stable and has lower enthalpy. To test this, differential scanning calorimetry should be used to find enthalpy changes between the monomer and trimer states. This would allow the stability of each form to be assessed. I would expect the homotrimer has lower enthalpy and is therefore more stable. This would explain why the trimer will not spontaneously convert to the monomer at lower temperatures. Additionally it would make sense the active form is more stable, as the trimer must be functional during heat stress.

If the differential scanning calorimetry results reveal that reverting from the trimer to monomer form is an energy-intensive process, then it could be assumed that it is an active process *in vitro* requiring ATP, or alternately HSF1 trimers are degraded by the proteasome [59, 60]. To test if the HSF1 trimer is converted back into the monomer within cells, [<sup>35</sup>S] methionine labeling may be required. Cells would be treated with [<sup>35</sup>S]methionine, subsequently heat shocked, and then allowed to recover. Protein lysate would then be separated by native polyacrylamide gel electrophoresis, and the oligomer status of HSF1 determined. If there is any monomeric radiolabeled HSF1 it would indicate the trimer to monomer conversion occurs *in vitro*.

If it is verified that active HSF1 is returned back the monomer, the next step would be to determine which proteins are responsible for converting the trimer to the monomeric form. The most likely candidates are the HSP90 and TRiC chaperone complexes. Both of these chaperone complexes are involved in actively refolding proteins [446, 447]. Additionally, inhibition of these chaperones leads to HSF1 activation [31, 418]. For these reasons, it is possible that chaperones not only provide negative feedback by binding the inactive monomer, but by also actively dismantling HSF1 trimers.

### **Mechanism of HSF1 Effect on EMT**

**Modulation of  $\beta$  Catenin and Wnt Signaling.** HSF1 promotes higher  $\beta$  Catenin levels, thereby supporting the Wnt/ $\beta$  Catenin pathway, and subsequently EMT [448]. This occurs via the HSF1 activation of ELAVL1 gene, not by direct activation of the  $\beta$  Catenin gene. The ELAVL1 protein then escalates  $\beta$  Catenin translation. Wnt/ $\beta$  Catenin signaling has been shown to promote EMT in ovarian cancer [449]. This suggests that it is possible that HSF1 supports EMT indirectly through regulation of  $\beta$  Catenin. Future studies could determine if  $\beta$  Catenin protein levels are reduced after HSF1 knockdown in ovarian cancer cell lines. If so, ELAVL1 mRNA levels should then be assessed under the same conditions to determine if HSF1 knockdown also has reduced ELAVL1 levels. HSF1 ChIP analysis of the ELAVL1 promoter could then be done to verify if the effect occurs by the previously elucidated pathway. Finally,  $\beta$  Catenin could be overexpressed during HSF1 knockdown to determine if HSF1 knockdown effects on EMT can be rescued by  $\beta$  Catenin.

**Direct Activation of EMT Transcription Factors.** Multiple EMT transcription factors have putative heat shock elements (Table S2). It is possible that HSF1 directly facilitates EMT behavior after TGF $\beta$  treatment. While these genes are not upregulated during a classic heat shock response, studies have shown that unique gene sets can be regulated by HSF1 in cancer under

non heat shock conditions [133]. One such EMT related gene, *slug*, has previously been found to be regulated by HSF1 during EMT despite the presence of only a weak heat shock element [450]. To explore this possibility, HSF1 CHIP could be performed to determine if HSF1 is in fact binding to these putative HSEs. These possible EMT-associated HSF1 targets include *fibronectin*, *vimentin*, *SNAIL*, *N-cadherin*, *ZEB*, and *TWIST* (Table S2).

### **Direct Activation of Interleukin Genes**

A less often discussed target of HSF1 and the heat shock response is the interleukin family of cytokines. These cytokines regulate the inflammatory and immune response [451]. These cytokines were first discovered in leukocytes, but have since been found to be produced by a wide variety of cells. Interleukins have been shown to have a significant and complicated role in cancer biology [452]. While some members of the interleukin family can be used to treat tumors, others are associated with tumorigenesis and poor patient outcomes [452]. Among interleukins involved in cancer, IL-8 and IL-6 are well understood to promote oncogenic behavior in ovarian cancer [453, 454]. IL-8 promotes anchorage-independent growth, while IL-6 promotes STAT3-driven proliferation [455, 456]. HSF1 has previously been reported to co-activate the IL-8 and IL-6 genes, and may be doing so during EMT [48, 120, 456]. To investigate this, qPCR could be used to determine if TGF $\beta$  induces IL-8 and IL-6 in SKOV-3 and HEY ovarian cancer cell lines. If IL-8 and IL-6 are induced, CHIP could be used to see if HSF1 is binding the HSEs within the IL-8 and IL-6 promoters during TGF $\beta$ -induced EMT.

## REFERENCES

1. Ritossa, F., *Discovery of the heat shock response*. Cell Stress Chaperones, 1996. **1**(2): p. 97-8.
2. Ritossa, F.M., *Behaviour of Rna and DNA Synthesis at the Puff Level in Salivary Gland Chromosomes of Drosophila*. Exp Cell Res, 1964. **36**: p. 515-23.
3. Ritossa, F.M., *Experimental Activation of Specific Loci in Polytene Chromosomes of Drosophila*. Exp Cell Res, 1964. **35**: p. 601-7.
4. McKenzie, S.L., S. Henikoff, and M. Meselson, *Localization of RNA from heat-induced polysomes at puff sites in Drosophila melanogaster*. Proc Natl Acad Sci U S A, 1975. **72**(3): p. 1117-21.
5. Bardwell, J.C. and E.A. Craig, *Major heat shock gene of Drosophila and the Escherichia coli heat-inducible dnaK gene are homologous*. Proc Natl Acad Sci U S A, 1984. **81**(3): p. 848-52.
6. Silver, P.A. and J.C. Way, *Eukaryotic DnaJ homologs and the specificity of Hsp70 activity*. Cell, 1993. **74**(1): p. 5-6.
7. Craig, E.A., *The heat shock response*. CRC Crit Rev Biochem, 1985. **18**(3): p. 239-80.
8. Ellis, J., *Proteins as molecular chaperones*. Nature, 1987. **328**(6129): p. 378-9.
9. Pelham, H.R., *Speculations on the functions of the major heat shock and glucose-regulated proteins*. Cell, 1986. **46**(7): p. 959-61.
10. Mirault, M.E., R. Southgate, and E. Delwart, *Regulation of heat-shock genes: a DNA sequence upstream of Drosophila hsp70 genes is essential for their induction in monkey cells*. EMBO J, 1982. **1**(10): p. 1279-85.
11. Wu, B.J., R.E. Kingston, and R.I. Morimoto, *Human HSP70 promoter contains at least two distinct regulatory domains*. Proc Natl Acad Sci U S A, 1986. **83**(3): p. 629-33.
12. Tanguay, R.M., *Transcriptional activation of heat-shock genes in eukaryotes*. Biochem Cell Biol, 1988. **66**(6): p. 584-93.
13. Akerfelt, M., R.I. Morimoto, and L. Sistonen, *Heat shock factors: integrators of cell stress, development and lifespan*. Nat Rev Mol Cell Biol, 2010. **11**(8): p. 545-55.
14. Wu, C., *An exonuclease protection assay reveals heat-shock element and TATA box DNA-binding proteins in crude nuclear extracts*. Nature, 1985. **317**(6032): p. 84-7.
15. Parker, C.S. and J. Topol, *A Drosophila RNA polymerase II transcription factor binds to the regulatory site of an hsp 70 gene*. Cell, 1984. **37**(1): p. 273-83.
16. Topol, J., D.M. Ruden, and C.S. Parker, *Sequences required for in vitro transcriptional activation of a Drosophila hsp 70 gene*. Cell, 1985. **42**(2): p. 527-37.
17. Goldenberg, C.J., et al., *Purified human factor activates heat shock promoter in a HeLa cell-free transcription system*. J Biol Chem, 1988. **263**(36): p. 19734-9.
18. Pirkkala, L., P. Nykanen, and L. Sistonen, *Roles of the heat shock transcription factors in regulation of the heat shock response and beyond*. FASEB J, 2001. **15**(7): p. 1118-31.
19. McMillan, D.R., et al., *Targeted disruption of heat shock transcription factor 1 abolishes thermotolerance and protection against heat-inducible apoptosis*. J Biol Chem, 1998. **273**(13): p. 7523-8.
20. Xiao, X., et al., *HSF1 is required for extra-embryonic development, postnatal growth and protection during inflammatory responses in mice*. EMBO J, 1999. **18**(21): p. 5943-52.
21. Vujanac, M., A. Fenaroli, and V. Zimarino, *Constitutive nuclear import and stress-regulated nucleocytoplasmic shuttling of mammalian heat-shock factor 1*. Traffic, 2005. **6**(3): p. 214-29.

22. Sarge, K.D., S.P. Murphy, and R.I. Morimoto, *Activation of heat shock gene transcription by heat shock factor 1 involves oligomerization, acquisition of DNA-binding activity, and nuclear localization and can occur in the absence of stress*. Mol Cell Biol, 1993. **13**(3): p. 1392-407.
23. Amin, J., J. Ananthan, and R. Voellmy, *Key features of heat shock regulatory elements*. Mol Cell Biol, 1988. **8**(9): p. 3761-9.
24. Xiao, H. and J.T. Lis, *Germline transformation used to define key features of heat-shock response elements*. Science, 1988. **239**(4844): p. 1139-42.
25. Wu, C., *Heat shock transcription factors: structure and regulation*. Annu Rev Cell Dev Biol, 1995. **11**: p. 441-69.
26. Westerheide, S.D., et al., *Stress-inducible regulation of heat shock factor 1 by the deacetylase SIRT1*. Science, 2009. **323**(5917): p. 1063-6.
27. Shi, Y., D.D. Mosser, and R.I. Morimoto, *Molecular chaperones as HSF1-specific transcriptional repressors*. Genes Dev, 1998. **12**(5): p. 654-66.
28. Yang, J., et al., *Riluzole increases the amount of latent HSF1 for an amplified heat shock response and cytoprotection*. PLoS One, 2008. **3**(8): p. e2864.
29. Hentze, N., et al., *Molecular mechanism of thermosensory function of human heat shock transcription factor Hsf1*. Elife, 2016. **5**.
30. Ali, A., et al., *HSP90 interacts with and regulates the activity of heat shock factor 1 in Xenopus oocytes*. Mol Cell Biol, 1998. **18**(9): p. 4949-60.
31. Neef, D.W., et al., *A direct regulatory interaction between chaperonin TRiC and stress-responsive transcription factor HSF1*. Cell Rep, 2014. **9**(3): p. 955-66.
32. Jurivich, D.A., et al., *Effect of sodium salicylate on the human heat shock response*. Science, 1992. **255**(5049): p. 1243-5.
33. Cotto, J., S. Fox, and R. Morimoto, *HSF1 granules: a novel stress-induced nuclear compartment of human cells*. J Cell Sci, 1997. **110 ( Pt 23)**: p. 2925-34.
34. Kline, M.P. and R.I. Morimoto, *Repression of the heat shock factor 1 transcriptional activation domain is modulated by constitutive phosphorylation*. Mol Cell Biol, 1997. **17**(4): p. 2107-15.
35. Holmberg, C.I., et al., *Phosphorylation of serine 230 promotes inducible transcriptional activity of heat shock factor 1*. EMBO J, 2001. **20**(14): p. 3800-10.
36. Xu, Y.M., et al., *Post-translational modification of human heat shock factors and their functions: a recent update by proteomic approach*. J Proteome Res, 2012. **11**(5): p. 2625-34.
37. Dayalan Naidu, S., et al., *Heat Shock Factor 1 Is a Substrate for p38 Mitogen-Activated Protein Kinases*. Mol Cell Biol, 2016. **36**(18): p. 2403-17.
38. Chou, S.D., et al., *mTOR is essential for the proteotoxic stress response, HSF1 activation and heat shock protein synthesis*. PLoS One, 2012. **7**(6): p. e39679.
39. Zhang, Y., et al., *Protein kinase A regulates molecular chaperone transcription and protein aggregation*. PLoS One, 2011. **6**(12): p. e28950.
40. Murshid, A., et al., *Protein kinase A binds and activates heat shock factor 1*. PLoS One, 2010. **5**(11): p. e13830.
41. Guettouche, T., et al., *Analysis of phosphorylation of human heat shock factor 1 in cells experiencing a stress*. BMC Biochem, 2005. **6**: p. 4.
42. Wang, X., et al., *Interactions between extracellular signal-regulated protein kinase 1, 14-3-3epsilon, and heat shock factor 1 during stress*. J Biol Chem, 2004. **279**(47): p. 49460-9.
43. Wang, X., et al., *Regulation of molecular chaperone gene transcription involves the serine phosphorylation, 14-3-3 epsilon binding, and cytoplasmic sequestration of heat shock factor 1*. Mol Cell Biol, 2003. **23**(17): p. 6013-26.

44. Biamonti, G. and C. Vourc'h, *Nuclear stress bodies*. Cold Spring Harb Perspect Biol, 2010. **2**(6): p. a000695.
45. Goenka, A., et al., *Human satellite-III non-coding RNAs modulate heat-shock-induced transcriptional repression*. J Cell Sci, 2016. **129**(19): p. 3541-3552.
46. Jaeger, A.M., et al., *Genomic heat shock element sequences drive cooperative human heat shock factor 1 DNA binding and selectivity*. J Biol Chem, 2014. **289**(44): p. 30459-69.
47. Crinelli, R., et al., *Molecular Dissection of the Human Ubiquitin C Promoter Reveals Heat Shock Element Architectures with Activating and Repressive Functions*. PLoS One, 2015. **10**(8): p. e0136882.
48. Maity, T.K., et al., *Distinct, gene-specific effect of heat shock on heat shock factor-1 recruitment and gene expression of CXC chemokine genes*. Cytokine, 2011. **54**(1): p. 61-7.
49. Damberger, F.F., et al., *Solution structure of the DNA-binding domain of the heat shock transcription factor determined by multidimensional heteronuclear magnetic resonance spectroscopy*. Protein Sci, 1994. **3**(10): p. 1806-21.
50. Littlefield, O. and H.C. Nelson, *A new use for the 'wing' of the 'winged' helix-turn-helix motif in the HSF-DNA cocystal*. Nat Struct Biol, 1999. **6**(5): p. 464-70.
51. Vihervaara, A., et al., *Transcriptional response to stress in the dynamic chromatin environment of cycling and mitotic cells*. Proc Natl Acad Sci U S A, 2013. **110**(36): p. E3388-97.
52. Xiao, H., O. Perisic, and J.T. Lis, *Cooperative binding of Drosophila heat shock factor to arrays of a conserved 5 bp unit*. Cell, 1991. **64**(3): p. 585-93.
53. Zou, J., et al., *Repression of heat shock transcription factor HSF1 activation by HSP90 (HSP90 complex) that forms a stress-sensitive complex with HSF1*. Cell, 1998. **94**(4): p. 471-80.
54. Abravaya, K., et al., *The human heat shock protein hsp70 interacts with HSF, the transcription factor that regulates heat shock gene expression*. Genes Dev, 1992. **6**(7): p. 1153-64.
55. Wang, X., et al., *Phosphorylation of HSF1 by MAPK-activated protein kinase 2 on serine 121, inhibits transcriptional activity and promotes HSP90 binding*. J Biol Chem, 2006. **281**(2): p. 782-91.
56. Baler, R., J. Zou, and R. Voellmy, *Evidence for a role of Hsp70 in the regulation of the heat shock response in mammalian cells*. Cell Stress Chaperones, 1996. **1**(1): p. 33-9.
57. Raychaudhuri, S., et al., *Interplay of acetyltransferase EP300 and the proteasome system in regulating heat shock transcription factor 1*. Cell, 2014. **156**(5): p. 975-85.
58. Raynes, R., et al., *The SIRT1 modulators AROS and DBC1 regulate HSF1 activity and the heat shock response*. PLoS One, 2013. **8**(1): p. e54364.
59. Hu, Y. and N.F. Mivechi, *Promotion of heat shock factor Hsf1 degradation via adaptor protein filamin A-interacting protein 1-like (FILIP-1L)*. J Biol Chem, 2011. **286**(36): p. 31397-408.
60. Kim, E., et al., *NEDD4-mediated HSF1 degradation underlies alpha-synucleinopathy*. Hum Mol Genet, 2016. **25**(2): p. 211-22.
61. Kazemi, Z., et al., *O-linked beta-N-acetylglucosamine (O-GlcNAc) regulates stress-induced heat shock protein expression in a GSK-3beta-dependent manner*. J Biol Chem, 2010. **285**(50): p. 39096-107.
62. Hietakangas, V., et al., *Phosphorylation of serine 303 is a prerequisite for the stress-inducible SUMO modification of heat shock factor 1*. Mol Cell Biol, 2003. **23**(8): p. 2953-68.
63. Brunet Simioni, M., et al., *Heat shock protein 27 is involved in SUMO-2/3 modification of heat shock factor 1 and thereby modulates the transcription factor activity*. Oncogene, 2009. **28**(37): p. 3332-44.
64. Ehrnsperger, M., M. Gaestel, and J. Buchner, *Analysis of chaperone properties of small Hsp's*. Methods Mol Biol, 2000. **99**: p. 421-9.



65. Van Montfort, R., C. Slingsby, and E. Vierling, *Structure and function of the small heat shock protein/alpha-crystallin family of molecular chaperones*. Adv Protein Chem, 2001. **59**: p. 105-56.
66. Jakob, U., et al., *Small heat shock proteins are molecular chaperones*. J Biol Chem, 1993. **268**(3): p. 1517-20.
67. Lelj-Garolla, B. and A.G. Mauk, *Roles of the N- and C-terminal sequences in Hsp27 self-association and chaperone activity*. Protein Sci, 2012. **21**(1): p. 122-33.
68. Wettstein, G., et al., *Small heat shock proteins and the cytoskeleton: an essential interplay for cell integrity?* Int J Biochem Cell Biol, 2012. **44**(10): p. 1680-6.
69. Bitar, K.N., *HSP27 phosphorylation and interaction with actin-myosin in smooth muscle contraction*. Am J Physiol Gastrointest Liver Physiol, 2002. **282**(5): p. G894-903.
70. Pandey, P., et al., *Hsp27 functions as a negative regulator of cytochrome c-dependent activation of procaspase-3*. Oncogene, 2000. **19**(16): p. 1975-81.
71. Tsai, J. and M.G. Douglas, *A conserved HPD sequence of the J-domain is necessary for YDJ1 stimulation of Hsp70 ATPase activity at a site distinct from substrate binding*. J Biol Chem, 1996. **271**(16): p. 9347-54.
72. Kampinga, H.H. and E.A. Craig, *The HSP70 chaperone machinery: J proteins as drivers of functional specificity*. Nat Rev Mol Cell Biol, 2010. **11**(8): p. 579-92.
73. Ajit Tamadaddi, C. and C. Sahi, *J domain independent functions of J proteins*. Cell Stress Chaperones, 2016. **21**(4): p. 563-70.
74. Rudiger, S., A. Buchberger, and B. Bukau, *Interaction of Hsp70 chaperones with substrates*. Nat Struct Biol, 1997. **4**(5): p. 342-9.
75. Garrido, C., et al., *Heat shock proteins 27 and 70: anti-apoptotic proteins with tumorigenic properties*. Cell Cycle, 2006. **5**(22): p. 2592-601.
76. Elsner, L., et al., *The endogenous danger signals HSP70 and MICA cooperate in the activation of cytotoxic effector functions of NK cells*. J Cell Mol Med, 2010. **14**(4): p. 992-1002.
77. Zhao, R., et al., *Navigating the chaperone network: an integrative map of physical and genetic interactions mediated by the hsp90 chaperone*. Cell, 2005. **120**(5): p. 715-27.
78. McClellan, A.J., et al., *Diverse cellular functions of the Hsp90 molecular chaperone uncovered using systems approaches*. Cell, 2007. **131**(1): p. 121-35.
79. Wandinger, S.K., K. Richter, and J. Buchner, *The Hsp90 chaperone machinery*. J Biol Chem, 2008. **283**(27): p. 18473-7.
80. Wang, X.Y. and J.R. Subjeck, *High molecular weight stress proteins: Identification, cloning and utilisation in cancer immunotherapy*. Int J Hyperthermia, 2013. **29**(5): p. 364-75.
81. Easton, D.P., Y. Kaneko, and J.R. Subjeck, *The hsp110 and Grp1 70 stress proteins: newly recognized relatives of the Hsp70s*. Cell Stress Chaperones, 2000. **5**(4): p. 276-90.
82. Oh, H.J., X. Chen, and J.R. Subjeck, *Hsp110 protects heat-denatured proteins and confers cellular thermoresistance*. J Biol Chem, 1997. **272**(50): p. 31636-40.
83. Zuo, D., J. Subjeck, and X.Y. Wang, *Unfolding the Role of Large Heat Shock Proteins: New Insights and Therapeutic Implications*. Front Immunol, 2016. **7**: p. 75.
84. Hartl, F.U., *Molecular chaperones in cellular protein folding*. Nature, 1996. **381**(6583): p. 571-9.
85. Lee, Y.J., et al., *HSF1 as a mitotic regulator: phosphorylation of HSF1 by Plk1 is essential for mitotic progression*. Cancer Res, 2008. **68**(18): p. 7550-60.
86. Uchiyama, T., et al., *Constitutively active heat shock factor 1 enhances glucose-driven insulin secretion*. Metabolism, 2011. **60**(6): p. 789-98.
87. Takaki, E., et al., *Heat shock transcription factor 1 is required for maintenance of ciliary beating in mice*. J Biol Chem, 2007. **282**(51): p. 37285-92.

88. Li, Q. and J.D. Martinez, *P53 is transported into the nucleus via an Hsf1-dependent nuclear localization mechanism*. Mol Carcinog, 2011. **50**(2): p. 143-52.
89. Liu, Y. and A. Chang, *Heat shock response relieves ER stress*. EMBO J, 2008. **27**(7): p. 1049-59.
90. Tong, Z., et al., *HSF-1 is involved in attenuating the release of inflammatory cytokines induced by LPS through regulating autophagy*. Shock, 2014. **41**(5): p. 449-53.
91. Dokladny, K., et al., *LPS-induced cytokine levels are repressed by elevated expression of HSP70 in rats: possible role of NF-kappaB*. Cell Stress Chaperones, 2010. **15**(2): p. 153-63.
92. Cooper, Z.A., et al., *Febrile-range temperature modifies cytokine gene expression in LPS-stimulated macrophages by differentially modifying NF-kappaB recruitment to cytokine gene promoters*. Am J Physiol Cell Physiol, 2010. **298**(1): p. C171-81.
93. Singh, I.S., et al., *Inhibition of tumor necrosis factor-alpha transcription in macrophages exposed to febrile range temperature. A possible role for heat shock factor-1 as a negative transcriptional regulator*. J Biol Chem, 2000. **275**(13): p. 9841-8.
94. Xie, Y., et al., *Heat shock factor 1 represses transcription of the IL-1beta gene through physical interaction with the nuclear factor of interleukin 6*. J Biol Chem, 2002. **277**(14): p. 11802-10.
95. Inouye, S., et al., *Heat shock transcription factor 1 opens chromatin structure of interleukin-6 promoter to facilitate binding of an activator or a repressor*. J Biol Chem, 2007. **282**(45): p. 33210-7.
96. Takii, R., et al., *Heat shock transcription factor 1 inhibits expression of IL-6 through activating transcription factor 3*. J Immunol, 2010. **184**(2): p. 1041-8.
97. Muralidharan, S., et al., *Moderate alcohol induces stress proteins HSF1 and hsp70 and inhibits proinflammatory cytokines resulting in endotoxin tolerance*. J Immunol, 2014. **193**(4): p. 1975-87.
98. Fattori, E., et al., *Functional analysis of IL-6 and IL-6DBP/C/EBP beta by gene targeting*. Ann N Y Acad Sci, 1995. **762**: p. 262-73.
99. Wang, Y., et al., *Role of C/EBP homologous protein and endoplasmic reticulum stress in asthma exacerbation by regulating the IL-4/signal transducer and activator of transcription 6/transcription factor EC/IL-4 receptor alpha positive feedback loop in M2 macrophages*. J Allergy Clin Immunol, 2017.
100. van der Krieken, S.E., et al., *CCAAT/enhancer binding protein beta in relation to ER stress, inflammation, and metabolic disturbances*. Biomed Res Int, 2015. **2015**: p. 324815.
101. Xie, Y., et al., *Heat shock factor 1 contains two functional domains that mediate transcriptional repression of the c-fos and c-fms genes*. J Biol Chem, 2003. **278**(7): p. 4687-98.
102. Zhang, L., et al., *HSF1 regulates expression of G-CSF through the binding element for NF-IL6/CCAAT enhancer binding protein beta*. Mol Cell Biochem, 2011. **352**(1-2): p. 11-7.
103. Li, H., et al., *Inhibition of the JNK/Bim pathway by Hsp70 prevents Bax activation in UV-induced apoptosis*. FEBS Lett, 2010. **584**(22): p. 4672-8.
104. Stankiewicz, A.R., et al., *Hsp70 inhibits heat-induced apoptosis upstream of mitochondria by preventing Bax translocation*. J Biol Chem, 2005. **280**(46): p. 38729-39.
105. Saleh, A., et al., *Negative regulation of the Apaf-1 apoptosome by Hsp70*. Nat Cell Biol, 2000. **2**(8): p. 476-83.
106. Ravagnan, L., et al., *Heat-shock protein 70 antagonizes apoptosis-inducing factor*. Nat Cell Biol, 2001. **3**(9): p. 839-43.
107. Johnson, T.R., et al., *The proteasome inhibitor PS-341 overcomes TRAIL resistance in Bax and caspase 9-negative or Bcl-xL overexpressing cells*. Oncogene, 2003. **22**(32): p. 4953-63.
108. Charette, S.J. and J. Landry, *The interaction of HSP27 with Daxx identifies a potential regulatory role of HSP27 in Fas-induced apoptosis*. Ann N Y Acad Sci, 2000. **926**: p. 126-31.

109. Voss, O.H., et al., *Binding of caspase-3 prodomain to heat shock protein 27 regulates monocyte apoptosis by inhibiting caspase-3 proteolytic activation*. J Biol Chem, 2007. **282**(34): p. 25088-99.
110. Paul, C., et al., *Hsp27 as a negative regulator of cytochrome C release*. Mol Cell Biol, 2002. **22**(3): p. 816-34.
111. Jacobs, A.T. and L.J. Marnett, *HSF1-mediated BAG3 expression attenuates apoptosis in 4-hydroxynonenal-treated colon cancer cells via stabilization of anti-apoptotic Bcl-2 proteins*. J Biol Chem, 2009. **284**(14): p. 9176-83.
112. Franceschelli, S., et al., *Bag3 gene expression is regulated by heat shock factor 1*. J Cell Physiol, 2008. **215**(3): p. 575-7.
113. Liang, W., et al., *Heat shock factor 1 inhibits the mitochondrial apoptosis pathway by regulating second mitochondria-derived activator of caspase to promote pancreatic tumorigenesis*. J Exp Clin Cancer Res, 2017. **36**(1): p. 64.
114. Degenhardt, K., et al., *Autophagy promotes tumor cell survival and restricts necrosis, inflammation, and tumorigenesis*. Cancer Cell, 2006. **10**(1): p. 51-64.
115. Desai, S., et al., *Heat shock factor 1 (HSF1) controls chemoresistance and autophagy through transcriptional regulation of autophagy-related protein 7 (ATG7)*. J Biol Chem, 2013. **288**(13): p. 9165-76.
116. Watanabe, Y., et al., *HSF1 stress response pathway regulates autophagy receptor SQSTM1/p62-associated proteostasis*. Autophagy, 2017. **13**(1): p. 133-148.
117. Kim, E.H., et al., *Heat shock factor 1-mediated aneuploidy requires a defective function of p53*. Cancer Res, 2009. **69**(24): p. 9404-12.
118. Dai, B., et al., *Forkhead box M1 is regulated by heat shock factor 1 and promotes glioma cells survival under heat shock stress*. J Biol Chem, 2013. **288**(3): p. 1634-42.
119. Lee, Y.J., et al., *A novel function for HSF1-induced mitotic exit failure and genomic instability through direct interaction between HSF1 and Cdc20*. Oncogene, 2008. **27**(21): p. 2999-3009.
120. Rokavec, M., W. Wu, and J.L. Luo, *IL6-mediated suppression of miR-200c directs constitutive activation of inflammatory signaling circuit driving transformation and tumorigenesis*. Mol Cell, 2012. **45**(6): p. 777-89.
121. Jin, X., D. Moskophidis, and N.F. Mivechi, *Heat shock transcription factor 1 is a key determinant of HCC development by regulating hepatic steatosis and metabolic syndrome*. Cell Metab, 2011. **14**(1): p. 91-103.
122. Li, J., J. Labbadia, and R.I. Morimoto, *Rethinking HSF1 in Stress, Development, and Organismal Health*. Trends Cell Biol, 2017.
123. Akerfelt, M., et al., *Heat shock factors at a crossroad between stress and development*. Ann N Y Acad Sci, 2007. **1113**: p. 15-27.
124. Cui, J., H. Tian, and G. Chen, *Upregulation of Nuclear Heat Shock Factor 1 Contributes to Tumor Angiogenesis and Poor Survival in Patients With Non-Small Cell Lung Cancer*. Ann Thorac Surg, 2015. **100**(2): p. 465-72.
125. Hoang, A.T., et al., *A novel association between the human heat shock transcription factor 1 (HSF1) and prostate adenocarcinoma*. Am J Pathol, 2000. **156**(3): p. 857-64.
126. Cen, H., et al., *Induction of HSF1 expression is associated with sporadic colorectal cancer*. World J Gastroenterol, 2004. **10**(21): p. 3122-6.
127. Ciocca, D.R., et al., *Co-expression of steroid receptors (estrogen receptor alpha and/or progesterone receptors) and Her-2/neu: Clinical implications*. J Steroid Biochem Mol Biol, 2006. **102**(1-5): p. 32-40.
128. Ishiwata, J., et al., *State of heat shock factor 1 expression as a putative diagnostic marker for oral squamous cell carcinoma*. Int J Oncol, 2012. **40**(1): p. 47-52.

129. Fang, F., R. Chang, and L. Yang, *Heat shock factor 1 promotes invasion and metastasis of hepatocellular carcinoma in vitro and in vivo*. *Cancer*, 2012. **118**(7): p. 1782-94.
130. Heimberger, T., et al., *The heat shock transcription factor 1 as a potential new therapeutic target in multiple myeloma*. *Br J Haematol*, 2013. **160**(4): p. 465-76.
131. Dai, C., et al., *Loss of tumor suppressor NF1 activates HSF1 to promote carcinogenesis*. *J Clin Invest*, 2012. **122**(10): p. 3742-54.
132. Chen, Y.F., et al., *Nucleoside analog inhibits microRNA-214 through targeting heat-shock factor 1 in human epithelial ovarian cancer*. *Cancer Sci*, 2013. **104**(12): p. 1683-9.
133. Mendillo, M.L., et al., *HSF1 drives a transcriptional program distinct from heat shock to support highly malignant human cancers*. *Cell*, 2012. **150**(3): p. 549-62.
134. Santagata, S., et al., *High levels of nuclear heat-shock factor 1 (HSF1) are associated with poor prognosis in breast cancer*. *Proc Natl Acad Sci U S A*, 2011. **108**(45): p. 18378-83.
135. Wu, J., et al., *Heat Shock Proteins and Cancer*. *Trends Pharmacol Sci*, 2017. **38**(3): p. 226-256.
136. Dai, C., et al., *Heat shock factor 1 is a powerful multifaceted modifier of carcinogenesis*. *Cell*, 2007. **130**(6): p. 1005-18.
137. Solimini, N.L., J. Luo, and S.J. Elledge, *Non-oncogene addiction and the stress phenotype of cancer cells*. *Cell*, 2007. **130**(6): p. 986-8.
138. Jiang, S., et al., *Multifaceted roles of HSF1 in cancer*. *Tumour Biol*, 2015. **36**(7): p. 4923-31.
139. Vydra, N., et al., *Overexpression of Heat Shock Transcription Factor 1 enhances the resistance of melanoma cells to doxorubicin and paclitaxel*. *BMC Cancer*, 2013. **13**: p. 504.
140. Xi, C., et al., *Heat shock factor Hsf1 cooperates with ErbB2 (Her2/Neu) protein to promote mammary tumorigenesis and metastasis*. *J Biol Chem*, 2012. **287**(42): p. 35646-57.
141. Chuma, M., et al., *Heat shock factor 1 accelerates hepatocellular carcinoma development by activating nuclear factor-kappaB/mitogen-activated protein kinase*. *Carcinogenesis*, 2014. **35**(2): p. 272-81.
142. Schopf, F.H., M.M. Biebl, and J. Buchner, *The HSP90 chaperone machinery*. *Nat Rev Mol Cell Biol*, 2017. **18**(6): p. 345-360.
143. Howlader N, N.A., Krapcho M, Miller D, Bishop K, Kosary CL, Yu M, Ruhl J, Tatalovich Z, Mariotto A, Lewis DR, Chen HS, Feuer EJ, Cronin KA (eds). *SEER Cancer Statistics Review, 1975-2014*. 2017.
144. Torre, L.A., et al., *Global cancer statistics, 2012*. *CA Cancer J Clin*, 2015. **65**(2): p. 87-108.
145. Leung, F., E.P. Diamandis, and V. Kulasingam, *Ovarian cancer biomarkers: current state and future implications from high-throughput technologies*. *Adv Clin Chem*, 2014. **66**: p. 25-77.
146. Matulonis, U.A., et al., *Ovarian cancer*. *Nat Rev Dis Primers*, 2016. **2**: p. 16061.
147. Koshiyama, M., N. Matsumura, and I. Konishi, *Subtypes of Ovarian Cancer and Ovarian Cancer Screening*. *Diagnostics (Basel)*, 2017. **7**(1).
148. Ramalingam, P., *Morphologic, Immunophenotypic, and Molecular Features of Epithelial Ovarian Cancer*. *Oncology (Williston Park)*, 2016. **30**(2): p. 166-76.
149. Klotz, D.M. and P. Wimberger, *Cells of origin of ovarian cancer: ovarian surface epithelium or fallopian tube?* *Arch Gynecol Obstet*, 2017.
150. Oren, M. and V. Rotter, *Mutant p53 gain-of-function in cancer*. *Cold Spring Harb Perspect Biol*, 2010. **2**(2): p. a001107.
151. Biegging, K.T., S.S. Mello, and L.D. Attardi, *Unravelling mechanisms of p53-mediated tumour suppression*. *Nat Rev Cancer*, 2014. **14**(5): p. 359-70.
152. Herzog, T.J. and B.J. Monk, *Bringing new medicines to women with epithelial ovarian cancer: what is the unmet medical need?* *Gynecol Oncol Res Pract*, 2017. **4**: p. 13.
153. Lamouille, S., J. Xu, and R. Derynck, *Molecular mechanisms of epithelial-mesenchymal transition*. *Nat Rev Mol Cell Biol*, 2014. **15**(3): p. 178-96.

154. Mani, S.A., et al., *The epithelial-mesenchymal transition generates cells with properties of stem cells*. Cell, 2008. **133**(4): p. 704-15.
155. Shirkoohi, R., *Epithelial mesenchymal transition from a natural gestational orchestration to a bizarre cancer disturbance*. Cancer Sci, 2013. **104**(1): p. 28-35.
156. Sabe, H., *Cancer early dissemination: cancerous epithelial-mesenchymal transdifferentiation and transforming growth factor beta signalling*. J Biochem, 2011. **149**(6): p. 633-9.
157. Auersperg, N., et al., *Ovarian surface epithelium: biology, endocrinology, and pathology*. Endocr Rev, 2001. **22**(2): p. 255-88.
158. Lengyel, E., *Ovarian cancer development and metastasis*. Am J Pathol, 2010. **177**(3): p. 1053-64.
159. Matte, I., et al., *Ovarian cancer ascites enhance the migration of patient-derived peritoneal mesothelial cells via cMet pathway through HGF-dependent and -independent mechanisms*. Int J Cancer, 2015. **137**(2): p. 289-98.
160. Kolomeyevskaya, N., et al., *Cytokine profiling of ascites at primary surgery identifies an interaction of tumor necrosis factor-alpha and interleukin-6 in predicting reduced progression-free survival in epithelial ovarian cancer*. Gynecol Oncol, 2015. **138**(2): p. 352-7.
161. Huang, R.Y., P. Guilford, and J.P. Thiery, *Early events in cell adhesion and polarity during epithelial-mesenchymal transition*. J Cell Sci, 2012. **125**(Pt 19): p. 4417-22.
162. Theveneau, E. and R. Mayor, *Cadherins in collective cell migration of mesenchymal cells*. Curr Opin Cell Biol, 2012. **24**(5): p. 677-84.
163. Maschler, S., et al., *Tumor cell invasiveness correlates with changes in integrin expression and localization*. Oncogene, 2005. **24**(12): p. 2032-41.
164. Peinado, H., D. Olmeda, and A. Cano, *Snail, Zeb and bHLH factors in tumour progression: an alliance against the epithelial phenotype?* Nat Rev Cancer, 2007. **7**(6): p. 415-28.
165. Postigo, A.A., et al., *Regulation of Smad signaling through a differential recruitment of coactivators and corepressors by ZEB proteins*. EMBO J, 2003. **22**(10): p. 2453-62.
166. Kim, S.A., E.K. Lee, and H.J. Kuh, *Co-culture of 3D tumor spheroids with fibroblasts as a model for epithelial-mesenchymal transition in vitro*. Exp Cell Res, 2015. **335**(2): p. 187-96.
167. Giarnieri, E., et al., *EMT markers in lung adenocarcinoma pleural effusion spheroid cells*. J Cell Physiol, 2013. **228**(8): p. 1720-6.
168. Rafehi, S., et al., *TGFbeta signaling regulates epithelial-mesenchymal plasticity in ovarian cancer ascites-derived spheroids*. Endocr Relat Cancer, 2016. **23**(3): p. 147-59.
169. Zhu, Y., M. Nilsson, and K. Sundfeldt, *Phenotypic plasticity of the ovarian surface epithelium: TGF-beta 1 induction of epithelial to mesenchymal transition (EMT) in vitro*. Endocrinology, 2010. **151**(11): p. 5497-505.
170. Garg, M., *Epithelial-mesenchymal transition - activating transcription factors - multifunctional regulators in cancer*. World J Stem Cells, 2013. **5**(4): p. 188-95.
171. Dunfield, L.D. and M.W. Nachtigal, *Inhibition of the antiproliferative effect of TGFbeta by EGF in primary human ovarian cancer cells*. Oncogene, 2003. **22**(30): p. 4745-51.
172. Vergara, D., et al., *Epithelial-mesenchymal transition in ovarian cancer*. Cancer Lett, 2010. **291**(1): p. 59-66.
173. Dunfield, L.D., E.J. Dwyer, and M.W. Nachtigal, *TGF beta-induced Smad signaling remains intact in primary human ovarian cancer cells*. Endocrinology, 2002. **143**(4): p. 1174-81.
174. Seoane, J. and R.R. Gomis, *TGF-beta Family Signaling in Tumor Suppression and Cancer Progression*. Cold Spring Harb Perspect Biol, 2017.
175. Massague, J., *TGFbeta signalling in context*. Nat Rev Mol Cell Biol, 2012. **13**(10): p. 616-30.
176. Derynck, R. and Y.E. Zhang, *Smad-dependent and Smad-independent pathways in TGF-beta family signalling*. Nature, 2003. **425**(6958): p. 577-84.

177. Moustakas, A. and C.H. Heldin, *Non-Smad TGF-beta signals*. J Cell Sci, 2005. **118**(Pt 16): p. 3573-84.
178. Dunker, A.K., et al., *Protein disorder and the evolution of molecular recognition: theory, predictions and observations*. Pac Symp Biocomput, 1998: p. 473-484.
179. Wright, P.E. and H.J. Dyson, *Intrinsically unstructured proteins: re-assessing the protein structure-function paradigm*. J Mol Biol, 1999. **293**(2): p. 321-331.
180. Uversky, V.N., J.R. Gillespie, and A.L. Fink, *Why are "natively unfolded" proteins unstructured under physiologic conditions?* Proteins, 2000. **41**(3): p. 415-427.
181. Dunker, A.K. and Z. Obradovic, *The protein trinity--linking function and disorder*. Nat Biotechnol, 2001. **19**(9): p. 805-6.
182. Tompa, P., *Intrinsically unstructured proteins*. Trends Biochem Sci, 2002. **27**(10): p. 527-533.
183. Daughdrill, G.W., et al., *Natively disordered proteins*, in *Handbook of Protein Folding*, J. Buchner and T. Kiefhaber, Editors. 2005, Wiley-VCH, Verlag GmbH & Co. KGaA: Weinheim, Germany. p. 271-353.
184. Uversky, V.N. and A.K. Dunker, *Understanding protein non-folding*. Biochim Biophys Acta, 2010. **1804**(6): p. 1231-64.
185. Holt, C. and L. Sawyer, *Caseins as rheomorphic proteins: interpretation of primary and secondary structures of the  $\alpha$ 1-,  $\beta$ -, and  $\kappa$ -caseins*. J Chem Soc Faraday Trans, 1993. **89**: p. 2683-2692.
186. Pullen, R.A., et al., *The relation of polypeptide hormone structure and flexibility to receptor binding: the relevance of X-ray studies on insulins, glucagon and human placental lactogen*. Mol. Cell. Biochem., 1975. **8**(1): p. 5-20.
187. Cary, P.D., T. Moss, and E.M. Bradbury, *High-resolution proton-magnetic-resonance studies of chromatin core particles*. Eur. J. Biochem., 1978. **89**(2): p. 475-82.
188. Linderstrom-Lang, K. and J.A. Schellman, *Protein structure and enzyme activity*, in *The Enzymes*, P.D. Boyer, H. Lardy, and K. Myrback, Editors. 1959, Academic Press: New York. p. 443-510.
189. Schweers, O., et al., *Structural studies of tau protein and Alzheimer paired helical filaments show no evidence for beta-structure*. J Biol Chem, 1994. **269**(39): p. 24290-24297.
190. Weinreb, P.H., et al., *NACP, a protein implicated in Alzheimer's disease and learning, is natively unfolded*. Biochemistry, 1996. **35**(43): p. 13709-13715.
191. Dunker, A.K., et al., *Intrinsically disordered protein*. J Mol Graph Model, 2001. **19**(1): p. 26-59.
192. Chen, J., H. Liang, and A. Fernandez, *Protein structure protection commits gene expression patterns*. Genome Biol, 2008. **9**(7): p. R107.
193. Uversky, V.N., *A protein-chameleon: conformational plasticity of alpha-synuclein, a disordered protein involved in neurodegenerative disorders*. J Biomol Struct Dyn, 2003. **21**(2): p. 211-34.
194. Fuxreiter, M., et al., *Malleable machines take shape in eukaryotic transcriptional regulation*. Nat Chem Biol, 2008. **4**(12): p. 728-37.
195. Tsvetkov, P., et al., *Operational definition of intrinsically unstructured protein sequences based on susceptibility to the 20S proteasome*. Proteins, 2008. **70**(4): p. 1357-66.
196. Dunker, A.K. and V.N. Uversky, *Drugs for 'protein clouds': targeting intrinsically disordered transcription factors*. Curr Opin Pharmacol, 2010. **10**(6): p. 782-8.
197. Livesay, D.R., *Protein dynamics: dancing on an ever-changing free energy stage*. Curr Opin Pharmacol, 2010. **10**(6): p. 706-8.
198. Uversky, V.N., *The mysterious unfoldome: structureless, underappreciated, yet vital part of any given proteome*. J Biomed Biotechnol, 2010. **2010**: p. 568068.
199. Uversky, V.N., *Natively unfolded proteins: a point where biology waits for physics*. Protein Sci, 2002. **11**(4): p. 739-56.

200. Iakoucheva, L.M., et al., *Intrinsic disorder in cell-signaling and cancer-associated proteins*. J Mol Biol, 2002. **323**(3): p. 573-84.
201. Dunker, A.K., et al., *Flexible nets: The roles of intrinsic disorder in protein interaction networks*. FEBS Journal, 2005. **272**(20): p. 5129-5148.
202. Uversky, V.N., C.J. Oldfield, and A.K. Dunker, *Showing your ID: intrinsic disorder as an ID for recognition, regulation and cell signaling*. J Mol Recognit, 2005. **18**(5): p. 343-384.
203. Radivojac, P., et al., *Intrinsic Disorder and Functional Proteomics*. Biophys J, 2007.
204. Uversky, V.N., C.J. Oldfield, and A.K. Dunker, *Intrinsically disordered proteins in human diseases: introducing the D2 concept*. Annu Rev Biophys, 2008. **37**: p. 215-46.
205. Lee, H., et al., *Local structural elements in the mostly unstructured transcriptional activation domain of human p53*. J Biol Chem, 2000. **275**(38): p. 29426-32.
206. Adkins, J.N. and K.J. Lumb, *Intrinsic structural disorder and sequence features of the cell cycle inhibitor p57Kip2*. Proteins, 2002. **46**(1): p. 1-7.
207. Chang, B.S., et al., *Identification of a novel regulatory domain in Bcl-X(L) and Bcl-2*. Embo J, 1997. **16**(5): p. 968-77.
208. Campbell, K.M., et al., *Intrinsic structural disorder of the C-terminal activation domain from the bZIP transcription factor Fos*. Biochemistry, 2000. **39**(10): p. 2708-13.
209. Sunde, M., et al., *TC-1 is a novel tumorigenic and natively disordered protein associated with thyroid cancer*. Cancer Res, 2004. **64**(8): p. 2766-73.
210. Glenner, G.G. and C.W. Wong, *Alzheimer's disease and Down's syndrome: sharing of a unique cerebrovascular amyloid fibril protein*. Biochem Biophys Res Commun, 1984. **122**(3): p. 1131-5.
211. Masters, C.L., et al., *Neuronal origin of a cerebral amyloid: neurofibrillary tangles of Alzheimer's disease contain the same protein as the amyloid of plaque cores and blood vessels*. Embo J, 1985. **4**(11): p. 2757-63.
212. Lee, V.M., et al., *A68: a major subunit of paired helical filaments and derivatized forms of normal Tau*. Science, 1991. **251**(4994): p. 675-8.
213. Ueda, K., et al., *Molecular cloning of cDNA encoding an unrecognized component of amyloid in Alzheimer disease*. Proc Natl Acad Sci U S A, 1993. **90**(23): p. 11282-6.
214. Wisniewski, K.E., et al., *Alzheimer's disease in Down's syndrome: clinicopathologic studies*. Neurology, 1985. **35**(7): p. 957-61.
215. Dev, K.K., et al., *Part II: alpha-synuclein and its molecular pathophysiological role in neurodegenerative disease*. Neuropharmacology, 2003. **45**(1): p. 14-44.
216. Prusiner, S.B., *Shattuck lecture--neurodegenerative diseases and prions*. N Engl J Med, 2001. **344**(20): p. 1516-26.
217. Zoghbi, H.Y. and H.T. Orr, *Polyglutamine diseases: protein cleavage and aggregation*. Curr Opin Neurobiol, 1999. **9**(5): p. 566-70.
218. Uversky, V.N., et al., *Protein intrinsic disorder and human papillomaviruses: increased amount of disorder in E6 and E7 oncoproteins from high risk HPVs*. J Proteome Res, 2006. **5**(8): p. 1829-42.
219. Cheng, Y., et al., *Abundance of intrinsic disorder in protein associated with cardiovascular disease*. Biochemistry, 2006. **45**(35): p. 10448-60.
220. Uversky, V.N., *Intrinsic disorder in proteins associated with neurodegenerative diseases*. Front Biosci, 2009. **14**: p. 5188-238.
221. Mohan, A., et al., *Intrinsic disorder in pathogenic and non-pathogenic microbes: discovering and analyzing the unfoldomes of early-branching eukaryotes*. Mol Biosyst, 2008. **4**(4): p. 328-40.
222. Uversky, V.N., *Targeting intrinsically disordered proteins in neurodegenerative and protein dysfunction diseases: another illustration of the D(2) concept*. Expert Rev Proteomics, 2010. **7**(4): p. 543-64.

223. Uversky, V.N., *Amyloidogenesis of natively unfolded proteins*. *Curr Alzheimer Res*, 2008. **5**(3): p. 260-87.
224. Midic, U., et al., *Protein disorder in the human diseasome: Unfoldomics of human genetic diseases*. *PLoS Computational Biology*, 2008: p. In press.
225. Xie, H., et al., *Functional anthology of intrinsic disorder. 1. Biological processes and functions of proteins with long disordered regions*. *J Proteome Res*, 2007. **6**(5): p. 1882-98.
226. Vucetic, S., et al., *Functional anthology of intrinsic disorder. 2. Cellular components, domains, technical terms, developmental processes, and coding sequence diversities correlated with long disordered regions*. *J Proteome Res*, 2007. **6**(5): p. 1899-916.
227. Xie, H., et al., *Functional anthology of intrinsic disorder. 3. Ligands, post-translational modifications, and diseases associated with intrinsically disordered proteins*. *J Proteome Res*, 2007. **6**(5): p. 1917-32.
228. Uversky, V.N., et al., *Unfoldomics of human diseases: linking protein intrinsic disorder with diseases*. *BMC Genomics*, 2009. **10 Suppl 1**: p. S7.
229. Liu, J., et al., *Intrinsic disorder in transcription factors*. *Biochemistry*, 2006. **45**(22): p. 6873-88.
230. Minezaki, Y., et al., *Human transcription factors contain a high fraction of intrinsically disordered regions essential for transcriptional regulation*. *J Mol Biol*, 2006. **359**(4): p. 1137-49.
231. Fukuchi, S., et al., *Development of an accurate classification system of proteins into structured and unstructured regions that uncovers novel structural domains: its application to human transcription factors*. *BMC Struct Biol*, 2009. **9**: p. 26.
232. Toth-Petroczy, A., et al., *Malleable machines in transcription regulation: the mediator complex*. *PLoS Comput Biol*, 2008. **4**(12): p. e1000243.
233. Singh, G.P. and D. Dash, *Intrinsic disorder in yeast transcriptional regulatory network*. *Proteins*, 2007. **68**(3): p. 602-5.
234. Singh, G.P., M. Ganapathi, and D. Dash, *Role of intrinsic disorder in transient interactions of hub proteins*. *Proteins*, 2007. **66**(4): p. 761-5.
235. Patil, A. and H. Nakamura, *Disordered domains and high surface charge confer hubs with the ability to interact with multiple proteins in interaction networks*. *FEBS Lett*, 2006. **580**(8): p. 2041-5.
236. Ekman, D., et al., *What properties characterize the hub proteins of the protein-protein interaction network of *Saccharomyces cerevisiae*?* *Genome Biol*, 2006. **7**(6): p. R45.
237. Haynes, C., et al., *Intrinsic disorder is a common feature of hub proteins from four eukaryotic interactomes*. *PLoS Comput Biol*, 2006. **2**(8): p. e100.
238. Dosztanyi, Z., et al., *Disorder and sequence repeats in hub proteins and their implications for network evolution*. *J Proteome Res*, 2006. **5**(11): p. 2985-95.
239. Cortese, M.S., V.N. Uversky, and A.K. Dunker, *Intrinsic disorder in scaffold proteins: getting more from less*. *Prog Biophys Mol Biol*, 2008. **98**(1): p. 85-106.
240. Buday, L. and P. Tompa, *Accessory proteins in signal transduction: scaffold proteins and beyond*. *FEBS J*, 2010. **277**(21): p. 4347.
241. Buday, L. and P. Tompa, *Functional classification of scaffold proteins and related molecules*. *FEBS J*, 2010. **277**(21): p. 4348-55.
242. Balazs, A., et al., *High levels of structural disorder in scaffold proteins as exemplified by a novel neuronal protein, CASK-interactive protein1*. *FEBS J*, 2009. **276**(14): p. 3744-56.
243. Uversky, V.N., *Flexible Nets of Malleable Guardians: Intrinsically Disordered Chaperones in Neurodegenerative Diseases*. *Chem Rev*, 2010.
244. Hegyi, H. and P. Tompa, *Intrinsically disordered proteins display no preference for chaperone binding in vivo*. *PLoS Comput Biol*, 2008. **4**(3): p. e1000017.



245. Kovacs, D., et al., *Chaperone activity of ERD10 and ERD14, two disordered stress-related plant proteins*. *Plant Physiol*, 2008. **147**(1): p. 381-90.
246. Farkas, A., et al., *DUK114, the Drosophila orthologue of bovine brain calpain activator protein, is a molecular chaperone*. *Biochem J*, 2004. **383**(Pt 1): p. 165-70.
247. Tompa, P. and D. Kovacs, *Intrinsically disordered chaperones in plants and animals*. *Biochem Cell Biol*, 2010. **88**(2): p. 167-74.
248. Kovacs, D., B. Agoston, and P. Tompa, *Disordered plant LEA proteins as molecular chaperones*. *Plant Signal Behav*, 2008. **3**(9): p. 710-3.
249. Kovacs, D., et al., *Janus chaperones: assistance of both RNA- and protein-folding by ribosomal proteins*. *FEBS Lett*, 2009. **583**(1): p. 88-92.
250. Tompa, P. and P. Csermely, *The role of structural disorder in the function of RNA and protein chaperones*. *FASEB J*, 2004. **18**(11): p. 1169-75.
251. Dunker, A.K., et al., *Intrinsic protein disorder in complete genomes*. *Genome Inform Ser Workshop Genome Inform*, 2000. **11**: p. 161-71.
252. Ward, J.J., et al., *Prediction and functional analysis of native disorder in proteins from the three kingdoms of life*. *J Mol Biol*, 2004. **337**(3): p. 635-45.
253. Oldfield, C.J., et al., *Comparing and combining predictors of mostly disordered proteins*. *Biochemistry*, 2005. **44**(6): p. 1989-2000.
254. Dyson, H.J. and P.E. Wright, *Coupling of folding and binding for unstructured proteins*. *Curr Opin Struct Biol*, 2002. **12**(1): p. 54-60.
255. Spolar, R.S. and M.T. Record, Jr., *Coupling of local folding to site-specific binding of proteins to DNA*. *Science*, 1994. **263**(5148): p. 777-84.
256. Shoemaker, B.A., J.J. Portman, and P.G. Wolynes, *Speeding molecular recognition by using the folding funnel: the fly-casting mechanism*. *Proc Natl Acad Sci U S A*, 2000. **97**(16): p. 8868-73.
257. Williamson, J.R., *Proteins that bind RNA and the labs who love them*. *Nat Struct Biol*, 2001. **8**(5): p. 390-1.
258. Patikoglou, G. and S.K. Burley, *Eukaryotic transcription factor-DNA complexes*. *Annu Rev Biophys Biomol Struct*, 1997. **26**: p. 289-325.
259. Laity, J.H., H.J. Dyson, and P.E. Wright, *DNA-induced alpha-helix capping in conserved linker sequences is a determinant of binding affinity in Cys(2)-His(2) zinc fingers*. *J Mol Biol*, 2000. **295**(4): p. 719-27.
260. Laity, J.H., H.J. Dyson, and P.E. Wright, *Molecular basis for modulation of biological function by alternate splicing of the Wilms' tumor suppressor protein*. *Proc Natl Acad Sci U S A*, 2000. **97**(22): p. 11932-5.
261. Frankel, A.D. and P.S. Kim, *Modular structure of transcription factors: implications for gene regulation*. *Cell*, 1991. **65**(5): p. 717-9.
262. Radhakrishnan, I., et al., *Solution structure of the KIX domain of CBP bound to the transactivation domain of CREB: a model for activator:coactivator interactions*. *Cell*, 1997. **91**(6): p. 741-52.
263. Ayed, A., et al., *Latent and active p53 are identical in conformation*. *Nat Struct Biol*, 2001. **8**(9): p. 756-60.
264. Grossmann, J.G., et al., *Molecular shapes of transcription factors TFIIIB and VP16 in solution: implications for recognition*. *Biochemistry*, 2001. **40**(21): p. 6267-74.
265. Crick, F.H., *On protein synthesis*. *Symp Soc Exp Biol*, 1958. **12**: p. 138-63.
266. Anfinsen, C.B., *Principles that govern the folding of protein chains*. *Science*, 1973. **181**(96): p. 223-30.
267. Bukau, B., J. Weissman, and A. Horwich, *Molecular chaperones and protein quality control*. *Cell*, 2006. **125**(3): p. 443-51.

268. Hartl, F.U. and M. Hayer-Hartl, *Molecular chaperones in the cytosol: from nascent chain to folded protein*. Science, 2002. **295**(5561): p. 1852-8.
269. Slepnev, S.V. and S.N. Witt, *The unfolding story of the Escherichia coli Hsp70 DnaK: is DnaK a holdase or an unfoldase?* Mol Microbiol, 2002. **45**(5): p. 1197-206.
270. Lindquist, S., *The heat-shock response*. Annu Rev Biochem, 1986. **55**: p. 1151-91.
271. Lindquist, S. and E.A. Craig, *The heat-shock proteins*. Annu Rev Genet, 1988. **22**: p. 631-77.
272. Young, J.C., et al., *Pathways of chaperone-mediated protein folding in the cytosol*. Nat Rev Mol Cell Biol, 2004. **5**(10): p. 781-91.
273. Goldberger, R.F., C.J. Epstein, and C.B. Anfinsen, *Acceleration of reactivation of reduced bovine pancreatic ribonuclease by a microsomal system from rat liver*. J Biol Chem, 1963. **238**: p. 628-35.
274. Hatahet, F., et al., *Protein disulfide isomerase: a critical evaluation of its function in disulfide bond formation*. Antioxid Redox Signal, 2009. **11**(11): p. 2807-50.
275. Nagradova, N., *Enzymes catalyzing protein folding and their cellular functions*. Curr Protein Pept Sci, 2007. **8**(3): p. 273-82.
276. Fischer, G., H. Bang, and C. Mech, *[Determination of enzymatic catalysis for the cis-trans-isomerization of peptide binding in proline-containing peptides]*. Biomed Biochim Acta, 1984. **43**(10): p. 1101-11.
277. Jorgensen, S., K.W. Skov, and B. Diderichsen, *Cloning, sequence, and expression of a lipase gene from Pseudomonas cepacia: lipase production in heterologous hosts requires two Pseudomonas genes*. J Bacteriol, 1991. **173**(2): p. 559-67.
278. Westerheide, S.D. and R.I. Morimoto, *Heat shock response modulators as therapeutic tools for diseases of protein conformation*. The Journal of biological chemistry, 2005. **280**(39): p. 33097-100.
279. Clos, J., et al., *Molecular cloning and expression of a hexameric Drosophila heat shock factor subject to negative regulation*. Cell, 1990. **63**(5): p. 1085-97.
280. Sorger, P.K. and H.R. Pelham, *Yeast heat shock factor is an essential DNA-binding protein that exhibits temperature-dependent phosphorylation*. Cell, 1988. **54**(6): p. 855-64.
281. Wiederrecht, G., D. Seto, and C.S. Parker, *Isolation of the gene encoding the S. cerevisiae heat shock transcription factor*. Cell, 1988. **54**(6): p. 841-53.
282. Fernandes, M., H. Xiao, and J.T. Lis, *Fine structure analyses of the Drosophila and Saccharomyces heat shock factor--heat shock element interactions*. Nucleic Acids Res, 1994. **22**(2): p. 167-73.
283. Green, M., et al., *A heat shock-responsive domain of human HSF1 that regulates transcription activation domain function*. Mol Cell Biol, 1995. **15**(6): p. 3354-62.
284. Newton, E.M., et al., *The regulatory domain of human heat shock factor 1 is sufficient to sense heat stress*. Mol Cell Biol, 1996. **16**(3): p. 839-46.
285. Sorger, P.K. and H.C. Nelson, *Trimerization of a yeast transcriptional activator via a coiled-coil motif*. Cell, 1989. **59**(5): p. 807-13.
286. Harrison, C.J., A.A. Bohm, and H.C. Nelson, *Crystal structure of the DNA binding domain of the heat shock transcription factor*. Science, 1994. **263**(5144): p. 224-7.
287. Vuister, G.W., et al., *Solution structure of the DNA-binding domain of Drosophila heat shock transcription factor*. Nat Struct Biol, 1994. **1**(9): p. 605-14.
288. Fernandes, M., H. Xiao, and J.T. Lis, *Fine structure analyses of the Drosophila and Saccharomyces heat shock factor--heat shock element interactions*. Nucleic acids research, 1994. **22**(2): p. 167-73.

289. Vuister, G.W., et al., *NMR evidence for similarities between the DNA-binding regions of Drosophila melanogaster heat shock factor and the helix-turn-helix and HNF-3/forkhead families of transcription factors*. *Biochemistry*, 1994. **33**(1): p. 10-6.
290. Rabindran, S.K., et al., *Regulation of heat shock factor trimer formation: role of a conserved leucine zipper*. *Science*, 1993. **259**(5092): p. 230-4.
291. Zuo, J., et al., *Activation of the DNA-binding ability of human heat shock transcription factor 1 may involve the transition from an intramolecular to an intermolecular triple-stranded coiled-coil structure*. *Mol Cell Biol*, 1994. **14**(11): p. 7557-68.
292. Chen, Y., et al., *Identification of the C-terminal activator domain in yeast heat shock factor: independent control of transient and sustained transcriptional activity*. *EMBO J*, 1993. **12**(13): p. 5007-18.
293. Brown, S.A., A.N. Imbalzano, and R.E. Kingston, *Activator-dependent regulation of transcriptional pausing on nucleosomal templates*. *Genes Dev*, 1996. **10**(12): p. 1479-90.
294. Shi, Y., P.E. Kroeger, and R.I. Morimoto, *The carboxyl-terminal transactivation domain of heat shock factor 1 is negatively regulated and stress responsive*. *Mol Cell Biol*, 1995. **15**(8): p. 4309-18.
295. Zuo, J., D. Rungger, and R. Voellmy, *Multiple layers of regulation of human heat shock transcription factor 1*. *Mol Cell Biol*, 1995. **15**(8): p. 4319-30.
296. Brown, S.A., et al., *Transcriptional activation domains stimulate initiation and elongation at different times and via different residues*. *Embo Journal*, 1998. **17**(11): p. 3146-54.
297. Chu, B., et al., *Sequential phosphorylation by mitogen-activated protein kinase and glycogen synthase kinase 3 represses transcriptional activation by heat shock factor-1*. *J Biol Chem*, 1996. **271**(48): p. 30847-57.
298. Goodson, M.L. and K.D. Sarge, *Regulated expression of heat shock factor 1 isoforms with distinct leucine zipper arrays via tissue-dependent alternative splicing*. *Biochem Biophys Res Commun*, 1995. **211**(3): p. 943-9.
299. Romero, P.R., et al., *Alternative splicing in concert with protein intrinsic disorder enables increased functional diversity in multicellular organisms*. *Proc Natl Acad Sci U S A*, 2006. **103**(22): p. 8390-5.
300. Sorger, P.K., M.J. Lewis, and H.R. Pelham, *Heat shock factor is regulated differently in yeast and HeLa cells*. *Nature*, 1987. **329**(6134): p. 81-4.
301. Sorger, P.K., *Yeast heat shock factor contains separable transient and sustained response transcriptional activators*. *Cell*, 1990. **62**(4): p. 793-805.
302. Cotto, J.J., M. Kline, and R.I. Morimoto, *Activation of heat shock factor 1 DNA binding precedes stress-induced serine phosphorylation. Evidence for a multistep pathway of regulation*. *J Biol Chem*, 1996. **271**(7): p. 3355-8.
303. Xia, W. and R. Voellmy, *Hyperphosphorylation of heat shock transcription factor 1 is correlated with transcriptional competence and slow dissociation of active factor trimers*. *J Biol Chem*, 1997. **272**(7): p. 4094-102.
304. Knauf, U., et al., *Repression of human heat shock factor 1 activity at control temperature by phosphorylation*. *Genes Dev*, 1996. **10**(21): p. 2782-93.
305. Knauf, U., et al., *Repression of human heat shock factor 1 activity at control temperature by phosphorylation*. *Genes & development*, 1996. **10**(21): p. 2782-93.
306. Chu, B., et al., *Transcriptional activity of heat shock factor 1 at 37 degrees C is repressed through phosphorylation on two distinct serine residues by glycogen synthase kinase 3 and protein kinases Calpha and Czeta*. *J Biol Chem*, 1998. **273**(29): p. 18640-6.

307. Dai, R., et al., *c-Jun NH2-terminal kinase targeting and phosphorylation of heat shock factor-1 suppress its transcriptional activity*. J Biol Chem, 2000. **275**(24): p. 18210-8.
308. Wang, X., et al., *Phosphorylation of HSF1 by MAPK-activated protein kinase 2 on serine 121, inhibits transcriptional activity and promotes HSP90 binding*. The Journal of biological chemistry, 2006. **281**(2): p. 782-91.
309. Hahn, J.S. and D.J. Thiele, *Activation of the Saccharomyces cerevisiae heat shock transcription factor under glucose starvation conditions by Snf1 protein kinase*. J Biol Chem, 2004. **279**(7): p. 5169-76.
310. Dunker, A.K., C.J. Brown, and Z. Obradovic, *Identification and functions of usefully disordered proteins*. Adv. Protein Chem., 2002. **62**: p. 25-49.
311. Dunker, A.K., et al., *Intrinsic disorder and protein function*. Biochemistry, 2002. **41**(21): p. 6573-82.
312. Marks, F., *Protein Phosphorylation*. 1996, New York, Basel, Cambridge, Tokyo: VCH Weinheim.
313. Johnson, L.N. and R.J. Lewis, *Structural basis for control by phosphorylation*. Chem. Rev., 2001. **101**(8): p. 2209-2242.
314. Iakoucheva, L.M., et al., *The importance of intrinsic disorder for protein phosphorylation*. Nucleic Acids Res., 2004. **32**(3): p. 1037-49.
315. Bossemeyer, D., et al., *Phosphotransferase and substrate binding mechanism of the cAMP-dependent protein kinase catalytic subunit from porcine heart as deduced from the 2.0 Å structure of the complex with Mn<sup>2+</sup> adenylyl imidodiphosphate and inhibitor peptide PKI(5-24)*. EMBO J., 1993. **12**(3): p. 849-59.
316. Narayana, N., et al., *Crystal structure of a polyhistidine-tagged recombinant catalytic subunit of cAMP-dependent protein kinase complexed with the peptide inhibitor PKI(5-24) and adenosine*. Biochemistry, 1997. **36**(15): p. 4438-4448.
317. Lowe, E.D., et al., *The crystal structure of a phosphorylase kinase peptide substrate complex: kinase substrate recognition*. Embo. J., 1997. **16**(22): p. 6646-6658.
318. ter Haar, E., et al., *Structure of GSK3beta reveals a primed phosphorylation mechanism*. Nat. Struct. Biol., 2001. **8**(7): p. 593-596.
319. Hubbard, S.R., *Crystal structure of the activated insulin receptor tyrosine kinase in complex with peptide substrate and ATP analog*. Embo. J., 1997. **16**(18): p. 5572-5581.
320. McDonald, I.K. and J.M. Thornton, *Satisfying hydrogen bonding potential in proteins*. J. Mol. Biol., 1994. **238**(5): p. 777-793.
321. Radivojac, P., et al., *Identification, analysis, and prediction of protein ubiquitination sites*. Proteins, 2010. **78**(2): p. 365-80.
322. Shamovsky, I., et al., *RNA-mediated response to heat shock in mammalian cells*. Nature, 2006. **440**(7083): p. 556-60.
323. Lis, J.T., et al., *P-TEFb kinase recruitment and function at heat shock loci*. Genes Dev, 2000. **14**(7): p. 792-803.
324. Sullivan, E.K., et al., *Transcriptional activation domains of human heat shock factor 1 recruit human SWI/SNF*. Mol Cell Biol, 2001. **21**(17): p. 5826-37.
325. Corey, L.L., et al., *Localized recruitment of a chromatin-remodeling activity by an activator in vivo drives transcriptional elongation*. Genes Dev, 2003. **17**(11): p. 1392-401.
326. Park, J.M., et al., *Mediator, not holoenzyme, is directly recruited to the heat shock promoter by HSF upon heat shock*. Mol Cell, 2001. **8**(1): p. 9-19.
327. Saunders, A., et al., *Tracking FACT and the RNA polymerase II elongation complex through chromatin in vivo*. Science, 2003. **301**(5636): p. 1094-6.

328. Hong, S., et al., *Coactivator ASC-2 mediates heat shock factor 1-mediated transactivation dependent on heat shock*. FEBS Lett, 2004. **559**(1-3): p. 165-70.
329. Xing, H., et al., *HSF1 modulation of Hsp70 mRNA polyadenylation via interaction with symplekin*. J Biol Chem, 2004. **279**(11): p. 10551-5.
330. Baler, R., W.J. Welch, and R. Voellmy, *Heat shock gene regulation by nascent polypeptides and denatured proteins: hsp70 as a potential autoregulatory factor*. J Cell Biol, 1992. **117**(6): p. 1151-9.
331. Guo, Y., et al., *Evidence for a mechanism of repression of heat shock factor 1 transcriptional activity by a multichaperone complex*. J Biol Chem, 2001. **276**(49): p. 45791-9.
332. Fujimoto, M. and A. Nakai, *The heat shock factor family and adaptation to proteotoxic stress*. FEBS J, 2010. **277**(20): p. 4112-25.
333. Pirkkala, L., P. Nykanen, and L. Sistonen, *Roles of the heat shock transcription factors in regulation of the heat shock response and beyond*. Faseb Journal, 2001. **15**(7): p. 1118-1131.
334. Alastalo, T.P., et al., *Formation of nuclear stress granules involves HSF2 and coincides with the nucleolar localization of Hsp70*. J Cell Sci, 2003. **116**(Pt 17): p. 3557-70.
335. Ostling, P., et al., *Heat shock factor 2 (HSF2) contributes to inducible expression of hsp genes through interplay with HSF1*. J Biol Chem, 2007. **282**(10): p. 7077-86.
336. Schuetz, T.J., et al., *Isolation of a cDNA for HSF2: evidence for two heat shock factor genes in humans*. Proc Natl Acad Sci U S A, 1991. **88**(16): p. 6911-5.
337. Sarge, K.D., et al., *Cloning and characterization of two mouse heat shock factors with distinct inducible and constitutive DNA-binding ability*. Genes Dev, 1991. **5**(10): p. 1902-11.
338. Sistonen, L., et al., *Activation of heat shock factor 2 during hemin-induced differentiation of human erythroleukemia cells*. Mol Cell Biol, 1992. **12**(9): p. 4104-11.
339. Mezger, V., et al., *Heat shock factor 2-like activity in mouse blastocysts*. Dev Biol, 1994. **166**(2): p. 819-22.
340. Murphy, S.P., et al., *Characterization of constitutive HSF2 DNA-binding activity in mouse embryonal carcinoma cells*. Mol Cell Biol, 1994. **14**(8): p. 5309-17.
341. Sarge, K.D., et al., *Expression of heat shock factor 2 in mouse testis: potential role as a regulator of heat-shock protein gene expression during spermatogenesis*. Biol Reprod, 1994. **50**(6): p. 1334-43.
342. Rallu, M., et al., *Function and regulation of heat shock factor 2 during mouse embryogenesis*. Proc Natl Acad Sci U S A, 1997. **94**(6): p. 2392-7.
343. Ahn, S.G., et al., *The loop domain of heat shock transcription factor 1 dictates DNA-binding specificity and responses to heat stress*. Genes Dev, 2001. **15**(16): p. 2134-45.
344. Yoshima, T., T. Yura, and H. Yanagi, *Function of the C-terminal transactivation domain of human heat shock factor 2 is modulated by the adjacent negative regulatory segment*. Nucleic Acids Res, 1998. **26**(11): p. 2580-5.
345. He, H., et al., *Elevated expression of heat shock factor (HSF) 2A stimulates HSF1-induced transcription during stress*. J Biol Chem, 2003. **278**(37): p. 35465-75.
346. Nakai, A., et al., *HSF4, a new member of the human heat shock factor family which lacks properties of a transcriptional activator*. Mol Cell Biol, 1997. **17**(1): p. 469-81.
347. Fujimoto, M., et al., *HSF4 is required for normal cell growth and differentiation during mouse lens development*. The EMBO journal, 2004. **23**(21): p. 4297-306.
348. Tanabe, M., et al., *The mammalian HSF4 gene generates both an activator and a repressor of heat shock genes by alternative splicing*. J Biol Chem, 1999. **274**(39): p. 27845-56.
349. Bu, L., et al., *Mutant DNA-binding domain of HSF4 is associated with autosomal dominant lamellar and Marner cataract*. Nat Genet, 2002. **31**(3): p. 276-8.

350. Smaoui, N., et al., *A homozygous splice mutation in the HSF4 gene is associated with an autosomal recessive congenital cataract*. Investigative ophthalmology & visual science, 2004. **45**(8): p. 2716-21.
351. Shi, Y., et al., *Mutation screening of HSF4 in 150 age-related cataract patients*. Molecular vision, 2008. **14**: p. 1850-5.
352. Nakai, A. and R.I. Morimoto, *Characterization of a novel chicken heat shock transcription factor, heat shock factor 3, suggests a new regulatory pathway*. Mol Cell Biol, 1993. **13**(4): p. 1983-97.
353. Torres, M.P., et al., *Immunopathogenesis of ovarian cancer*. Minerva Med, 2009. **100**(5): p. 385-400.
354. Jemal, A., et al., *Cancer statistics, 2002*. CA Cancer J Clin, 2002. **52**(1): p. 23-47.
355. Cannistra, S.A., *Cancer of the ovary*. N Engl J Med, 2004. **351**(24): p. 2519-29.
356. Cannistra, S.A., *Is there a "best" choice of second-line agent in the treatment of recurrent, potentially platinum-sensitive ovarian cancer?* J Clin Oncol, 2002. **20**(5): p. 1158-60.
357. Kelland, L., *The resurgence of platinum-based cancer chemotherapy*. Nat Rev Cancer, 2007. **7**(8): p. 573-84.
358. Moreno-Bueno, G., et al., *The morphological and molecular features of the epithelial-to-mesenchymal transition*. Nat Protoc, 2009. **4**(11): p. 1591-613.
359. Xu, J., S. Lamouille, and R. Derynck, *TGF-beta-induced epithelial to mesenchymal transition*. Cell Res, 2009. **19**(2): p. 156-72.
360. Thiery, J.P., *Epithelial-mesenchymal transitions in tumour progression*. Nat Rev Cancer, 2002. **2**(6): p. 442-54.
361. Cerami, E., et al., *The cBio cancer genomics portal: an open platform for exploring multidimensional cancer genomics data*. Cancer Discov, 2012. **2**(5): p. 401-4.
362. Gao, J., et al., *Integrative analysis of complex cancer genomics and clinical profiles using the cBioPortal*. Sci Signal, 2013. **6**(269): p. p11.
363. Korch, C., et al., *DNA profiling analysis of endometrial and ovarian cell lines reveals misidentification, redundancy and contamination*. Gynecol Oncol, 2012. **127**(1): p. 241-8.
364. Olson, A., et al., *RNAi Codex: a portal/database for short-hairpin RNA (shRNA) gene-silencing constructs*. Nucleic Acids Res, 2006. **34**(Database issue): p. D153-7.
365. Geback, T., et al., *TScratch: a novel and simple software tool for automated analysis of monolayer wound healing assays*. Biotechniques, 2009. **46**(4): p. 265-74.
366. Timmins, N.E. and L.K. Nielsen, *Generation of multicellular tumor spheroids by the hanging-drop method*. Methods in molecular medicine, 2007. **140**: p. 141-51.
367. Holmberg, C.I., et al., *Multisite phosphorylation provides sophisticated regulation of transcription factors*. Trends Biochem Sci, 2002. **27**(12): p. 619-27.
368. Hay, E.D., *An overview of epithelio-mesenchymal transformation*. Acta Anat (Basel), 1995. **154**(1): p. 8-20.
369. Kelm, J.M., et al., *Method for generation of homogeneous multicellular tumor spheroids applicable to a wide variety of cell types*. Biotechnol Bioeng, 2003. **83**(2): p. 173-80.
370. O'Callaghan-Sunol, C. and M.Y. Sherman, *Heat shock transcription factor (HSF1) plays a critical role in cell migration via maintaining MAP kinase signaling*. Cell Cycle, 2006. **5**(13): p. 1431-7.
371. Li, Y., et al., *MicroRNA-135b, a HSF1 target, promotes tumor invasion and metastasis by regulating RECK and EVI5 in hepatocellular carcinoma*. Oncotarget, 2015. **6**(4): p. 2421-33.
372. Nakamura, Y., et al., *Heat shock factor 1 is required for migration and invasion of human melanoma in vitro and in vivo*. Cancer Lett, 2014. **354**(2): p. 329-35.
373. Schilling, D., et al., *Sensitizing tumor cells to radiation by targeting the heat shock response*. Cancer Lett, 2015. **360**(2): p. 294-301.

374. Toma-Jonik, A., et al., *Active heat shock transcription factor 1 supports migration of the melanoma cells via vinculin down-regulation*. Cell Signal, 2015. **27**(2): p. 394-401.
375. Carpenter, R.L., et al., *Akt phosphorylates and activates HSF-1 independent of heat shock, leading to Slug overexpression and epithelial-mesenchymal transition (EMT) of HER2-overexpressing breast cancer cells*. Oncogene, 2014.
376. Shield, K., et al., *Multicellular spheroids in ovarian cancer metastases: Biology and pathology*. Gynecol Oncol, 2009. **113**(1): p. 143-8.
377. Kroeger, P.E. and R.I. Morimoto, *Selection of new HSF1 and HSF2 DNA-binding sites reveals difference in trimer cooperativity*. Mol Cell Biol, 1994. **14**(11): p. 7592-603.
378. Westerheide, S.D. and R.I. Morimoto, *Heat shock response modulators as therapeutic tools for diseases of protein conformation*. J Biol Chem, 2005. **280**(39): p. 33097-100.
379. Christians, E.S., L.J. Yan, and I.J. Benjamin, *Heat shock factor 1 and heat shock proteins: Critical partners in protection against acute cell injury*. Crit Care Med, 2002. **30**(1 Supp): p. S43-S50.
380. Dai, C. and S.B. Sampson, *HSF1: Guardian of Proteostasis in Cancer*. Trends Cell Biol, 2016. **26**(1): p. 17-28.
381. Morimoto, R.I., *The heat shock response: systems biology of proteotoxic stress in aging and disease*. Cold Spring Harb Symp Quant Biol, 2011. **76**: p. 91-9.
382. Bertram, J., et al., *Increase of P-glycoprotein-mediated drug resistance by hsp 90 beta*. Anticancer Drugs, 1996. **7**(8): p. 838-45.
383. Evans, C.G., L. Chang, and J.E. Gestwicki, *Heat shock protein 70 (hsp70) as an emerging drug target*. J Med Chem, 2010. **53**(12): p. 4585-602.
384. Ray, S., et al., *Genomic mechanisms of p210BCR-ABL signaling: induction of heat shock protein 70 through the GATA response element confers resistance to paclitaxel-induced apoptosis*. J Biol Chem, 2004. **279**(34): p. 35604-15.
385. Scherz-Shouval, R., et al., *The reprogramming of tumor stroma by HSF1 is a potent enabler of malignancy*. Cell, 2014. **158**(3): p. 564-78.
386. Page, T.J., et al., *Genome-wide analysis of human HSF1 signaling reveals a transcriptional program linked to cellular adaptation and survival*. Mol Biosyst, 2006. **2**(12): p. 627-39.
387. Chen, Y., et al., *Targeting HSF1 sensitizes cancer cells to HSP90 inhibition*. Oncotarget, 2013. **4**(6): p. 816-29.
388. Powell, C.D., et al., *The Heat Shock Transcription Factor HSF1 Induces Ovarian Cancer Epithelial-Mesenchymal Transition in a 3D Spheroid Growth Model*. PLoS One, 2016. **11**(12): p. e0168389.
389. Siddik, Z.H., *Cisplatin: mode of cytotoxic action and molecular basis of resistance*. Oncogene, 2003. **22**(47): p. 7265-79.
390. Agarwal, R. and S.B. Kaye, *Ovarian cancer: strategies for overcoming resistance to chemotherapy*. Nat Rev Cancer, 2003. **3**(7): p. 502-16.
391. Schiff, P.B., J. Fant, and S.B. Horwitz, *Promotion of microtubule assembly in vitro by taxol*. Nature, 1979. **277**(5698): p. 665-7.
392. Wani, M.C. and S.B. Horwitz, *Nature as a remarkable chemist: a personal story of the discovery and development of Taxol*. Anticancer Drugs, 2014. **25**(5): p. 482-7.
393. Torres, K. and S.B. Horwitz, *Mechanisms of Taxol-induced cell death are concentration dependent*. Cancer Res, 1998. **58**(16): p. 3620-6.
394. Ikui, A.E., et al., *Low concentrations of taxol cause mitotic delay followed by premature dissociation of p55CDC from Mad2 and BubR1 and abrogation of the spindle checkpoint, leading to aneuploidy*. Cell Cycle, 2005. **4**(10): p. 1385-8.
395. Kampan, N.C., et al., *Paclitaxel and Its Evolving Role in the Management of Ovarian Cancer*. Biomed Res Int, 2015. **2015**: p. 413076.

396. Vejpongsa, P. and E.T. Yeh, *Prevention of anthracycline-induced cardiotoxicity: challenges and opportunities*. J Am Coll Cardiol, 2014. **64**(9): p. 938-45.
397. Carvalho, C., et al., *Doxorubicin: the good, the bad and the ugly effect*. Curr Med Chem, 2009. **16**(25): p. 3267-85.
398. Minotti, G., et al., *Anthracyclines: molecular advances and pharmacologic developments in antitumor activity and cardiotoxicity*. Pharmacol Rev, 2004. **56**(2): p. 185-229.
399. Brucker, J., et al., *Non-pegylated liposomal doxorubicin for patients with recurrent ovarian cancer: A multicentric phase II trial*. Oncol Lett, 2016. **12**(2): p. 1211-1215.
400. Hatcher, H., et al., *Curcumin: from ancient medicine to current clinical trials*. Cell Mol Life Sci, 2008. **65**(11): p. 1631-52.
401. Kunnumakkara, A.B., P. Anand, and B.B. Aggarwal, *Curcumin inhibits proliferation, invasion, angiogenesis and metastasis of different cancers through interaction with multiple cell signaling proteins*. Cancer Lett, 2008. **269**(2): p. 199-225.
402. Deng, Y.I., E. Verron, and R. Rohanzadeh, *Molecular Mechanisms of Anti-metastatic Activity of Curcumin*. Anticancer Res, 2016. **36**(11): p. 5639-5647.
403. Gupta, S.C., S. Patchva, and B.B. Aggarwal, *Therapeutic roles of curcumin: lessons learned from clinical trials*. AAPS J, 2013. **15**(1): p. 195-218.
404. Reinhold, W.C., et al., *CellMiner: a web-based suite of genomic and pharmacologic tools to explore transcript and drug patterns in the NCI-60 cell line set*. Cancer Res, 2012. **72**(14): p. 3499-511.
405. Guo, W., et al., *Formation of 17-allylamino-demethoxygeldanamycin (17-AAG) hydroquinone by NAD(P)H:quinone oxidoreductase 1: role of 17-AAG hydroquinone in heat shock protein 90 inhibition*. Cancer Res, 2005. **65**(21): p. 10006-15.
406. Hadden, M.K., D.J. Lubbers, and B.S. Blagg, *Geldanamycin, radicicol, and chimeric inhibitors of the Hsp90 N-terminal ATP binding site*. Curr Top Med Chem, 2006. **6**(11): p. 1173-82.
407. Sidera, K. and E. Patsavoudi, *HSP90 inhibitors: current development and potential in cancer therapy*. Recent Pat Anticancer Drug Discov, 2014. **9**(1): p. 1-20.
408. Jhaveri, K. and S. Modi, *Ganetespib: research and clinical development*. Onco Targets Ther, 2015. **8**: p. 1849-58.
409. Ying, W., et al., *Ganetespib, a unique triazolone-containing Hsp90 inhibitor, exhibits potent antitumor activity and a superior safety profile for cancer therapy*. Mol Cancer Ther, 2012. **11**(2): p. 475-84.
410. Thakur, M.K., et al., *A phase II trial of ganetespib, a heat shock protein 90 (Hsp90) inhibitor, in patients with docetaxel-pretreated metastatic castrate-resistant prostate cancer (CRPC)-a prostate cancer clinical trials consortium (PCCTC) study*. Invest New Drugs, 2016. **34**(1): p. 112-8.
411. Ramalingam, S., et al., *A randomized phase II study of ganetespib, a heat shock protein 90 inhibitor, in combination with docetaxel in second-line therapy of advanced non-small cell lung cancer (GALAXY-1)*. Ann Oncol, 2015. **26**(8): p. 1741-8.
412. Cercek, A., et al., *Ganetespib, a novel Hsp90 inhibitor in patients with KRAS mutated and wild type, refractory metastatic colorectal cancer*. Clin Colorectal Cancer, 2014. **13**(4): p. 207-12.
413. Meng, J., et al., *Doxycycline as an inhibitor of the epithelial-to-mesenchymal transition and vasculogenic mimicry in hepatocellular carcinoma*. Mol Cancer Ther, 2014. **13**(12): p. 3107-22.
414. Zhong, W., et al., *Doxycycline directly targets PAR1 to suppress tumor progression*. Oncotarget, 2017.
415. Zhao, Y., et al., *Overcoming trastuzumab resistance in breast cancer by targeting dysregulated glucose metabolism*. Cancer Res, 2011. **71**(13): p. 4585-97.



416. Chai, R.C., et al., *Molecular stress-inducing compounds increase osteoclast formation in a heat shock factor 1 protein-dependent manner*. J Biol Chem, 2014. **289**(19): p. 13602-14.
417. Fujikake, N., et al., *Heat shock transcription factor 1-activating compounds suppress polyglutamine-induced neurodegeneration through induction of multiple molecular chaperones*. J Biol Chem, 2008. **283**(38): p. 26188-97.
418. Bagatell, R., et al., *Induction of a heat shock factor 1-dependent stress response alters the cytotoxic activity of hsp90-binding agents*. Clin Cancer Res, 2000. **6**(8): p. 3312-8.
419. Millson, S.H. and P.W. Piper, *Insights from yeast into whether the inhibition of heat shock transcription factor (Hsf1) by rapamycin can prevent the Hsf1 activation that results from treatment with an Hsp90 inhibitor*. Oncotarget, 2014. **5**(13): p. 5054-64.
420. Rabindran, S.K., et al., *Molecular cloning and expression of a human heat shock factor, HSF1*. Proc Natl Acad Sci U S A, 1991. **88**(16): p. 6906-10.
421. Clos, J., et al., *Induction temperature of human heat shock factor is reprogrammed in a Drosophila cell environment*. Nature, 1993. **364**(6434): p. 252-5.
422. Orosz, A., J. Wisniewski, and C. Wu, *Regulation of Drosophila heat shock factor trimerization: global sequence requirements and independence of nuclear localization*. Mol Cell Biol, 1996. **16**(12): p. 7018-30.
423. Zhang, Y. and S.K. Calderwood, *Autophagy, protein aggregation and hyperthermia: a mini-review*. Int J Hyperthermia, 2011. **27**(5): p. 409-14.
424. Hanahan, D. and R.A. Weinberg, *Hallmarks of cancer: the next generation*. Cell, 2011. **144**(5): p. 646-74.
425. Qiao, A., et al., *The transcriptional regulator of the chaperone response HSF1 controls hepatic bioenergetics and protein homeostasis*. J Cell Biol, 2017. **216**(3): p. 723-741.
426. Cigliano, A., et al., *Inhibition of HSF1 suppresses the growth of hepatocarcinoma cell lines in vitro and AKT-driven hepatocarcinogenesis in mice*. Oncotarget, 2017.
427. Wang, B., et al., *Heat shock factor 1 induces cancer stem cell phenotype in breast cancer cell lines*. Breast Cancer Res Treat, 2015. **153**(1): p. 57-66.
428. Jung, M., et al., *A Myc Activity Signature Predicts Poor Clinical Outcomes in Myc-Associated Cancers*. Cancer Res, 2017. **77**(4): p. 971-981.
429. Aunoble, B., et al., *Major oncogenes and tumor suppressor genes involved in epithelial ovarian cancer (review)*. Int J Oncol, 2000. **16**(3): p. 567-76.
430. Reyes-Gonzalez, J.M., et al., *Targeting c-MYC in Platinum-Resistant Ovarian Cancer*. Mol Cancer Ther, 2015. **14**(10): p. 2260-9.
431. Dalla-Favera, R., et al., *Human c-myc onc gene is located on the region of chromosome 8 that is translocated in Burkitt lymphoma cells*. Proc Natl Acad Sci U S A, 1982. **79**(24): p. 7824-7.
432. *Broad Institute TCGA Genome Data Analysis Center (2016): SNP6 Copy number analysis (GISTIC2)*. 2016.
433. Timmins, N.E., S. Dietmair, and L.K. Nielsen, *Hanging-drop multicellular spheroids as a model of tumour angiogenesis*. Angiogenesis, 2004. **7**(2): p. 97-103.
434. Raghavan, S., et al., *Comparative analysis of tumor spheroid generation techniques for differential in vitro drug toxicity*. Oncotarget, 2016. **7**(13): p. 16948-61.
435. Cao, L., et al., *Tissue transglutaminase links TGF-beta, epithelial to mesenchymal transition and a stem cell phenotype in ovarian cancer*. Oncogene, 2012. **31**(20): p. 2521-34.
436. de Billy, E., et al., *Drugging the heat shock factor 1 pathway: exploitation of the critical cancer cell dependence on the guardian of the proteome*. Cell Cycle, 2009. **8**(23): p. 3806-8.

437. Harada, M., et al., *The novel combination of dual mTOR inhibitor AZD2014 and pan-PIM inhibitor AZD1208 inhibits growth in acute myeloid leukemia via HSF pathway suppression*. *Oncotarget*, 2015. **6**(35): p. 37930-47.
438. Im, C.N., H.H. Yun, and J.H. Lee, *Heat Shock Factor 1 Depletion Sensitizes A172 Glioblastoma Cells to Temozolomide via Suppression of Cancer Stem Cell-Like Properties*. *Int J Mol Sci*, 2017. **18**(2).
439. Samarasinghe, B., et al., *Heat shock factor 1 confers resistance to Hsp90 inhibitors through p62/SQSTM1 expression and promotion of autophagic flux*. *Biochem Pharmacol*, 2014. **87**(3): p. 445-55.
440. Li, S., et al., *Upregulation of heat shock factor 1 transcription activity is associated with hepatocellular carcinoma progression*. *Mol Med Rep*, 2014. **10**(5): p. 2313-21.
441. Liao, Y., et al., *Higher heat shock factor 1 expression in tumor stroma predicts poor prognosis in esophageal squamous cell carcinoma patients*. *J Transl Med*, 2015. **13**: p. 338.
442. McConnell, J.R., L.K. Buckton, and S.R. McAlpine, *Regulating the master regulator: Controlling heat shock factor 1 as a chemotherapy approach*. *Bioorg Med Chem Lett*, 2015. **25**(17): p. 3409-14.
443. Kim, H.B., et al., *Sensitization of multidrug-resistant human cancer cells to Hsp90 inhibitors by down-regulation of SIRT1*. *Oncotarget*, 2015. **6**(34): p. 36202-18.
444. Su, Y.H., et al., *Targeting of multiple oncogenic signaling pathways by Hsp90 inhibitor alone or in combination with berberine for treatment of colorectal cancer*. *Biochim Biophys Acta*, 2015. **1853**(10 Pt A): p. 2261-72.
445. Friedland, J.C., et al., *Targeted inhibition of Hsp90 by ganetespib is effective across a broad spectrum of breast cancer subtypes*. *Invest New Drugs*, 2014. **32**(1): p. 14-24.
446. Lopez, T., K. Dalton, and J. Frydman, *The Mechanism and Function of Group II Chaperonins*. *J Mol Biol*, 2015. **427**(18): p. 2919-30.
447. Pearl, L.H. and C. Prodromou, *Structure and mechanism of the Hsp90 molecular chaperone machinery*. *Annu Rev Biochem*, 2006. **75**: p. 271-94.
448. Chou, S.D., et al., *HSF1 regulation of beta-catenin in mammary cancer cells through control of HuR/elavL1 expression*. *Oncogene*, 2015. **34**(17): p. 2178-88.
449. Arend, R.C., et al., *The Wnt/beta-catenin pathway in ovarian cancer: a review*. *Gynecol Oncol*, 2013. **131**(3): p. 772-9.
450. Carpenter, R.L., et al., *Akt phosphorylates and activates HSF-1 independent of heat shock, leading to Slug overexpression and epithelial-mesenchymal transition (EMT) of HER2-overexpressing breast cancer cells*. *Oncogene*, 2015. **34**(5): p. 546-57.
451. Dinarello, C.A., *Historical insights into cytokines*. *Eur J Immunol*, 2007. **37 Suppl 1**: p. S34-45.
452. Razavi, G.A., T., *Emerging Role of Interleukins in Cancer Treatment*. *Immunome Research*, 2015. **2**(006).
453. Wang, Y., et al., *Interleukin-8 secretion by ovarian cancer cells increases anchorage-independent growth, proliferation, angiogenic potential, adhesion and invasion*. *Cytokine*, 2012. **59**(1): p. 145-55.
454. Kumar, J. and A.C. Ward, *Role of the interleukin 6 receptor family in epithelial ovarian cancer and its clinical implications*. *Biochim Biophys Acta*, 2014. **1845**(2): p. 117-25.
455. Park, J.I., et al., *Transforming growth factor-beta1 activates interleukin-6 expression in prostate cancer cells through the synergistic collaboration of the Smad2, p38-NF-kappaB, JNK, and Ras signaling pathways*. *Oncogene*, 2003. **22**(28): p. 4314-32.
456. Singh, I.S., et al., *Heat shock co-activates interleukin-8 transcription*. *Am J Respir Cell Mol Biol*, 2008. **39**(2): p. 235-42.

## APPENDICES

## Appendix A: Supplementary Figures

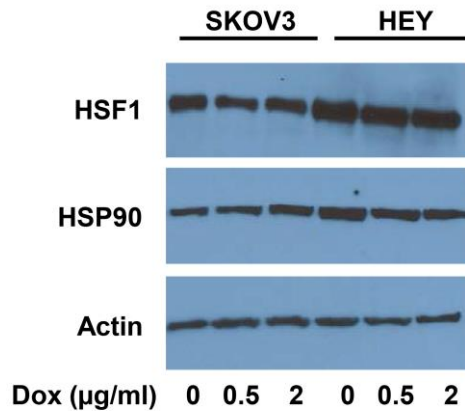


**Figure S.1. Doxycycline Treatment Alone Does Not Alter HSF1 Levels or Induce HSP90 Expression in Ovarian Cancer Cell Lines.** SKOV-3 and HEY cells were treated with 0–2 µg/ml doxycycline, as indicated, for 48 hours. Cell lysates were subjected to Western blot analysis using antibodies recognizing HSF1, HSP90, and actin as a loading control.

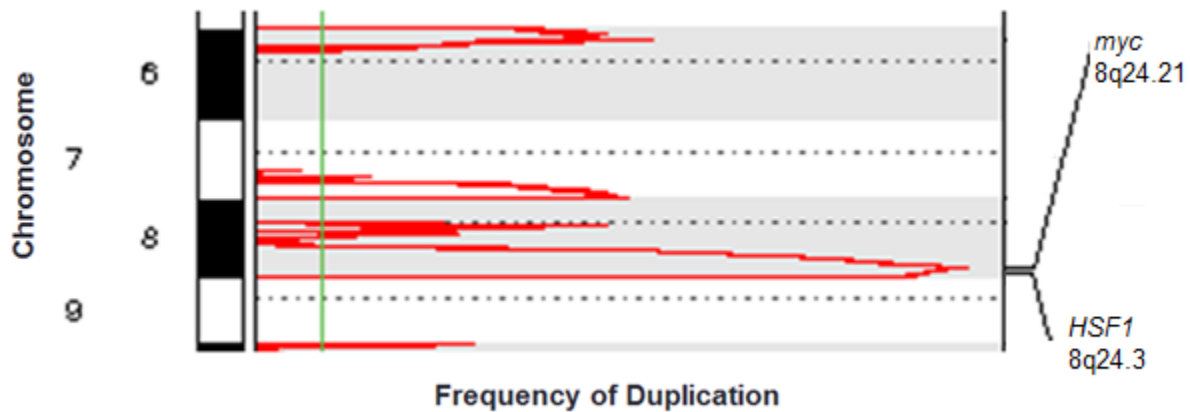


**Figure S.2. HSF1 Gene Locus is Highly Amplified in Serous Ovarian Cancer.** Data is based on GISTIC2 copy number analysis of 579 tumor samples from TCGA. Graphic adapted from Broad Institute TCGA Genome Data Analysis Center [doi:10.7908/C1P84B9Q](https://doi.org/10.7908/C1P84B9Q).

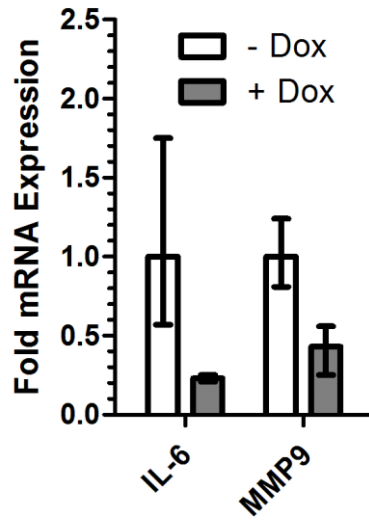


**Figure S.3. Knockdown of HSF1 Reduces IL-6 and MMP9 mRNA induction During TGF $\beta$  Treatment in SKOV-3.shHSF1B Cells.** SKOV-3.shHSF1b cells were treated with and without doxocycline for 48 hours, follow by 10 ng/ml TGF $\beta$  for 48 hr. qPCR was used to assess changes in mRNA levels compared to GAPDH.



**Figure S.4. SKOV-3 Short Tandem Repeat Analysis.** Genomic DNA was purified by phenol chloroform extraction and used to verify cell line authenticity. Short tandem repeat analysis was performed using PowerPlex® 16 HS System. Major peaks were found to match SKOV-3 with over 90% identity using American Type Culture Collection (ATCC) database.

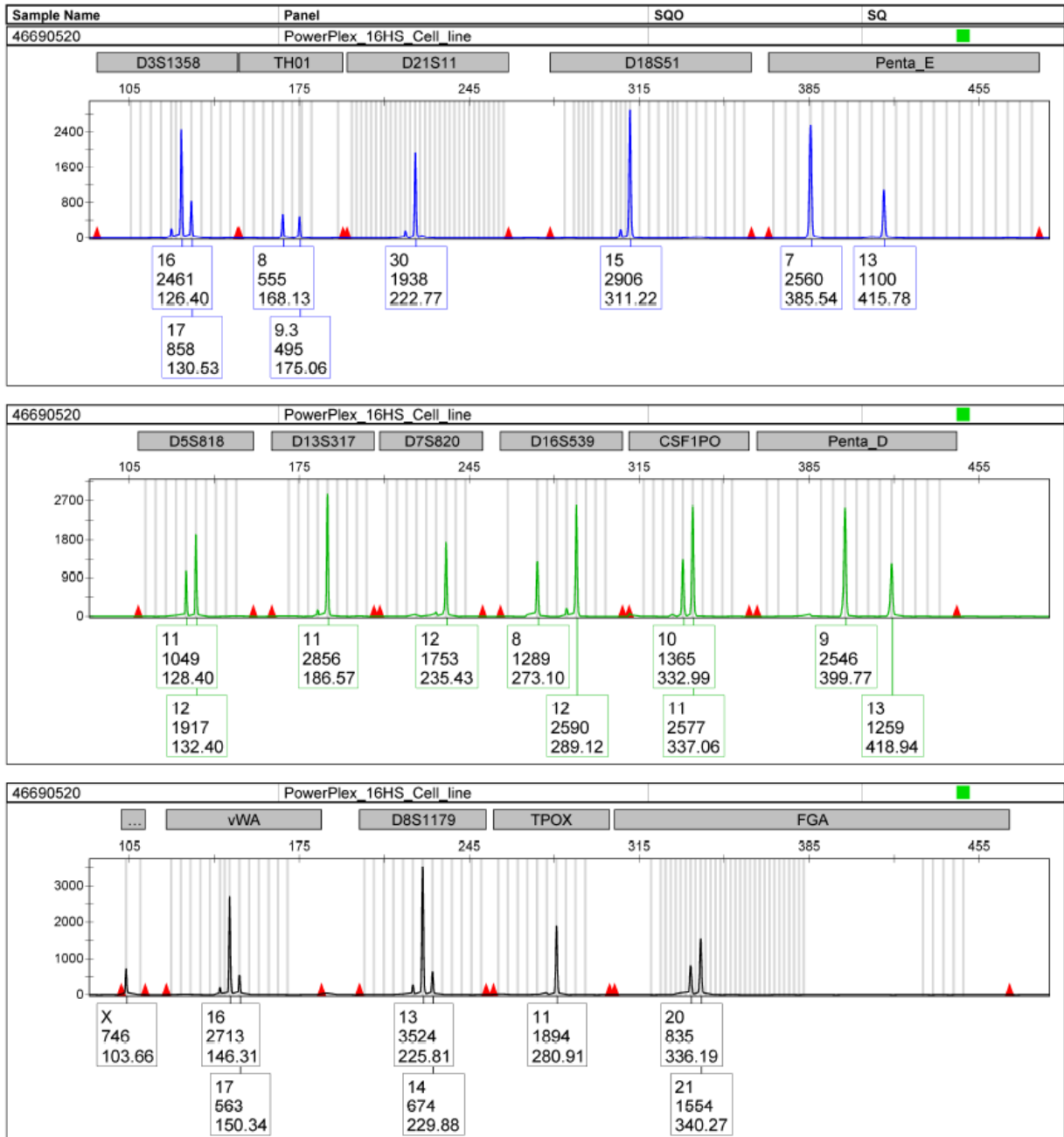


**Figure S.5. HEY Short Tandem Repeat Analysis.** Genomic DNA was purified by phenol chloroform extraction and used to verify cell line authenticity. Short tandem repeat analysis was performed using PowerPlex® 16 HS System. Major peaks were found to strongly match HEY results previously published [363].

## Appendix B: Supplementary Tables

**Table S.1. List of Primers Used in Quantitative RT-PCR.**

Gene Name	Common Name	Sequence
<i>GAPDH</i>	<i>GAPDH</i>	F: 5' - CCACTCCTCCACTTTGAC - 3' R: 5' - ACCCTGTTGCTGTAGCCA - 3'
<i>SNAI1</i>	<i>SNAIL</i>	F: 5' - TCCCAGATGAGCATTGGCAG - 3' R: 5' - CGCGCTCTTTCCTCGTCAG - 3'
<i>SNAI2</i>	<i>SLUG</i>	F: 5' - TTCGGACCCACACATTACCT - 3' R: 5' - GCAGTGAGGGCAAGAAAAG - 3'
<i>TWIST1</i>	<i>TWIST</i>	F: 5' - GGAGTCCGCAGTCTTACGAG - 3' R: 5' - TCTGGAGGACCTGGTAGAGG - 3'
<i>ZEB1</i>	<i>ZEB</i>	F: 5' - CAATACCGTCATCCTCAGCA - 3' R: 5' - CCAATCCCAGGAGGAAAAC - 3'

**Table S.2. Location of HSEs in EMT Genes.**

Gene Name	Common Name	Location from CDS	Sequence
<i>FN1</i>	<i>fibronectin</i>	-3254	<u>TTCTGCAACTTTCA</u>
<i>VIM</i>	<i>vimentin</i>	-3754	<u>TTCCAGAAGGTTAA</u>
<i>SNAI1</i>	<i>SNAIL</i>	-3201	<u>TTCTAGAAGCTTCA</u>
		-3207	<u>TTCTAGAAATTTTGG</u>
<i>CDH2</i>	<i>N-cadherin</i>	-4429	<u>TTCTGGGAAGTTCC</u>
		-2183	<u>TTCCGGAACCTTTT</u>
		-2177	<u>TTCCGGAAAATTTA</u>
		-2544	<u>TTCTGGATTTTCT</u>
<i>ZEB1</i>	<i>ZEB</i>	-289	<u>TTACTAACTTTCC</u>
<i>TWIST1</i>	<i>TWIST</i>	-1301	<u>TTCGAGCACCTTCC</u>
Consensus			<u>TTcnnGAA<sub>nn</sub>TTc<sub>n</sub></u>



**Table S.3. Antibody Dilutions and Incubation Times**

Target	Manufacturer (cat#)	Dilution	Species	Location	Notes
Actin	Santa Cruz sc1616R	1:5000	Rabbit	4°C	4C Overnight
Beta-tubulin	Cell Sig Tech 2128	1:1000	Rabbit	-20°C	4C Overnight
HSF1 Mono	Assay Design spa950	1:1000	Rat	-20°C	4C Overnight
HSP70	Cell Sig 4872	1:1000	Rabbit	-20°C	4C Overnight ; Detects all HSP70 and HSC70
Vimentin	Cell Sig 5741	1:5000	Rabbit	-20°C	RT 2 hours; Very strong - 5% BSA 0.1% tween recommended
Fibronectin	Thermo ms165	1:1000	Mouse	4°C	RT 2 hours; Not working?
N-Cadherin	BD 610920	1:5000	Mouse	-20°C	4C Overnight; Very strong (RT 2 Hours maybe better?)
HSF1 pS326	Epitomics 2092-1	1:5000	Rabbit	-20°C	4C Overnight; maybe weak?
HSP90 Alpha	Cell Sig 8156	1:2000	Rabbit	-20°C	4C Overnight; (Heat shock 90 only) 5%BSA 0.1%Tween recommended
HSP70	Thermo ma3009	1:1000	Mouse	-20°C	4C Overnight; only for heat shock hsp70, maybe weak?
HSP27	Thermo MS-101-P	1:1000	Mouse	4°C	4C Overnight; recognized HSP27 variants unkown
Slug	Thermo MA5-41881	1:1000	Mouse	-20°C	4C Overnight
Fibronectin (new)	Thermo MS 1351	1:5000	Mouse	4°C	4C Overnight
Fibronectin	BD 610077	1:1000	Mouse	-20°C	4C Overnight, Long Exp on PVDF, 2 Hour transfer Required

## Appendix C: Detailed Methods

### Thawing Cells

1. Remove the cryo-vial containing the frozen cells in DMSO freezing medium from liquid nitrogen storage and immediately place it into a 37°C water bath.
2. Quickly thaw the cells (< 1 minute) by gently swirling the vial in the 37°C water bath until there is little to no ice left in the vial.
3. Transfer the vial into a laminar flow hood. Before opening, thoroughly wipe the outside of the vial with 70% ethanol and dry.
4. Using a pipette, gently transfer thawed cells to a 60 mm culture dish with 5 ml warm medium. Rock plate to distribute cells.
5. The following morning, aspirate medium to remove residual DMSO and replace with fresh medium.

### **Creation of pTripZ Constructs**

Primers were created so that the shRNA targeting sequences CGCAGCTCCTTGAGAACATCAA (shHSF1A) and CCCACAGAGATACACAGATATA (shHSF1B) with the addition of the 5' EcoRI and 3' XhoI would be created upon annealing and extension of the primers. This was done to conserve costs. Alternatively the entire double stranded sequence could be ordered.

### **Generate Double Stranded Hairpin DNA**

1. Mix primers constituting the region to be cloned in a 1:1 ratio, heat to 95°C and slowly cool. This allows double stranded DNA formation.
2. Extend duplexed primers via PCR with standard TAQ polymerase using the maximum recommended primer concentrations for a single cycle. This extends the double stranded DNA sequence to the ends. Set up the reaction using 2.5 µl 10x Taq polymerase Buffer, 1µg DNA template, 0.5 µl dNTPs, 0.125 µl Taq polymerase. Bring to a final volume of 20 µl.
3. Extend using a single 20 minute step at 72°C.

### **Digest PCR Product Directly in the PCR Tube**

1. Add 5 µl 10X compatible NEB buffer, 2 µl of each restriction enzyme, 21 µl nuclease free water.
2. Digest for 1 – 2 hours at 37°C

### **Purify Digested DNA Using Qiagen PCR Clean Up**

1. Add 250  $\mu$ l buffer PB1.
2. Add to column, spin at 13,000 rpm for 1 minute; discard flow through.
3. Wash with 750  $\mu$ l buffer PE, spin, discard flow through.
4. Spin once more, then transfer column to a clean 1.5 ml tube.
5. Add 30  $\mu$ l buffer EB and let stand for 1 minute.
6. Spin to collect eluent.
7. Determine concentration using UV spectrophotometer.

### **Prepare Plasmid by Digest (pTripZ was digested with EcoRI and XhoI)**

1. Add 2  $\mu$ l of 10X compatible NEB buffer, 2  $\mu$ g of DNA, and 2  $\mu$ l of each restriction enzyme.  
1  $\mu$ g may be used if quantity is limited or the conc. is < 160 ng/ $\mu$ l.
2. Add Nuclease free water to 20  $\mu$ l total volume.
3. Incubate for 2 hours at 37°C.

### **Separate Digested Plasmid Backbone via Agarose Gel Electrophoresis**

1. Pour a 0.8% agarose gel with 1  $\mu$ l ethidium bromide.
2. Add 4ul of 6X dye to digest and load, leaving an empty well in-between each sample.
3. Use a 1kb ladder and run for approximately 45 minutes, photograph gel.

### **Purify Plasmid Backbone by Gel Extraction Using a Qiagen Gel Extraction Kit**

1. Extract desired bands under UV light using a clean blade for each excised band.
2. Place excised gel bands into to pre-weighed 1.5 ml tube and reweigh to determine mass of gel.

3. Add 3 volumes buffer QG. 0.100 g = 100  $\mu$ l e.g. gel weighs 0.32 g, add 960  $\mu$ l buffer QG
4. Incubate at 50°C for 10 minutes. Mix sample every 2 minutes. All gel should be dissolved when finished.
5. Add 1 volume isopropanol. e.g. gel weighs 0.32 g add 320  $\mu$ l isopropanol.
6. Add to column and spin at 13,000 rpm for 1 minute; discard the flow through.
7. Add 500  $\mu$ l buffer QG, spin, discard flow through.
8. Add 750  $\mu$ l buffer PE, spin, discard flow through.
9. Spin, move column to clean 1.5 ml tube.
10. Add 30  $\mu$ l buffer EB, wait 1 minute.
11. Spin, label and save the eluent. Note: Yield cannot be determined by UV spectrophotometry due to carryover from QG buffer.

#### **Ligate Plasmid and shRNA Sequence**

1. In a 1.5 ml tube, add 2  $\mu$ l 10X T4 ligase buffer, 8  $\mu$ l shRNA insert, 4  $\mu$ l backbone plasmid, 1  $\mu$ l ligase and nuclease free H<sub>2</sub>O.
2. Incubate at 15°C for 1 hour. Note: plasmid may be ligated overnight.

#### **Transform NEB5 $\alpha$ Cells with Ligation Product**

1. Thaw NEB5 alpha cells on ice.
2. Add 8  $\mu$ l of ligated product.
3. Incubate on ice for 15 minutes.
4. Heat shock cells at 42°C for 35 seconds.
5. Incubate on ice for 10 minutes.
6. Add 750  $\mu$ l room temp SOC medium.
7. Incubate at 37°C for 1 hour with 250rpm shaking.

8. Spread on appropriate LB agar plates.
  - i. Spread 20  $\mu$ l, 200  $\mu$ l, and the remainder across three plates.
9. Incubate overnight at 37°C.
  - i. Colonies should appear by morning, store at 4°C after 16 - 18 hours incubation.

### **Purify Plasmid DNA Using Qiagen Miniprep**

1. Prepare 15 ml conical tubes by adding 10 ml LB broth and appropriate antibiotic.
2. Inoculate each broth with a single colony using a flame sterilized inoculating wand.
3. Incubate overnight at 37°C with 250rpm shaking.
4. Pellet cells by spinning at 5,000rpm for 15 minutes at 4°C.
5. Aspirate media.
6. Re-suspend cells in 250  $\mu$ l buffer P1 and transfer to a new 1.5 ml tube.
7. Add 250  $\mu$ l buffer P2 and invert 4 - 6 times. Solution will be completely blue when done.
8. Add 350  $\mu$ l buffer N3 and invert 4 - 6 times. Blue color will be gone when done inverting.
9. Spin for 10 minutes at 13,000rpm.
10. Transfer supernatant to column.
11. Spin at 13,000rpm for 1 minute; discard flow through.
12. Add 500  $\mu$ l buffer PB, spin, discard flow through.
13. Add 750  $\mu$ l buffer PE, spin, discard flow through.
14. Spin at 13,000rpm and move column to new tube.
15. Add 30  $\mu$ l buffer EB, wait 1 minute then spin again.
16. Determine DNA concentration of eluent, label and save.

## Generation of Stable Cell Lines

The pTripZ doxycycline inducible targeting short hairpin RNA (shRNA) works with a second generation lentiviral system. This requires the use of pCGP packaging and pVSVG envelope plasmids. Retroviral plasmids may require different packaging and envelop plasmids.

1. Culture HEK293T cells in the cell medium the cell line that is to be infected uses. A single 10 cm dish will generate enough viral supernatant for multiple rounds of infection.
2. Transfect HEK293T cells with Polyfect Transfection Reagent (Qiagen) using a 1:1:1 ratio of pTripZ, pCGP, and pVSVG.
  - i. Culture cells to approximately 60% confluence
  - ii. Add 4 µg total plasmid DNA to 400 µl serum and antibiotic free medium. Use a 1:1:1 ratio of plasmids.
  - iii. Add 25 µl polyfect, vortex, spin and incubate at room temperature for 5 minutes.
  - iv. During incubation, aspirate medium from cells and replace with 8 ml complete medium.
  - v. Add 1 ml complete medium to polyfect mixture mix by pipetting and add to cells. Rock plates to mix.
3. 12 - 24 hours post-transfection, remove medium with transfection reagent and replace with fresh medium.
4. 24 hours later harvest medium containing viral stock.
5. Filter using a 0.45 micron PVDF filter with Leur lock attached to a syringe.
6. Viral stock may be frozen back at -80°C if it will not be used for 48 hours.
7. Add polybrene to a final concentration of 34.6 µg/ml. Save as 1.5 ml aliquots; when added to 5 ml medium this will yield a final concentration of 8µg/ml polybrene.
8. Infect actively dividing cells at approximately 30% confluency with 1.5 ml of viral supernatant per 5ml cell medium.

9. 12 – 24 hours later, replace cell medium and treat with 0.5 – 5 µg/ml puromycin. The amount needed depends on cell type and cell density.
10. Replace medium as cells die off. Passage cells as needed.

### **Freezing Cells**

It is imperative that cells are healthy and actively dividing to obtain viable cell stocks.

1. Remove medium from cells, wash, and release cells.
2. Once cells are detached add 5 ml warm medium, and transfer to centrifuge tube. Use 15 ml sterile centrifuge tubes and combine cells of same type.
3. Lightly pellet cells by spinning at 1,000 rpm for 5 minutes and remove medium. Up to 1,500rpm may be needed to pellet some cell lines.
4. Resuspend cells in enough freezing medium to create a cell suspension of 1 – 2 x 10<sup>6</sup> cells per ml.
5. Pipette up and down gently to ensure an even mixture. Aliquot approximately 1 ml into cryo-vials. This will provide 1 – 2 x 10<sup>6</sup> cells per cryo-vial.
6. Place cryo-vials into Mr. Frosty™ freezing container and store in -80°C freezer overnight.
7. Cells may be transferred to liquid nitrogen the next day. If a dedicated 1°C per hour freezing container is not available, place cells in a Styrofoam cooler to achieve a similar controlled freezing.

### **Clonogenicity Assay**

1. Culture cells to 70% confluence. It is critical that the cells are healthy and actively dividing.
2. Release cells with trypsin and break up cell clumps. Be thorough to ensure a single cell mixture is obtained.
3. Count cells using a hemocytometer. To ensure accuracy count cells twice.

4. Plate 500 cells per well in 6 well plates. Plating from the same cell pool to ensure all wells receive the same number of cells. Treat with doxycycline as needed.
5. Retreat doxycycline samples on day 4. Doxycycline has a 48 hour half-life.
6. Remove plates after 8 days or when discreet substantial colonies form.
7. Aspirate medium and stain cells with 1% crystal violet (w/v) in methanol for 10 minutes.
8. Gently rinse 3 times by submerging plates in clean deionized water.
9. Photograph and count colonies. Lyse stained colonies using 200  $\mu$ l per well of 1% SDS and placing plates on rocker for 30 minutes.
10. Measure absorbance from each well's lysate in triplicate at 590 nm using Biotek® plate reader.

### **Migration Assay**

1. Treat with doxycycline 48 hours before start of assay.
2. 24 hours before the assay cells should be approximately 75% confluent and serum starved by using serum free medium.
3. Thoroughly release cells with trypsin and pipette to ensure no cell aggregates are in solution.
4. To ensure accuracy count cells twice.
5. Dilute cells to  $1 \times 10^5$  cells/ml in serum free medium. Add 250  $\mu$ l to the upper chamber insert. Perform in triplicate.
6. Add 400  $\mu$ l of medium containing serum as chemoattractant to bottom of wells. Wells are filled second to avoid floating inserts.
7. After 16 hours, remove cells which did not migrate using a cotton swab. Do not let inserts and cells dry out.



8. Stain cells using 1% (w/v) crystal violet in methanol for 10 minutes. Wash 3 times by submerging in deionized water.
9. Cut out membrane from insert using scalpel and mount on glass slides; a cover slip is not needed.
10. Count and average 10 random field of views for each insert.

### **Viability Assay for Testing Drug Sensitivity**

1. Cells to be treated with doxycycline should be done 48 hours before plating. One 60% confluent 10 cm plate is needed for each 96 well plate.
2. Release with trypsin and count cells
3. Dilute to  $1.5 \times 10^5$  cell/ml in a multichannel boat. 10 ml of cell solution is needed per 96 well plate.
4. Using a multichannel pipette, add 100  $\mu$ l per well to 96 well black side clear bottom plates. Be sure to mix cell solution in boat to maintain homogeneous solution.
5. Incubate for 6 hours to allow cells to adhere. Treat with drugs or vehicle control in triplicate. Dilutions should be created fresh.
6. After a 16 hour treatment, wash cells 3 times with PBS. Note: More washes may be needed as doxorubicin and curcumin can affect PrestoBlue® assay due to strong color.
7. Add warm 50  $\mu$ l RPMI medium to each well followed by 5  $\mu$ l of PrestoBlue® Cell Viability reagent.
8. Incubate for 45 minute at 37°C. Incubation time is critical and may need to be adjusted for some treatments.
9. Measure fluorescence using excitation at 570 nm and emission at 600 nm using a microplate reader (BioTek).

10. Calculate percent viability, subtract dead cell control value from all wells and divide each sample reading by the vehicle control.
11. Kill curves can be calculated using variable slope linear regression analysis with GraphPad Prism® 7 software.

### **Wound Healing Assay**

This procedure can be performed with standard or fibronectin coated plates. It makes little difference in cell morphology and migration when using SKOV-3 and HEY cell lines. It is imperative that the cells are on the cusp of full confluence, and that the level of confluence is equal between treated and untreated pairs.

1. Plate cells at  $3 \times 10^5$  cells per ml in each well of a 6 well plate. Treat knockdown samples with 1  $\mu\text{g/ml}$  doxycycline.
2. After 36 – 48 hours use a sterile 2  $\mu\text{l}$  pipette tip to scrape 2 horizontal and 2 vertical lines, creating a “#” pattern. Be sure to use even pressure so the wounds are consistent.
3. Thoroughly aspirate and wash twice with PBS solution. Wash more if detached cells are not all removed from medium.
4. Aspirate PBS and replace with warm serum-free medium.
5. Photograph each of the intersections created by scraping; keeping track of each of the 4 individual scrape intersections.
6. Repeat photograph after 12 hours. None of the scrape intersections should be completely healed, but some should be close. The time interval may be adjusted as needed.
7. Analyze wound closure using TScratch software [365]. Be sure to use identical parameters for image analysis across the entire experiment.

## **BCA Protein Assay**

The bicinchoninic acid (BCA) assay is tolerant of ionic detergents and has a wide range of detection from 20 – 2000 µg/ml. This protocol calls for a clear 96 well plate and sample dilutions which serve to save sample and ensure the concentration is within range of the assay.

1. Prepare RIPA lysis buffer within a 1.5 ml tube, using 250 µl per cell pellet. Add appropriate amount of 100x protease inhibitors and 100x phosphatase inhibitors.
2. Add 250 µl RIPA buffer containing inhibitors to each pellet.
3. Place in 4°C mixer set at 1,000rpm for 10 minutes.
4. Pellet cell debris by spinning at 13,000rpm for 12 minutes at 4°C.
5. Transfer supernatant to new tubes. This step can be omitted if there is no debris.
6. Prepare working reagent by mixing BCA reagents A and B at a 50:1 ratio. Determine total amount needed as follows: number of samples X replicates X 200 µl + 100 µl.
7. Mix well. Working reagent may be stored for 5 days in a sealed container at room temperature.
8. Prepare a 2:3 dilution by the addition of 10 µl sample and 15 µl PBS followed by 200 µl working reagent.
9. Incubate at 37°C for 30 minutes and cover to prevent evaporation.
10. Read plate absorbance at 562 nm using BioTek microplate reader.
11. If available, use a quadratic fit curve to generate standard curve. Use curve to calculate concentrations. Correct for dilution factor as needed.

## **Western Blots**

For consistency, 10% SDS-PAGE gels should be used unless other percentages are absolutely required. Gels should be run at 125 volts until the dye front nears the bottom. A total of 25 µg protein should be run per well. If the lysate is not concentrated enough a lower amount

of total protein may be used. When possible, a positive control cell lysate sample should be run on the gel to serve as a reference point for signal intensity. Decaying signal intensity of the control sample indicates the antibody is going bad, or the western procedure was not performed optimally.

Antibodies should be aliquoted in glycerol and stored at  $-20^{\circ}\text{C}$ . This will ensure the longest shelf life possible and prevent contamination. While antibodies containing sodium azide are said to last a year or more at  $4^{\circ}\text{C}$  they often lose potency and become contaminated over time. Storing aliquots at  $-20^{\circ}\text{C}$  ensures there is another source of a given antibody to use if a current aliquot is thought to be bad. Used antibodies in TBST may be saved for 1 – 2 weeks if sodium azide is added to a final concentration of 0.05% (w/v). It is important to save antibodies in 1% (w/v) non-fat milk TBST instead of 5% milk because the milk component readily aggregates and falls out of solution at 5%. This precipitation can be further avoided by using BSA in lieu of non-fat milk. An additional consideration is that sodium azide irreversibly inhibits conjugated horseradish peroxidase secondary antibodies. Three washes between incubation with sodium azide solutions and the secondary horseradish peroxidase antibody is sufficient to remove residual sodium azide.

1. Cut a  $0.2\ \mu\text{m}$  pore polyvinylidene difluoride (PVDF) membrane to the exact size of gel to be transferred, or slightly larger.
2. Briefly soak PVDF membrane in methanol. Ethanol and isopropyl alcohol will also work if methanol is not available.
3. Transfer PVDF membrane to Towbin transfer buffer and allow to soak until membrane sinks. This takes about 3 minutes. Towbin buffer consists of 25 mM Tris, 192 mM glycine, 20% (v/v) methanol, pH 8.3. If probing for proteins larger than 100 kDa add 0.1% (m/v) sodium dodecyl sulphate.
4. Create a transfer sandwich top to bottom as follows: extra thick blotting paper, trimmed SDS-PAGE gel, PVDF membrane, extra thick blotting paper. Double layers of standard

thickness blotting paper may substituted if needed. Assemble the blot sandwich in transfer buffer, being sure to remove any air bubbles by massaging the transfer sandwich.

5. Move blot sandwich to semi dry transfer apparatus, being sure the layers of the blot have not shifted and do not hang over. Blots with hang over will allow the current to go around the membrane instead of through it, resulting in decreased transfer of proteins.
6. Transfer for 45 - 60 minutes at 150 mA. Double the current with each blot being transferred.
7. Rinse membrane for 2 minutes in TBS (20 mM Tris, 150 mM NaCl, pH 7.6). Repeat for a total of 3 times.
8. Briefly stain in Ponceau Red for 5 minutes (0.1% w/v ponceau, 5% v/v acetic acid, in diH<sub>2</sub>O).
9. Rinse 3 times in TBST (20 mM Tris, 150 mM NaCl, 0.1% Tween-20, pH 7.6).
10. Block in TBST 1% (w/v) non-fat milk for 30 minutes at room temperature.
11. Replace TBST milk and add antibody. Incubate as directed (Table S.3).
12. After incubation period wash 3 times with TBST milk.
13. Add appropriate secondary antibody and incubate for 2 hours at room temperature with agitation on a plate rocker.
14. Rinse 5 times, in 5 minutes intervals with TBST milk. It is imperative to remove any free secondary antibody.
15. Prepare 200 µl developing solution by mixing 100 µl ECL Prime working solution (50 µl reagent A and 50 µl reagent B) with 100 µl PBS. Further dilution of ECL Prime may be used if the signal is too intense, or there is substantial background signal.
16. Blot edge of membrane on a kimwipe to remove excess fluid.
17. Evenly distribute developing solution where protein bands are expected and cover membrane with plastic wrap.

18. Tape down covered membrane in the top left corner of developing cassette and expose. Use 15 seconds, 30 seconds, 1 minute, and 5 minute exposures. If developing 1 or 2 blots, use each corner of the x-ray film individually. This ensures that 4 exposures can be obtained from a single sheet by flipping the x-ray film over.

### **Stripping Western Blot PVDF Membranes**

Western blots using PVDF membranes may be striped of antibodies multiple times. This procedure will not work with nitrocellulose membranes. It is imperative to wash stripping solution off thoroughly to avoid denatured antibodies when re-probing.

1. Rinse blot for 5 minutes with 5 ml TBST.
2. Decant TBST and add 5 ml stripping solution (6M GnHCl, 0.2% Nonidet P-40, 0.1M  $\beta$ -mercaptoethanol, 20mM Tris-HCl,).  $\beta$ -mercaptoethanol should be added when it is fresh. Stripping solution may be warmed to help the GnHCl dissolve.
3. Place on a rocker or shaker for 10 minutes.
4. Decant stripping solution and briefly rinse with TBST.
5. Wash for 5 minutes with TBST. Repeat twice.
6. Re-block membrane with appropriate blocking solution.

### **RNA Extraction with Tri Reagent**

Samples should be prepared directly after harvest. If using frozen samples the time in storage should be minimized. The Tri reagent can be added directly to the frozen samples to thaw. The procedure should be performed in 1.5 ml tubes.

1. For monolayer cells, homogenize the cells by pipetting 1 ml Tri reagent per 10 cm plate. For spheroids add 1 ml Tri reagent and homogenize using a Dounce homogenizer in 1.5 ml tubes. After lysing spheroids, spin at 12,000g for 10 minutes at 4°C to pellet debris.

2. Incubate for 5 minutes at room temperature on plate rocker.
3. Add 0.2 ml chloroform and shake vigorously for 15 seconds. Allow to stand for 10 minutes.
4. Spin at 12,000g for 15 minutes at 4°C.
5. Transfer the top aqueous phase to a new tube. Avoid the white interphase as it contains DNA.
6. Add 0.5 ml of isopropanol. Mix and let stand 8 minutes at room temperature.
7. Centrifuge at 12,000g for 10 minutes at 4°C.
8. Remove supernatant and wash pellet with 1 ml cold 75% ethanol.
9. Vortex briefly and spin at 7,500g for 5 minutes at 4°C. If pellets floats, perform at 12,000g for 5 minutes. Samples can be saved after this step in ethanol for 4 days at 4°C, or 3 months at -20°C.
10. Aspirate ethanol wash with a micropipette and air dry for 20 minutes.
11. Dissolve remaining pellet in 20 µl DNase/RNase free water.

When assessing quality and yield, A260/A280 should be greater than 1.7. Yield from epithelial cells should be between 8 - 15 µg/1 x 10<sup>6</sup> cells. If the extracted RNA is resolved on an agarose gel, strong crisp bands should be observed at 2kb and 5kb if the sample is of good quality.

These bands result from the large and small ribosomal RNAs.

## Appendix D: Copyright Permissions

Copyright permission policy for *Current Peptide and Protein Science*:

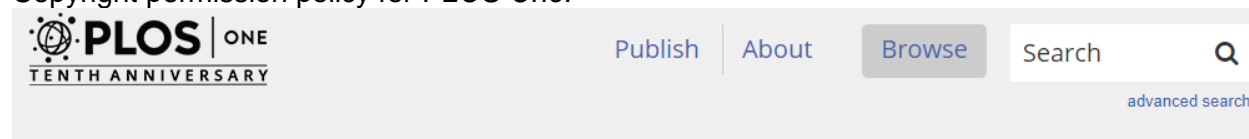
### SELF-ARCHIVING POLICIES

By signing the Copyright Letter the authors retain the rights of self-archiving. Following are the important features of self-archiving policy of *Bentham Science* journals:

1. Authors can deposit the first draft of a submitted article on their personal websites, their institution's repositories or any non-commercial repository for personal use, internal institutional use or for permitted scholarly posting.
2. Authors may deposit the ACCEPTED VERSION of the peer-reviewed article on their personal websites, their institution's repository or any non-commercial repository such as PMC, arXiv after **12 MONTHS of publication** on the journal website. In addition, an acknowledgement must be given to the original source of publication and a link should be inserted to the published article on the journal's/publisher's website.
3. If the research is funded by NIH, Wellcome Trust or any other Open Access Mandate, authors are allowed the archiving of published version of manuscripts in an institutional repository after the mandatory embargo period. Authors should first contact the Editorial Office of the journal for information about depositing a copy of the manuscript to a repository. Consistent with the copyright agreement, *Bentham Science* does not allow archiving of FINAL PUBLISHED VERSION of manuscripts.
4. The link to the original source of publication should be provided by inserting the DOI number of the article in the following sentence: "The published manuscript is available at EurekaSelect via [http://www.eurekalect.com/openurl/content.php?genre=article&doi=\[insert DOI\]](http://www.eurekalect.com/openurl/content.php?genre=article&doi=[insert DOI])."
5. There is no embargo on the archiving of articles published under the OPEN ACCESS PLUS category. Authors are allowed deposition of such articles on institutional, non-commercial repositories and personal websites immediately after publication on the journal website.

Retrieved from: <http://benthamscience.com/self-archiving-policies-main.php> on July 6, 2017.

Copyright permission policy for *PLOS One*:



## Licenses and Copyright

The following policy applies to all PLOS journals, unless otherwise noted.

### What Can Others Do with My Original Article Content?

PLOS applies the [Creative Commons Attribution \(CC BY\) license](#) to articles and other works we publish. If you submit your paper for publication by PLOS, you agree to have the CC BY license applied to your work. Under this Open Access license, you as the author agree that anyone can reuse your article in whole or part for any purpose, for free, even for commercial purposes. Anyone may copy, distribute, or reuse the content as long as the author and original source are properly cited. This facilitates freedom in re-use and also ensures that PLOS content can be mined without barriers for the needs of research.

Retrieved from: <http://journals.plos.org/plosone/s/licenses-and-copyright> on July 6, 2017.